A FINE-SCALE VOLUMETRIC CENSUS OF THE WATER MASSES OF THE AGULHAS RETROFLECTION AREA

by

Henry Richard Valentine

Submitted to the Faculty of Science of the University of Cape Town in fulfillment of the requirements for the degree of Master of Science.

April 1990

ABSTRACT

Two studies of the quantification of water masses around southern Africa are described in this thesis. The first, a pilot study, is concerned with the volumetric analysis of historic hydrographic data from the region off the South African west coast. It uses data that have been collected with various instruments over a considerable period of time and with relatively poor vertical and horizontal resolution. Nevertheless meaningful and significant results have been obtained:

(i) The T/S characteristics of the upwelling domain and the open-ocean are significantly different and show no overlap. Upwelled water is derived from different parts of the South Atlantic Central Water mass.

(ii) Upwelled water, irrespective of its particular origin the Central Water mass, eventually is heated to a limit of 23°C.

(iii) The volume of water in each bivariate T/S class of Central Water, which is available for upwelling, are constant. This implies that the intensity of upwelling may be estimated from the salinity of the upwelled water only.

The second or main study is concerned with the Agulhas Retroflection area. This is located in the broader South-East Atlantic/South West Indian ocean region, which is identified as a serious gap in a previously published fine-scale volumetric census of the world ocean. Recently collected, high quality hydrographic data make it possible to rectify this. This is the principle objective of this thesis. Some results include:

1. The subtle differences between the Central water of South Atlantic Ocean origin and that of the South Indian ocean were addressed. These differences are real and distinguishable as is shown using both historic data and high quality hydrographic data.

2. For the first time, reliable quantitative estimates for the warm and thermocline water masses are produced. The warm, saline surface water of the Agulhas Retroflection area contributes very little to the overall volume of the upper 1500 m of the water column.

3. The low salinity water from south of the Subtropical Convergence is spread widely (in T/S space) on the less saline side of the three-dimensional volumetric diagrams and has very little volume (less than 1 % of the total volume).

4. The more saline, higher volume section of the Central Water in this region corresponds to South West Indian Central Water.

5. Twenty five percent of the total volume of water in this region is contained in only 21 fine-scale bivariate classes.

6. Fifty percent of the water (contained in 71 classes) has a temperature below 3°C. If the lower volume, non-ranked classes were added then almost seventy percent (67,26%) of all the water in the Retroflection area would be colder than 3°C.

The results of this census are compared with those of the world ocean census. Although the volume per bivariate class interval is not of the same order of magnitude, the results are remarkably similar. The water masses of the Retroflection area are less diverse than those of the world ocean.

CONTENTS

PREVIEW AND OBJECTIVES

The Agulhas Retroflection area has been the focus of a considerable number of investigations and studies. This area is a crossroad for water masses from several different geographical regions. It is recognised as an ocean area that plays a crucial role in influencing global climatic patterns because of the globally important exchange of water between the Indian and Atlantic oceans that takes place here. This area, in fact, forms a 'bottle neck' as the two opposing flows (shallow/warm from Indian to Atlantic and deep/cold from Atlantic to Indian ocean) are restricted to a limited area south of Africa (Gordon, 1986). This area also has an influence on local weather and climate patterns because of the oceanic and atmospheric heat fluxes that take place here.

Despite the recognised importance of the area and the vast number of publications on the Retroflection, certain limitations in our knowledge and understanding of this area do exist. One such limitation concerns water characteristics and water masses. There is a need for a thorough detailed description of water properties (eg. temperature, salinity, oxygen content, nutrients, etc.) based on all available high quality hydrographic data. Average tables or curves per area (degree of latitude x degree of longitude) could be produced. These curves could then provide a comprehensive picture of the distribution of such water properties in the Retroflection area; in much the same way as the work done by Emery and Dewar (1982) in the North Pacific and North Atlantic oceans. Such a description would serve as a foundation for work such as that done by Fine et al. (1988) who addressed more dynamic aspects like water mass interrelations and modifications. This is not the objective or thrust of this thesis.

Another fundamental gap in our existing knowledge of the Retroflection area (related to the above) is the quantification of water properties or volumetric analysis. Pollak (1958) considered this as essential for the understanding of the circulation: "A quantitative inventory of water characteristics is virtually a prerequisite to the development of a valid theory of oceanic circulation". This has never been attempted in the Retroflection area. This gap has been recognised before but the lack of suitable data prevented it from being filled. Worthington (1981) undertook a fine-scale volumetric census of the world ocean and concluded: "The most serious gap in the census is in the south-eastern Atlantic and south-western Indian Ocean, where the transition between Atlantic and Indian Ocean water masses has not been properly observed" (see figure A.1). The Agulhas Retroflection area lies in the centre of the vast area of several thousand square kilometers referred to by Worthington that at the time, contained less than ten high quality deep (bottom) hydrographic stations. Since then an excellent data set consisting of several hydrographic sections from several cruises has been built up. The main objective of this thesis will be to address this gap in the volumetric census of the world ocean by analysing the above-mentioned data set.

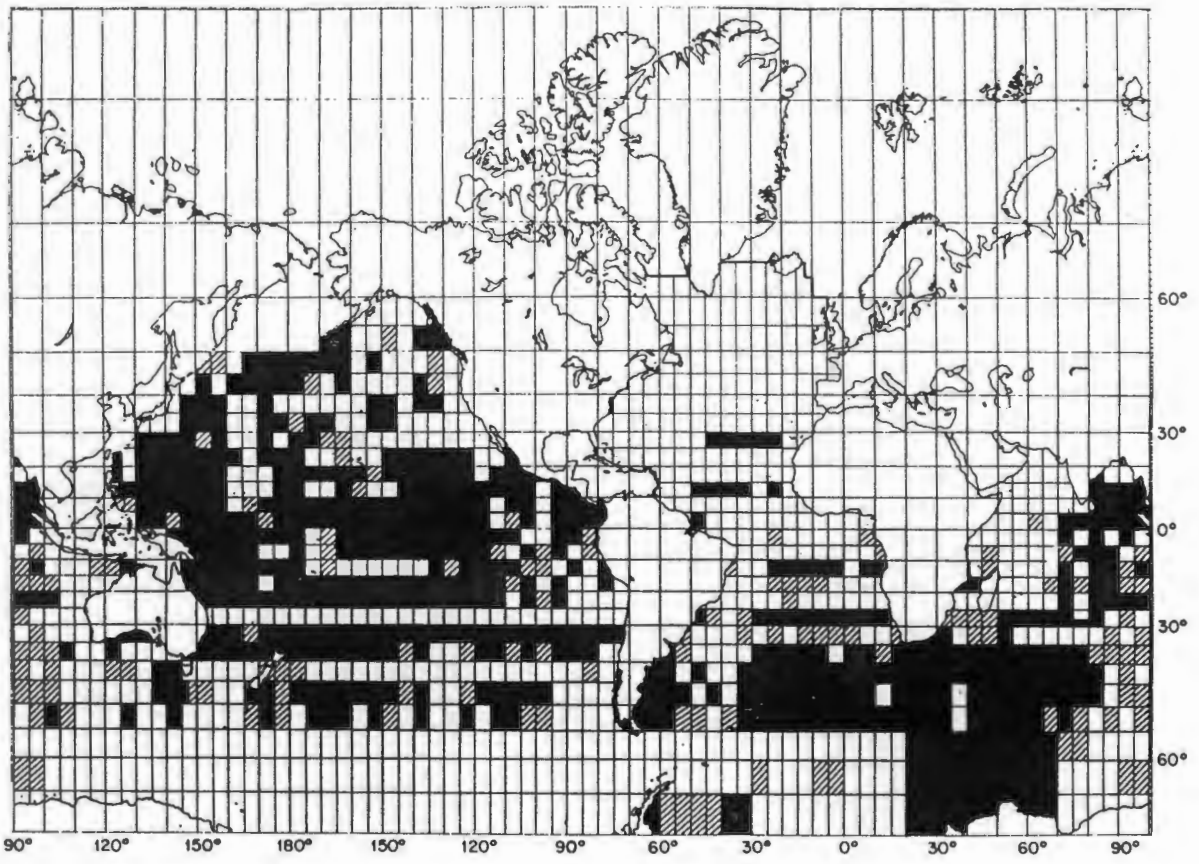

Figure A.1 Chart showing where high-quality deep stations are available (up to June 1977) in the world ocean. Unshaded 5°-squares contain at least one high-quality deep station; crosshatched 5°-squares contain at least one high-quality shallow station; and black 5°-squares contain no high-quality deep stations (from Worthington, 1981).

A volumetric analysis, using historic data, of the Benguela upwelling region will also be carried out as a pilot study. The motivation for this is basically three-fold and is listed below. A vast quantity of historic data is available for the area off the South African west coast. An excellent overview of the area, its physical features and processes has already been done (Shannon, 1985). A comparative study (Carmack and Aagaard, 1977) in this area has been carried out which will allow the results of this pilot study to be viewed in perspective. The experience gained with this pilot study will be incorporated in the main volumetric analysis carried out in the Retroflection area.

The main objectives of this thesis, therefore, are:

1. *to carry out a volumetric analysis of the Benguela upwelling regime as a pilot study.*

2. *to carry out a fine-scale volumetric analysis (census) of the Agulhas Retroflection area to address the serious gap in the global volumetric census.*

A review of the lower Agulhas Current and the Retroflection area will be presented in CHAPTER 1 as introduction. The various contributions that have led to our present understanding and knowledge of the area will be discussed.

Because a volumetric analysis is essentially a quantification of water characteristics and because these water characteristics are employed to identify and describe water masses, it is necessary to give a description of the water masses and water types concerned in a volumetric analysis. This will be done in CHAPTER 2. The description will be brief with the objective of facilitating comparison of the volumetric results only.

Volumetric analyses are not very common. (A possible reason for this may be that they are dependant on good quality deep stations over extensive areas, which are not readily available.) It therefore seems appropriate to give an historic introductory review of the use of T/S diagrams (which forms the basis for volumetric studies) and volumetric census. This is dealt with in CHAPTER 3.

In CHAPTER 4 the data and methodology will be discussed. The data and methods of historical volumetric census will be discussed first while those of the pilot study and the Retroflection area volumetric census will follow.

The results will be discussed in CHAPTER 5. The use of historic data with poor vertical resolution, collected with various instruments over a time-scale of decades, will obviously have some limitations in a volumetric analysis. Despite the above, significant results are possible as shown by the pilot study, and are presented here.

Central Water of the South Atlantic Ocean and that of the South Indian Ocean are very similar as far as their temperature and salinity characteristics are concerned. Since both types of Central Water are present in the Retroflection area, I will show that one can distinguish between the two types of Central Water on the basis of their T/S characteristics with good quality data. Attempts to do this have been made before by for example Clowes (1950) and also by Chapman (1988).

The volumetric results of the Retroflection area are compared with the fine-scale census of the world ocean which inspired this study.

A summary of the results and a few concluding remarks are presented in the final chapter, CHAPTER 6.

ACKNOWLEDGEMENTS

I acknowledge with gratitude, the contributions of various people towards the research for this thesis. Dr John Toole of Woods Hole Oceanographic Institution allowed me access to the *Thomas Washington* hydrographic data before it was published for which I am most grateful. I am also grateful to Professor Joe Reid of Scripps Institution of Oceanography for sending me the calibrated high resolution data of the Ajax cruise.

The many stimulating discussions and the constructive suggestions of Dr Johann Lutjeharms are greatly appreciated. My colleague Mr Roy van Ballegooyen was most helpful in acting as a sounding board for my ideas. He also wrote the original computer programme for the three-dimensional plots. Miss Rosemary Mey's comments are also acknowledged. For the advice and guidance of Professor Geoff Brundritt who acted as supervisor for this thesis, I am most grateful.

I also wish to thank Miss Jill Slinger for assistance in editing the thesis. A very special thank you is extended to Mrs Juanita van Heerden who patiently decyphered my scribbling and diligently typed this thesis from the first draft through the various iterations till its final form. And lastly, I would like to thank my wife, Claudine, and children for their support and encouragement.

LIST OF FIGURES

Figure Page

LIST OF TABLES

CHAPTER 1

INTRODUCTION

The Agulhas Retroflection area is generally referred to as that geographic area south-southwest of the sub-continent where the Agulhas Current retroflects, and its immediate vicinity. The southern boundary of the retroflection area is generally taken as the Subtropical Convergence.

As far as the bottom topography of this area is concerned, there are two prominent and distinct features, namely the Agulhas Plateau and the Agulhas Bank and a less prominent Cape Rise to the southwest of this area (see figure 1.1). The former two features exert a major influence on the behaviour of the Agulhas Current and the Agulhas Return Current in this area. The Cape Rise would have a significant impact as far as the control of the retroflection of the current is concerned if the current usually retroflected that far west (~15°E). To date there is very little evidence of a retroflection that far west (Lutjeharms and van Ballegooyen, 1984). Lutjeharms (1988a) however has produced some evidence from thermal infrared imagery that suggests an extreme retroflection at about 8°E. The topography where the current normally retroflects is relatively flat.

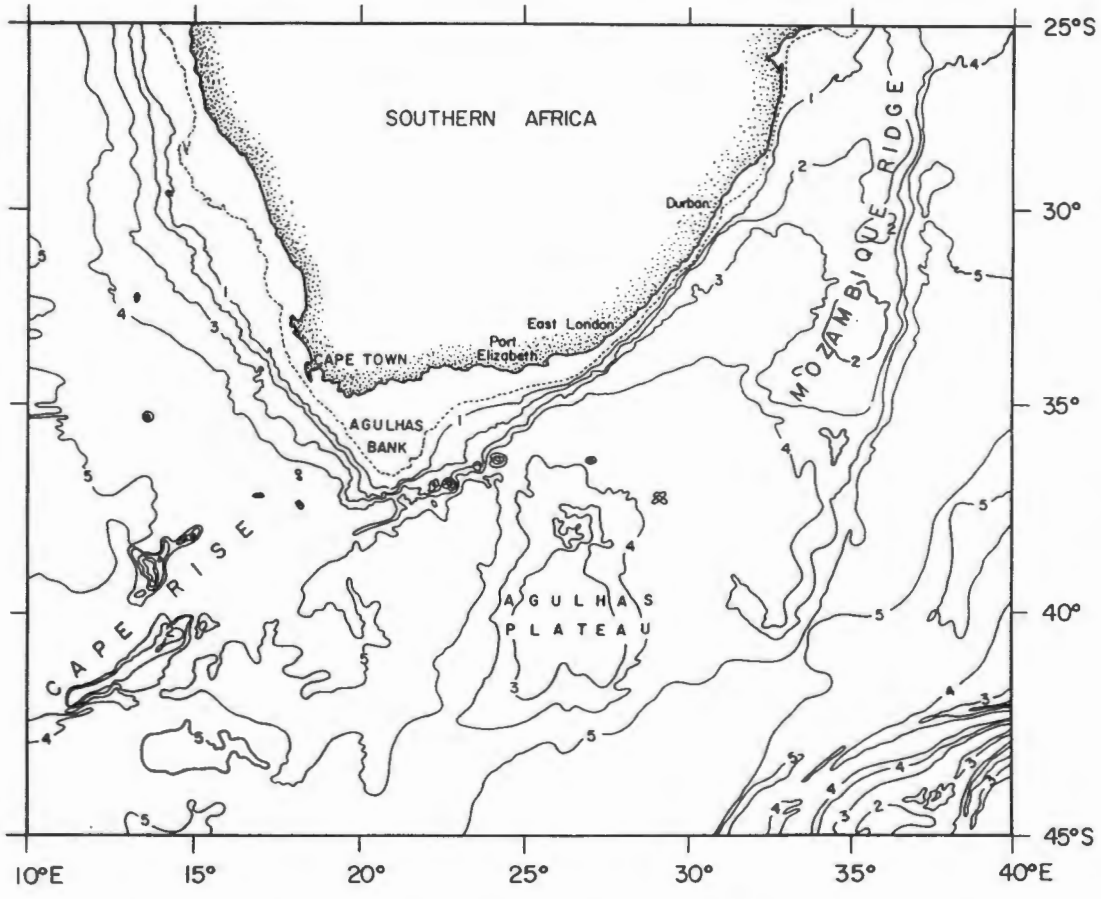

Figure 1.1 The bottom topography of the ocean area adjacent to South Africa (after Simpson, 1974). The contours are in 1000 m intervals. The continental shelf is indicated by the 200 m contour (dotted line).

The Agulhas Retroflection area is dominated by the three components of the southern part of the Agulhas Current system namely the southern Agulhas Current, its retroflection and the Agulhas Return Current. The Agulhas Current is a warm, strongly developed western boundary current (Pearce, 1970; Harris and Van Foreest, 1978; Gründlingh and Lutjeharms, 1979) flowing along the southeastern coast of southern Africa. The current hugs the coast (continental shelf) and near the southern tip of the continent where the continental shelf is at its widest, it separates from the coast as a free jet and curves around in a large anticyclonic loop called the Agulhas Retroflection. Nils Bang (Bang and Pearce, 1970) was the first to coin the term 'retroflect' for this abrupt turn of the Agulhas Current south of Africa. The fact that it separates from its western boundary at the southern tip of the continental shelf makes the Agulhas Current different from all other western boundary currents which separate from a meridional coast that continues poleward. On retroflecting the warm subtropical Agulhas water flows eastward along the Subtropical Convergence as the South Indian Ocean Current. The first section of this eastward flowing current is known as the Agulhas Return Current.

On a global scale this Retroflection area is one of the most important oceanic areas of comparable size for various reasons. Gordon (1986) and Lutjeharms and Gordon (1987) have described the Agulhas Current as the major, most energetic western boundary current in the Southern Hemisphere. The Retroflection region is furthermore subject to active temporal variability (Colton and Chase, 1983; Cheney et al., 1983; Lutjeharms and Baker, 1980). The Agulhas Current loop encloses a pool of Indian Ocean water south of Africa whose temperature is more than 5°C higher than South Atlantic Surface Water at similar latitude. This feature supports a large average heat flux into the atmosphere of about 100 - 125 W/m^2 (Bunker, 1980). These fluxes could even be substantially larger at specific times (Walker and Mey, 1988). Satellite and hydrographic data suggest an exchange of Indian and South Atlantic water at the Retroflection.

The transfer of Indian Ocean water into the South Atlantic (via eddies, Agulhas rings, filaments, etc.) at the Retroflection area introduces warmer, saltier water into the eastern boundary regime of the South Atlantic subtropical gyre and may be of importance to the overall heat and salinity budgets of the South Atlantic. The heat of the surface layers may be quickly lost to the colder atmosphere but the salt has a more lasting influence. It has been proposed (Gordon, 1986) that this transfer (Indian Ocean to South Atlantic Ocean) may play a role in the global thermohaline circulation by providing a relatively warm and salty return path for the Atlantic Ocean export of North Atlantic Deep Water (NADW). In the Atlantic Ocean, NADW, after formation, spreads south throughout the Atlantic and is exported to the Indian and Pacific Oceans, as part of the deep circulation. To compensate for the NADW the bulk of the upper layer return flow (according to Hastenrath's 1982 calculations) must reside within the thermocline. The only source for such water south of 30°S is the Indian Ocean thermocline water within the Agulhas Current. Not all of the Agulhas water participates in the Retroflection. Eddies, filaments and rings shed along the western margins of the Agulhas Retroflection introduce variable amounts of warm water into the Southeast Atlantic

(Lutjeharms, 1981b; Gordon, 1985; Walker, 1986). Up to 20 percent of the Agulhas Current can leak into the South Atlantic in this way (Gordon et al.,1987). Gordon (1985) has also shown that between the centres of isolated Agulhas rings west of the retroflection and the African mainland an 'Agulhas Current branch' transporting 14 Sv (Sv = Sverdrup = $10^6 m^3 s^{-1}$) into the South Atlantic existed during November-December 1983. This situation was not unique. Synoptic data of a cruise in March 1969 (Harris and Van Foreest, 1978) indicated that 5 Sv of Agulhas water entered the South Atlantic. Model studies also depict linkage between the subtropical gyres of the South Atlantic and Indian Oceans (Veronis, 1973; de Ruijter and Boudra, 1985).

Because ocean heat and freshwater flux influences global climate patterns, the possible warmwater link between the Indian and Atlantic Oceans might be an important climate factor (Veronis, 1973; de Ruijter, 1982). The wind-driven non-linear barotropic model of de Ruijter and Boudra (1985) showed that changes to the connection between the subtropical gyres of the two oceans could be forced by changing the wind field: as the zero wind stress curl moves further south of Africa, exchange between the two subtropical gyres increases. Ou and de Ruijter (1986) find that as the Agulhas transport decreases the Agulhas Current separation from the continental shelf becomes less complete and more water flows into the Atlantic. Thus the presence of strong seasonal variation of the wind stress over the South Atlantic - Indian Ocean basin (as reported by Hellerman and Rosenstein, 1983) may be expected to have an impact on the South Atlantic circulation and climatology.

The Retroflection area also has an impact on local climate and weather. Recent hydrographic studies (Gordon et al., 1987) have underscored the key role this area plays in the ventilation of the Atlantic and Indian ocean thermocline through the exchange of water south of Africa (Gordon, 1985). This process has been shown to depend to a large extent on ring shedding at the Retroflection (Lutjeharms and Gordon, 1987; Olson and Evans, 1986). Once these Agulhas rings (and also eddies) are spawned they lose heat and moisture to the atmosphere which alters their mixed layer characteristics of temperature and salinity and therefore density. The interocean heat transfer therefore, also has water modification implications. Furthermore, oceanic heat losses induce atmospheric modifications via the marine boundary layer which influence local weather and climate patterns (Jury and Walker, 1988; Harrison et al., submitted).

The leakage of warm water from Agulhas origin into the South Atlantic may contribute to a large extent to the anomalous equator-ward transport of warm water in the South Atlantic, which also has climatic implications. The equator-ward heat flux is in the range of 54 to 86 x 10^{13}W (Hastenrath, 1982). The variable amounts of warm Agulhas water advected into the South Atlantic also may have implications for the fishing industry at the South African west coast. Shannon et al. (1988) have for instance noted that historical performances of a number of key fish stocks in the Southeast Atlantic appear to be related to trends in sea surface temperature (SST). Brundrit et al. (in press) have explored the possibility of using SST in linear stochastic models to forecast hake recruitment.

From the above it is thus clear that the Agulhas Retroflection area is a very dynamic area with high temporal variation. It is a area with high ocean to atmosphere heat fluxes all year round. It plays a crucial role in the global oceanic thermohaline circulation. The area also has an influence on local weather and climate, especially the summer rainfall areas of Southern Africa (Walker, in press). It has some implications for the west coast fishing industry and it contributes to the anomalous equator-ward heat transport in the South Atlantic ocean with subsequent climatic implications.

The recognition of this global significance of the Agulhas Current system only come about during the early nineteen seventies. The real emphasis only occurred the last decade or so when the Retroflection area has been high-lighted as one of the most important oceanic areas of the world due to the tremendous implications and influence this area has on global as well as local climate and weather. It is appropriate to give here a brief overview of some of the work done that contributed to our present understanding and knowledge of the Agulhas Current system in general and the Retroflection in particular.

Dietrich (1936) observed that the Agulhas Current forms part of the western boundary current system of the Southern Indian Ocean and that it is therefore dynamically similar to the Florida Current (Gulf Stream) and Kuroshio systems. He also stated that it had not, however, been studied in the same detail (then) as its northern hemisphere counterparts. However by the early seventies the overall circulation in the Agulhas Current system was reasonably well known mainly from large scale surveys of such investigators as Dietrich (1935), Clowes (1950), Darbyshire (1964), Duncan (1970), Bang (1970), Harris (1972) and (later) Lutjeharms (1976). The earlier work seemed to have emphasised investigations or research of a general or descriptive nature. Work by Duncan (1970) and Bang (1970) for example would fit in this category. As more and better quality data became available and as the knowledge base increased, the emphasis shifted towards addressing specific aspects of the Agulhas Current system, and the dynamic processes involved. Fine et al.'s (1988) work on water mass modification in the Retroflection area is a good example of this category. There can be no clear chronological cut-off though. Better understanding will inevitably lead to new discoveries which in turn have to be described. So descriptive papers will allways constitute a fair component of the published literature. The work on the Agulhas Current system is no different. The usefulness of the descriptive papers is that they usually not only incorporate all the available data but also all of the latest information (at the time). An example here is the work by Lutjeharms and Van Ballegooyen (1988) on the Agulhas Retroflection.

The introduction of satellite remote sensing and its application to oceanography has lead to a significant increase in the rate of growth of our knowledge base of the Agulhas Current system. Infrared satellite imagery has since been used extensively as a tool in studies on the western boundary currents (the Agulhas Current is no exception). The high thermal contrast between the currents proper and their surroundings make them most suitable for satellite imagery investigations.

Based on these two traditions of research, the following is now known. The Agulhas Current which flows poleward along the southeast coast of the sub-continent, has an average width of about 90 km (Pearce, 1977) and is about 1000 to 2500 m deep (Duncan, 1970). It has as its sources water from the Mozambique Channel (Saetre and Jorge da Silva, 1984; Lutjeharms, 1976; Harris, 1972) and from the area east of Madagascar (Lutjeharms et al., 1981) and reaches its full stature at about 26°S. However, the source of Agulhas Current water entering the Retroflection is primarily the southwest Indian Ocean anticyclonic gyre (Gordon et al., 1987). There is secondary input through the Mozambique Channel, which is very variable (Lutjeharms, 1972). Estimates of transport through the Mozambique Channel are small, [ranging from 6 x $10^6 m^3 s^{-1}$ (Fu, 1986) to 10 x $10^6 m^3 s^{-1}$ (Harris, 1972)] compared to those of the Agulhas Current [95 x $10^6 m^3 s^{-1}$ (Gordon et al., 1987)]. Most of the direct measurements of the Agulhas Current structure have been made in the northern section off the Natal coast (Pearce, 1977). Current speeds in excess of 2,5m s^{-1} have been measured (Gründlingh, 1977), while the volume flow has been estimated at about 70 x $10^6 m^3 s^{-1}$ (Gründling, 1980). There seems to be an apparent increase in volume flow down stream e.g. Jacobs and Georgi (1977) derived a value of 137 x $10^6 m^3 s^{-1}$ adjacent to the Agulhas Bank. Gordon et al. (1987) estimated a southwest transport into the Retroflection area through the Agulhas passage of 95 x $10^6 m^3 s^{-1}$ though.

As a major western boundary current the Agulhas is unusual in showing very little meandering or divergence from its average position for a considerable part of its length. Gründlingh (1983) showed that between 28°30'S (Cape St. Lucia) and 34°S (Port Elizabeth) the Agulhas Current follows the continental slope with a lateral meandering displacement of less than 15 km, on average. However in 5 percent of more than 300 cross current hydrographic sections, exceptional current core meanders in excess of 100 km were observed. Satellite imagery was successfully employed to identify sideways waves on the current border south of East London (Harris et al., 1978). These had phase velocities of about 20 cm s^{-1} which were very similar to those of extreme meanders observed in 1973 (Gründlingh, 1979) and October 1983 (Gründlingh, 1986). Lutjeharms (1981a) distinguished two types of perturbation features. Downstream of Port Elizabeth the presence of a wider shelf facilitates the growth of small perturbations into substantial meanders with attendant shear-edge features and trailing plumes over the shelf. Up stream of Port Elizabeth at irregular intervals excursions of the current with substantially larger amplitudes (the Natal pulse) have been observed. Both perturbation features of the Current have implications for the circulation further downstream. Lutjeharms and Roberts (1988) estimated a rate of about 21 cm s^{-1} for the downstream progress of the Natal pulse until the Agulhas Bank is reached, from where the progress rates decline to about 5 cm s^{-1}. The downstream progress of the cyclonic eddy within a Natal pulse may cause intermittent coastal counter currents (Lutjeharms and Connell 1989) as have been observed in numerous hydrographic surveys and current measurements (Schumann, 1981, 1982; Pearce, 1977; Pearce et al., 1978).

South of Mossel Bay the Agulhas Bank widens considerably, causing the general flow of the Current to veer southwards. It is in this region that the most dramatic changes occur in the

developing meanders, with shear-edge features in the form of plumes and eddies a common occurrence. The warm water trailing edges extend in a northeasterly direction, generally separated from the main flow of the Current by a core of cold water. In common with conditions in other western boundary currents, upwelling occurs along the inshore front of the Agulhas Current (Walker, 1986). This could be a result of Ekman veering (Schumann, 1986; Hsueh and O'Brien, 1971) or hydraulic control as suggested by Gill and Schumann (1979). The existence of the frontal features (eddies and plumes) increases the effect that the Agulhas Current has on the Agulhas Bank. Catzel and Lutjeharms (1987), Lutjeharms, Catzel and Valentine (1988) have established the degree of penetration of warm Agulhas Current water over the shelf. The shear-edge eddies were established as the source of these penetrations. Swart and Largier (1987) have speculated that advection of Agulhas Current water plays an important role in the thermocline structure on the Agulhas Bank. Lutjeharms (1981b) concluded that these shear-edge phenomena are a consistent and an ever present part of the landward border of the Agulhas Current.

As the Agulhas Current veers south, it executes a large anticyclonic loop (retroflects) and flows eastward along the Subtropical Convergence as the Agulhas Return Current. The latter is part of the South Indian Ocean Current. At the Retroflection deep-sea eddies had been observed before (Duncan, 1968) but Bang (1970) was the first to show the inherent generic nature of the Agulhas Retroflection and that the terminal region of the Agulhas Current was populated by a range of eddies. Results of a three-ship cruise (March 1969) showed the connection between these features (Harris and Van Foreest, 1978) and the Agulhas Current. The geopotential anomaly of the sea surface relative to 1500 db [based on hydrographic data of the *R.V. Knorr* and the *R.V. Meiring Naudé* (Gordon et al., 1987)] (figure 1.2) revealed a geostrophic circulation pattern remarkably similar to that found in March 1969. With serial satellite imagery, Lutjeharms (1981b) showed for the first time that the Agulhas Retroflection loop was unstable and that it could coalesce and form Agulhas rings.

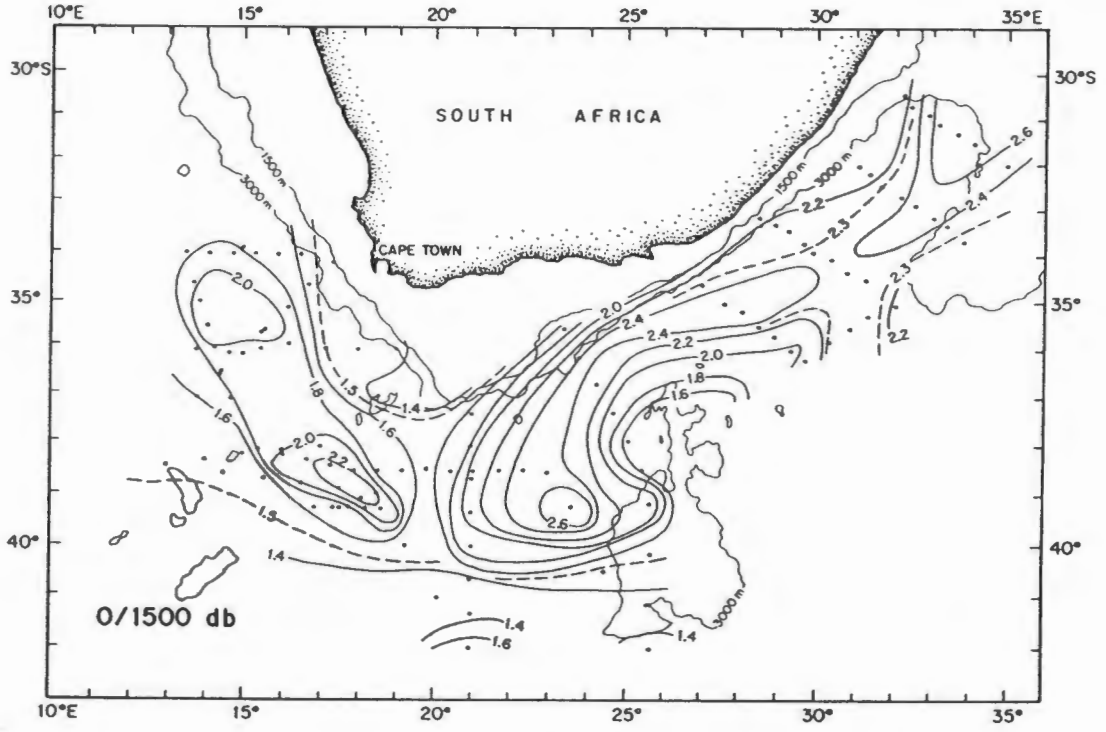

Figure 1.2 Dynamic height anomaly of the sea surface relative to the 1500 decibar surface. Values are given in dynamic meters. The black dots indicate the station positions of the R.V. Knorr (Nov/Dec 1983) and the R.V. Meiring Naudé (Oct 1983). Adapted from Gordon et. al., 1987.

The Agulhas Return Current describes a series of meanders which coincide with features of the bottom topography such as the Agulhas Plateau and the extension of the Mozambique Ridge (Gründlingh, 1978). Harris and Bang (1974) investigated the topographic control in the main part of the Current and concluded that the deflection offshore of the Current near East London has its origin in topographic Rossby waves. The factor responsible for the singular Current behaviour manifested in the Retroflection could be the conservation of potential vorticity. To test this hypothesis the Current may be modelled as a free inertial jet. Various degrees of success have been achieved to date in simulating certain components of the Agulhas Current system with inertial jet models. Gill and Schumann (1979) and Lutjeharms and Van Ballegooyen (1984) have successfully modelled the Retroflection in this manner under a range of possible conditions. The model shows that the magnitude of the volume transport is decisive in causing either westward penetration or early retroflection of the Current; and that strong topographic control is indicated for the offshore deflection near Port Elizabeth.

De Ruijter (1982) modelled the Current from a large-scale wind-driven ocean circulation (incorporating inertia) point of view. He showed that the existence of the retroflection is critically dependent on the wind stress curl decreasing substantially in the region adjacent to South Africa. Subsequently, De Ruijter and Boudra (1985) also found that the Agulhas Retroflection is largely due to the net accumulation of anticyclonic relative vorticity as the Current flows southward. By including baroclinicity in their model, Boudra and De Ruijter (1986) have facilitated the simulation of ring formation at the Retroflection.

The large and meso-scale features of the Agulhas Current system described above have been observed on numerous occasions and have been confirmed by trajectories of drifting bouys (free drifting and drogued) (Stavropoulos and Duncan, 1974; Gründlingh, 1977, 1978; Garrett, 1981; Patterson, 1985) and by hydrographic measurements (Gründlingh and Lutjeharms, 1979; Gründlingh, 1980; Pearce, 1977; Harris and Van Foreest, 1978; Gordon et al., 1987) and from satellite imagery (Harris et al., 1978; Lutjeharms, 1979, 1981; Lutjeharms and Roberts, 1988; Lutjeharms and Valentine, 1981b, 1988; Walker, 1986).

The Agulhas Retroflection is associated with a very active meso-scale field (Lutjeharms and Baker, 1980). The highest variability (up to 40cm) in sea level change (measured by SEASAT) in the Southern Hemisphere was found south of Africa (Colton and Chase, 1983). Variability is also in the surface temperature patterns observed from satellites (Catzel and Lutjeharms, 1987; Lutjeharms and Van Ballegooyen, 1988), from satellite-tracked drifters and from hydrographic data. The variability is dominated by shear-edge eddies along the inshore side of the Agulhas and by changes in the position of the Retroflection associated with the generation of warm-core rings (Lutjeharms, 1981b; Olson and Evans, 1986). Lutjeharms and Van Ballegooyen (1988) found the Agulhas Retroflection to occur between 16°E and 20°E. The zonal location is not stable but shows a characteristic progradation into the South Atlantic and sudden subsequent reinitiation in the east. Each progradation event is concluded with the shedding of a warm-core Agulhas ring. Cheney et al. (1983) found the variability most intense between 11°E and 16°E, which is west of the Retroflection. Lutjeharms and Van Ballegooyen (1988) observed the behaviour of the Agulhas Retroflection and the shedding of rings and eddies to be analogous to similar features of other western boundary currents of the Southern Hemisphere, but more intense. This seems to be confirmed by Olson and Evans (1986) who showed that two eddies observed in 1983 west of the Retroflection to be four times more energetic relative to other western boundary generated eddies and rings. This supports Cheney et al.'s (1983) claim of high variability west of the Retroflection. In contrast to other western boundary currents no re-absorption events or eddy-coalescence events have yet been observed.

Duncan (1970) proposed a seasonal variation in the transport of the source of the Agulhas Current (higher in winter than in summer). This pattern is reflected in the mass transport of the Agulhas Current despite different winter/summer ratios in the connecting currents (Mozambique Current and East Madagascar Current). The seasonal variation of volume transport has been confirmed by Gründlingh (1980). Although the geostrophic calculations alone exhibited a seasonal variation similar to that obtained by Duncan, the transports resulting from the matched velocity profiles had no variation at all. Eagle and Orren (1985) speculated that the penetration of Agulhas water along the bottom of the Agulhas Bank may occur on a seasonal basis. Lutjeharms and Van Ballegooyen (1984) also speculated that the most westerly retroflections which occur for lower volume transports of the Current (according to their model) may be a seasonally induced occurrence. Pearce and Gründlingh (1982), using hydrographic data could, however, find no appreciable seasonal trends in the mean current speeds nor any significant seasonal variation of the core speed.

From the above it is clear that the Agulhas Current system (whether as a whole or certain aspects of it) has been well documented in a substantial number of publications. The majority of these publications emphasize the upper 1500 - 2000 m of the water column. This is the generally accepted depth extent of the Agulhas Current. The deeper water masses in this region have not received the same kind of attention at all. The warm, thermocline and even intermediate waters of the world oceans are much more dynamic and have high variability compared with the deep waters, which are much more stable and have very tight temperature/salinity characteristics. In fact their T/S characteristics are often used to calibrate data and even instruments. So the emphases on the upper ~2000 m of the water column is understandable especially in the Retroflection area where we have a major western boundary current as the key factor. On the other hand almost all volumetric studies by definition emphasize the deeper waters which make up most of the world ocean's volume (as will be shown in chapters 3-5). Since no volumetric census has been conducted in the Retroflection area, the concentration on the upper water masses is even greater than usual. With the volumetric analysis of this study the emphasis will be shifted towards the deeper waters. This may also be seen as an attempt to start to amend the imbalance. The Retroflection area is being recognised as very important due to the potential influence it may have on global climate. Quite a number of researchers are still actively working on this region. Our knowledge base of this area is however far from complete. There are several limitations in our knowledge and understanding that still have to be addressed. One such a limitation is the question of oceanic as well as ocean-atmosphere heat fluxes in this area. This aspect has only recently (Fu, 1986; Lutjeharms, 1988b; Walker and Mey, 1988) received some attention. If we accept that statistically significant links between oceanic and atmospheric properties may have important implications for climate prediction, then the subject of heat fluxes and their implications has to be understood better .

Another example of a limitation to our knowledge is the question of whether the Agulhas Current, especially in Retroflection area, does exhibit significant seasonal variation. This aspect has not been conclusively addressed. More fundamental though, as far as I am concerned, are the limitations to our knowledge regarding the water masses of this area. Here I refer to water mass identification and description, water mass formation and modification and water mass and/or water type quantification. The latter is inevitably linked to a volumetric analysis; which has never been attempted for the Retroflection area. This will be discussed in the next chapter which addresses the historical definitions of the water masses of the Agulhas Retroflection area.

CHAPTER 2

THE WATER MASSES OF THE AGULHAS RETROFLECTION AREA

Bennett (1988) has referred to the Agulhas Retroflection area as the area where three oceans (Atlantic, Indian and Southern oceans) meet, because of its geographical location in relation to the world oceans. It can be expected then that, due to the area's proximity to the three oceans, water masses that are typical of one or more of these may be found here. Water masses from the different oceans may also interact with one another in the Retroflection area. If one adds to this scenario : the fast flowing Agulhas Current that transports waters of Indian Ocean origin, not only into the Retroflection area, but also into the South Atlantic; the compensating flow and transport from the Atlantic to the Indian ocean; factors such as mixing and heat fluxes which alter the composition of water masses; and the dynamics and high variability of the area, then it can be appreciated that the water mass composition of the Retroflection area can be expected to be very complex.

Because data collected over several years are usually combined for a volumetric analysis and because the objective of this chapter is to describe the water masses only to facilitate comparison with volumetric results, only a general description of the waters that can generally be expected to be present in the Retroflection area is offered. Although not ideal, the simplistic description of the water masses of the Atlantic and Indian Oceans by Sverdrup et al. (1942) and the attempt by Emery and Meincke (1986) to combine and describe the major water masses of the world will be used as the basis for this description of the waters of this area. No attempt will be made to describe the complexities and intricate detail of the water masses and their interrelationships of the Retroflection area. Such descriptions have been attempted (Gordon et al., 1987; Fine et al., 1988) but were based on quasi-synoptic data so the water masses were described as they existed at the time of the hydrographic survey.

The injection of South Indian water via the Agulhas Current into the South Atlantic, interocean exchange of thermocline water at the Retroflection (Gordon, 1986), heat fluxes (both vertical and horizontal) and mixing are some of the processes that influence the constitution of the water masses in this area. The water masses of the Retroflection area are primarily Subtropical Surface Water, South Indian Central Water, South Atlantic Central Water, Antarctic Intermediate Water, Deep Water and Antarctic Bottom Water. To address the waters that the Agulhas Current introduces to this area one has to look at the source of the Current. The source of Agulhas Current water entering the Retroflection region is primarily the southwest Indian Ocean anticyclonic gyre (Gordon et al., 1987). There is secondary input through the Mozambique Channel, which is, as has been noted before, very variable (Lutjeharms, 1972).

The surface waters in the Retroflection area have temperatures in the range of about 16°C - 26°C and salinity in excess of 35,5 per mille (‰) or practical salinity units (psu). This water has its origin in the tropical zone (Tropical Thermocline Water) of the Indian Ocean. Further south the surface salinity is higher due to excessive evaporation encountered in the Subtropical zone (25-35°S). This subtropical water sinks and produces subsurface salinity maxima throughout the South Indian Ocean. This water is called Subtropical Surface Water and is transported by the Agulhas into the Retroflection area. Underneath this water is the Central Water.

Central Water is formed at the Subtropical Convergence region by the sinking and northward spreading of mixed subtropical and subantarctic surface water masses (Sverdrup et al., 1942; Orren, 1963 and 1966). Emery and Meincke (1986) do not distinguish between surface water and Central Water. They refer to the upper water mass in the South Indian Ocean as South Indian Central Water with temperature and salinity (T/S) ranges of 8,0 - 25,0 °C and 34,60 - 35,80 ‰. Sverdrup et al., (1942) classified Central Water in the Southwest Indian Ocean as that with a T/S range of 8,0 - 15,0°C and 34,60 - 35,50 ‰ which corresponds with the lower section of Emery and Meincke's range. Gordon et al. (1987) confirmed Sverdrup et al.'s description by referring to South Indian Central Water (SICW) as thermocline water which spans the interval from the more saline surface water to the salinity minimum of the Antarctic Intermediate Water (AAIW). This water is also transported by the Agulhas Current into the Retroflection area.

Central Water in the South Indian Ocean and in the Southeast Atlantic Ocean has very similar T/S characteristics (Orren, 1963; Shannon, 1966). Gordon (1986) has pointed out that between 7° and 15°C the South Atlantic and South Indian thermoclines are similar in potential temperature/salinity (θ-S) properties. The T/S range for the South Atlantic Central Water (SACW) is 6,0 - 16,0°C and 34.50 - 35,50 ‰. South Atlantic Water does not enter the Retroflection region via the Agulhas Current. It is formed from a blend of thermocline water and Subantarctic Surface Water (Gordon, 1981) and enters the Retroflection area from the South. The common (similar) θ-S curves of the South Atlantic and Indian thermoclines (basically Central Water) between 15° and 7°C may be a consequence of exchange between these basins across the Retroflection (Gordon, 1985). According to Fine et al. (1988) the coincidence in θ-S space may be due to a combination of mixing and similarity in the ventilation processes along the poleward outcropping of the thermocline and Intermediate Water isopycnals.

At the base of the Central Water at intermediate depths Antarctic Intermediate Water (AAIW) is found. The traditionally held view is that Antarctic Intermediate Water is formed continuously or intermittantly near the Antarctic Polar front, which lies around 50-55°S, where water of about 2,2°C and 33,87 ‰ salinity sinks and spreads northwards in the Atlantic, Indian and Pacific oceans (Sverdrup et. al., 1942). So at its source it has a characteristic T/S of 2,2°C and 33,87 ‰. McCartney (1977), however, suggested that it is the Subantarctic Mode Water that penetrates the Atlantic ocean via the Drake Passage which gives the AAIW in this region its

low salinity and low temperature characteristics. The salinity minimum which marks the core of the AAIW is gradually eroded with distance from source. The salinity range for the AAIW in the South Atlantic as well as the South Indian Ocean is 33,80 - 34,80 ‰ while the temperature ranges for the two oceans are 2,0 - 6,0°C and 2,0 - 10,0°C respectively (Emery and Meincke, 1986). In the southeast Atlantic the salinity minimum is usually between 34,30 and 34,50 ‰ and the temperature between 4,0 and 5,0°C (Clowes, 1950; Stander, 1964; Shannon, 1966). Clowes (1950) and Fuglister (1960) suggest the depth of the salinity minimum to be between 600 and 1000m. Clowes (1950) and Shannon (1966) also suggested a northwesterly flow of AAIW south of latitude 25°S. This was supported by Visser (1969). Some AAIW may also be advected from the Indian Ocean into the Atlantic around the Agulhas Bank (Clowes, 1950; Shannon, 1966). The large range of salinity values within the AAIW indicate some influence of Red Sea Water (RSW). The northward penetration of AAIW encounters the southward spreading of the very saline RSW at about the same depth at about 20°S off the east coast of Africa (Gründlingh, 1985). So in the western South Indian Ocean AAIW and RSW intermingle but their opposing characteristics (high temperature/high salinity of RSW and lower temperature/lower salinity of AAIW) make it possible to distinguish between the two water masses. Clowes and Deacon (1935) found traces of RSW at intermediate depths as far as 40°S.

Gordon et al. (1987) found RSW present between 4 and 6°C in the Retroflection area from synoptic hydrographic data. Jacobs and Georgi (1977) noted that in the Retroflection region AAIW is strongly eroded by high salinity intrusions. Piola and Georgi (1982) and Jacobs and Georgi (1977) suggested that RSW mixes with AAIW and provides the high salinity component for the Antarctic Intermediate Water observed in the Retroflection area.

Below the AAIW (and RSW) in the Retroflection region, is the North Atlantic Deep Water (NADW) and the Circumpolar Deep Water (CDW). The NADW marks the salinity maximum. This high salinity water has its origin in the North Atlantic Ocean and is found as far south as 56°S (Clowes, 1950). Its T/S range is 1,5 - 4,0°C and 34,80 - 35,00 ‰ (Emery and Meincke, 1986) and it dominates the deep water not only in the South Atlantic but also within the western Indian Ocean. Gordon et al. (1987) distinguished between NADW and Indian Deep Water (IDW) on the basis of their oxygen content. The latter is also less saline. They could, however, not find any evidence of IDW entering the Retroflection area. In the Indian Ocean the AAIW and RSW overlies the Circumpolar Deep Water. The latter has a T/S range of 0,1 - 2,0°C and 34,62 - 34,73 ‰ (Emery and Meincke, 1986). In the Southern Ocean sector the NADW lies between two layers of CDW (subdivided into Upper CDW and Lower CDW). In the Retroflection area, using synoptic hydrographic data, Gordon et al. (1987) found very little CDW based on θ -S properties only, in this area, but with oxygen content instead of salinity as a parameter they distinguished Upper CDW, above, and Lower CDW, beneath, the NADW.

The Deep Water layers overlie the Antarctic Bottom Water (AABW) in the Retroflection area. This water has a T/S range of -0,9 - 1,7°C and 34,64 - 34,72 ‰. Very little of the cold, high oxygen water that usually is found on the ocean floor (AABW) is present in the Retroflection region.

In the upper layers of the Retroflection area, water masses of Indian Ocean origin are introduced by the Agulhas Current, but water masses from the Atlantic are introduced at the intermediate and deep layer levels. The injection of Agulhas water into the South Atlantic has been noted by various authors (Dietrich, 1935; Clowes, 1950; Shannon, 1966; Harris and Van Foreest, 1978; Pearce, 1980 and Gordon, 1985, amongst others). It was only very recently that an attempt to quantify the amount of this Agulhas water has been made. Gordon et al. (1987) calculated a transport of 10 x $10^6 m^3 S^{-1}$ (relative to 1500 db) of Agulhas water into the South Atlantic, which is about 13 percent of the total transport (relative to 1500 db) of the Agulhas. This figure could in fact be as high as 20 percent of the Agulhas Current transport (Gordon, 1985). Calculations by Fine et al. (1988) show that substantial quantities of the Agulhas water inflow to the Atlantic are replaced by water from the South Atlantic subantarctic zone at least between 15 and 4°C (SACW). Some portion of the subantarctic zone water is modified South Atlantic water. Thus the 10 x $10^6 m^3 S^{-1}$ of Indian Ocean water entering the South Atlantic may partially be balanced by returning in the Agulhas Return Current. If this is the case it means that South Atlantic Water is returned to the Indian Ocean at the thermocline (Central Water) and intermediate (AAIW) depths. Gordon et al. (1987) concluded that waters below 1500 m, which represent about 20 percent of the Agulhas transport, in the Retroflection area were entirely of South Atlantic origin. Thus it is also possible that South Atlantic water colder than 4°C is returned to the Indian Ocean. Negative salinity anomalies in hydrographic data (Gordon et al. 1987) indicate that the Agulhas Return Current carries Atlantic AAIW characteristics into the South Indian subtropical gyre. Shannon and Hunter (1988) also produced results, from historic data, that seem to indicate that the movement of AAIW, in many respects is similar to the surface circulation, which supports the hydrographic data anomalies. Throughout the hydrographic data of the 1983 Agulhas Retroflection survey, strong gradients and interleaving were observed. This reflected the fact that the retroflection region is a crossroads for water masses from several different geographical regions (Gordon, 1985). Table 2.1 gives a summary of the major water masses of the Retroflection area. Notice that this is a simplified summary of the water masses present in the Retroflection. The definitions come from various authors as discussed above.

Volumetric analyses are not very common. There may be a variety of reasons for this. I will not try to establish these reasons but rather give an overview of the evolution and background of volumetric studies. This will be done in the next chapter (chapter 3). This may be appropriate and useful and can be seen as an introduction to the volumetric analysis which is the main thrust of this thesis.

Table 2.1

Summary of the water masses of the Agulhas Retroflection Area

		TEMPERATURE RANGE	SALINITY RANGE
SURFACE WATER		~ 16.0 - 26.0°C	> 35.5 ‰
CENTRAL WATER			
(i)	South East Atlantic Ocean	6.0 - 16.0°C	34.5 - 35.5 ‰
(ii)	South West Indian Ocean	8.0 - 15.0°C	34.6 - 35.5 ‰
ANTARCTIC INTERMEDIATE WATER			
	Characteristic T/S	~ 2.2°C	~ 33.87 ‰
(i)	South East Atlantic	2.0 - 6.0°C	33.8 - 34.8 ‰
(ii)	South West Indian	2.0 - 10.0°C	33.8 - 34.8 ‰
DEEP WATER			
NORTH ATLANTIC DEEP WATER (South East Atlantic)		1.5 - 4.0°C	34.80 - 35.00 ‰
CIRCUMPOLAR DEEP WATER (South West Indian)		0.1 - 2.0°C	34.63 - 34.73 ‰
ANTARCTIC BOTTOM WATER		-0.9 - 1.7°C	34.64 - 34.72 ‰

CHAPTER 3

HISTORIC INTRODUCTORY REVIEW OF T/S DIAGRAMS AND VOLUMETRIC ANALYSES

The correlation of temperature and salinity, two conservative characteristics of sea water, was first put on a systematic basis when Helland-Hansen (1916) introduced the temperature-salinity diagram. This led the way for all the characteristic diagrams which are regarded as valuable tools in oceanography today.

The identification of ocean waters by their temperature-salinity correlation has subsequently became a standard technique in oceanography. It is common practice to present observations of temperature and salinity both as vertical profiles and as temperature-salinity (T/S) curves. The vertical profiles provide a natural description of the thermal and haline structure measured at a particular station, while the T/S relation indicates how these properties are interrelated.

As early as 1918 - Helland-Hansen recognised that T/S curves from adjacent stations were similar and that this similarity was due to the presence of water of similar character, called a water mass. Sverdrup et al. (1942) differentiated between water masses which were defined by characteristic T/S curves or parts thereof and "water types" characterized by an individual pair of temperature and salinity values - a point on a T/S curve. So the T/S curve is made up of an infinite number of water types.

Sverdrup et al. (1942) used a limited number of hydrographic stations to summarize the water mass distribution in the world's oceans with a set of T/S curves. This description has become the standard against which most subsequent observations have been compared. It remains today the most comprehensive review of global T/S curves and water masses available. (An example of a T/S plot is given in figure 3.1). A similar presentation was produced by Dietrich (1964), but since all the oceans were included in the same diagram it resulted in a resolution that was poorer than that of Sverdrup et al. (1942). In his book Mamayev (1975), rather than carry out a new summary analysis of temperature-salinity data, merely reproduces the figures from Dietrich (1964) and Sverdrup et al. (1942). Until very recently our knowledge of T/S curves globally, therefore, relied on relatively little hydrographic data.

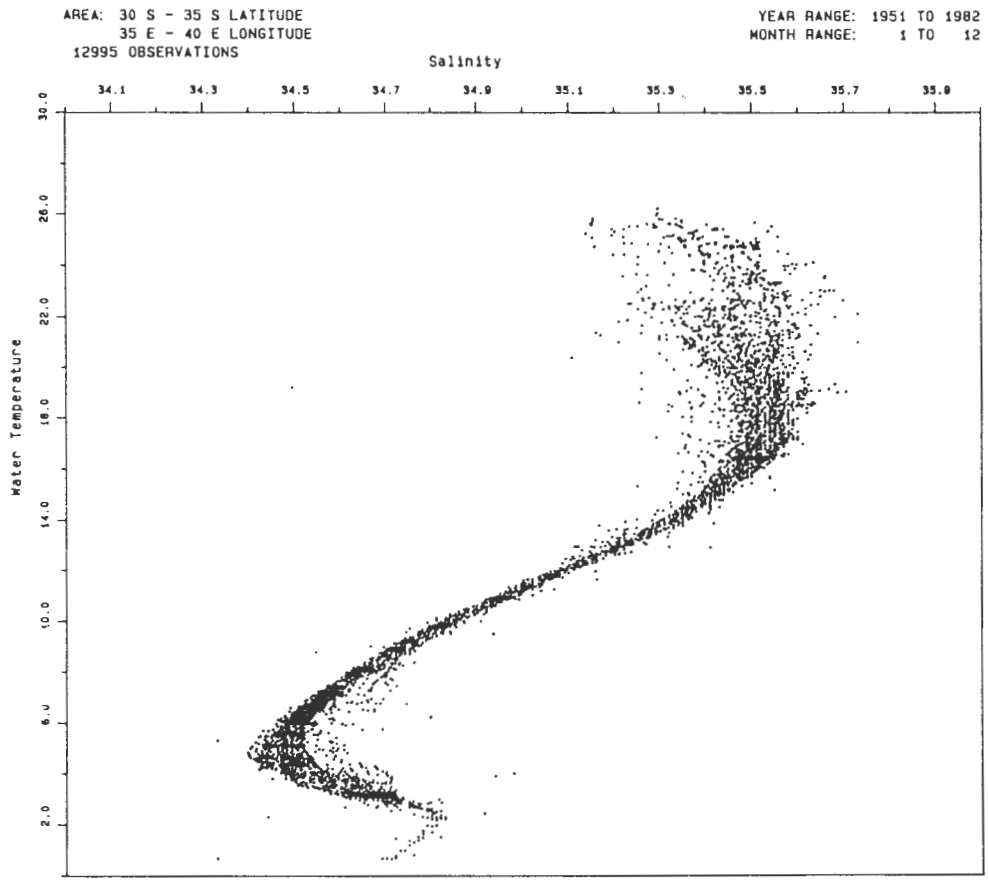

Figure 3.1 An example of a T/S scatter diagram which is a combination of several T/S curves. This diagram represents the historic data in the area 30 - 35°S and 35° - 40°E.

Since Sverdrup et al.'s (1942) estimates of global distributions of water masses many publications eg. Fuglister (1960), Wyrtki (1971), Wright and Worthington (1970), Worthington (1976), Emery and Dewar (1982), Pollard and Pu (1985), Reid (1965, 1973), Broecker and Takahashi (1985) and Harvey (1982) have examined the details of water masses in particular regions or oceans. The many descriptions and analyses of water masses have lead to a situation already observed in 1970 by Wright and Worthington (1970): "The nomenclature of the water masses in the North Atlantic has become bewilderingly confused in the past half century, although it is apparent that the water masses themselves have remained essentially the same". This observation can be applied easily to other oceans as well and the abundance of water mass nomenclature presently in use forces one to be selective and limit the description to (in broadest terms) the major water masses.

Very few attempts have been made to synthesize these regional studies (mentioned above) into a comprehensive overview of global water mass distribution. Mamayev's (1975) T/S analysis of the global ocean reviewed the characteristic limits for the global water masses. He also presented global maps of intermediate and deep water masses. Unfortunately these maps are produced on a very small scale and it is also difficult to determine the criteria used to define the water mass boundaries. The same problem arises in the characteristic T/S values in his table of global water masses.

The most recent attempt to synthesize the definitions and distributions of global water masses from the literature was that of Emery and Meincke (1986). They presented an updated global water masses summary in compact form rather than review all the regionally specific water masses that have been identified and studied.

The most important advance in water-mass analysis (according to Worthington 1981) since Helland-Hansen's (1916) concept of a water mass as defined by a temperature-salinity curve, came with the introduction of the volumetric-T/S curve by Montgomery (1958), Cochrane (1958) and Pollak (1958). These publications gave an estimate of the volumes of all the world water masses.

Although the T/S diagram has been, since its introduction, the most familiar means of comparing and classifying ocean waters, its suitability in representing bivariate frequency distributions of the water characteristics, temperature and salinity, had hardly been exploited before the above-mentioned publications. This aspect of the T/S diagram may be recognized partially when a large number of serial observations is plotted as a scatter diagram in temperature-salinity co-ordinates, as for example, by Helland-Hansen and Nansen (1926). But the first entirely quantitative representations of a distribution by means of the diagram seems to have been given by Montgomery (1955) for surface temperatures and salinities at Weather Ship J.

Cochrane's (1956) study to determine the prevalence of the T/S properties at the surface of the Pacific Ocean was one of a few (by then) attempts to describe the prevalence of different temperature and salinities at the sea surface, although many maps and tabulations then already existed to show the geographical distribution of average sea-surface temperature and salinity.

Nearly all previous studies of prevalence had been confined to temperature. (Sir) John Murray (1899) portrayed the area of sea surface having maximum and minimum temperatures within 10°F of each other, for each ocean. Spilhaus (1942) computed the percentage of ocean surface having annual mean temperatures within various 5°C temperature intervals. A complete series of sea surface temperature distributions for 5°F intervals for the world ocean and each ocean separately have been presented by Littlewood (1955).

Helland-Hansen and Nansen's (1926) scatter diagram concept (in temperature-salinity co-ordinates) gave some suggestion of the two-dimensional frequency distribution of T/S. While not directly concerned with prevalence, Wüst, Brogmus and Noodt (1954) presented related information. In a series of T/S diagrams they indicated the average annual temperatures and salinities for each 5° zone of the world ocean and of each ocean separately.

Cochrane (1956) introduced a few definitions regarding the volumetric T/S curve. As in Montgomery's (1955) paper, the term *characteristic* denotes a point on the T/S diagram (similar to Sverdrup et al., 1942 'water type'). *Characteristic class* refers to the area on the diagram included in a specified temperature/salinity interval. The frequency of a characteristic class means its prevalence in extent and duration within the region and period considered. I will

adhere to these definitions as far as possible, although Sverdrup et al.'s (1942) 'water type' is preferred to 'characteristic'.

Bivariate distributions for sea water were prepared for a point by Montgomery (1955) and for a surface by Cochrane (1956). Bivariate distributions for volumes were presented first in a group of three papers in a parallel study, namely Cochrane (1958), Pollak (1958) and Montgomery (1958). Pollak was convinced that a quantitative inventory of water characteristics is virtually a prerequisite to the development of a valid theory of oceanic circulation. His paper represented such an inventory for the Indian Ocean. Together with the parallel studies of the Atlantic ocean (Montgomery, 1958) and Pacific ocean (Cochrane, 1958) these papers helped to eliminate a substantial gap in descriptive oceanography. The purpose of these papers was to furnish some basic of statistics sea-water indicating the volume of each type according to temperature-salinity criteria. At that stage 'in-situ' temperatures (T) were used most commonly for T/S correlation. As water at all depths is treated together in the volume calculations, actual temperature is not sufficiently conservative. Therefore, these papers employ potential temperature (θ), computed for each sample using the method of Helland-Hansen (1930). The individual and world oceans were divided into bivariate classes of temperature and salinity each of which contained an assigned volume. Based on a volume of 1369 x $10^6 km^3$ for the world ocean (including adjacent seas) Montgomery (1958) found the most abundant class in the world ocean to lie between T = 1,0 - 1,5°C and S = 34,7 - 34,8 ‰. He calculated that this relatively small class contained 9 % of the water in the ocean.

A direct descendent of Montgomery's (1958) work was the volumetric census of the North Atlantic ocean by Wright and Worthington (1970). This census was motivated by the introduction of very accurate salinometers, pioneered by Schleicher and Bradshaw (1956), which were based on the measurement of electrical conductivity. The precision of data obtained with these salinometers enabled Wright and Worthington (1970) to divide the North Atlantic water masses into much smaller temperature-salinity classes than Montgomery and colleagues had used. Before the introduction of salinometers in 1954 the Wenner instrument, a shipborne electrical salinity bridge was in use (Wenner, Smith and Soule 1930). The use of the conductivity properties of sea water to measure salinity was introduced by Wenner in 1922. His instrument was always calibrated by chemical titration using the Knudsen method, however, so that its full precision was never realized. Wright and Worthington's smallest class (below 2°C) was 0,1°C x 0,01 ‰. This means that fifty of these classes make up one of Montgomery's classes (0,5°C x 0,1 ‰). This fine-scale census had clear advantages over the coarser-scale census that inspired it. In consequence Worthington (1981) undertook a census of the world-ocean water masses using the fine-scale classes that Wright and Worthington (1970) introduced.

The above comprises a background or an introduction to volumetric studies. In the next chapter (DATA and METHOD) more emphasis will be layed on the different methods the various investigators used and how the data have been adapted to suit the methods.

CHAPTER 4

DATA AND METHOD

In any volumetric analysis considerable effort is devoted to

(i) selecting the suitable hydrographic data and

(ii) adjusting or manipulating the selected data to make it more suitable for volumetric analysis.

Different methods or techniques have been developed in this regard and a number of assumptions are made along the way. One should be particularly aware of this when comparing results from different volumetric analyses.

4.1 Historical Volumetric Census

Although the temperature-salinity diagram (since its introduction by Helland-Hansen, 1916) has been the most familiar means of comparing and classifying ocean waters, its suitability in representing bivariate frequency distributions of water characteristics, temperature and salinity was only realized in the nineteen fifties. Montgomery (1955) was the first to demonstrate the suitability of the temperature-salinity diagram for the quantitative representation of the frequency distribution of water characteristics. He needed a uniform series of data to prepare a diagram for a fixed point in the ocean. He used three years of surface observations at Weather Ship J. for this purpose. On most days there was one observation of temperature and salinity, but on some days there was none. In order to obtain a homogeneous series from the somewhat irregular original series, 15 observations per month (odd days namely 1, 3, 5 ... 29) were chosen. Missing odd days were replaced with other days or with observations from nearby positions. The frequency was tabulated for each two-dimensional class with temperature interval 0.5°C and salinity interval 0.1 per mille. The frequency of a characteristic class means its prevalence in extent and duration within the region and period considered, while characteristic class refers to the area on the diagram included in a specified temperature and specified salinity (Cochrane, 1956). The two-dimensional distribution was summed horizontally and vertically, respectively, to yield the one-dimensional frequency distribution of salinity and temperature (salinity was plotted on the abscissa) in the form of a histogram. Isopleths of specific volume anomaly were included in the diagram. Any other temperature-salinity function, such as sound speed can be shown in the same manner by including the appropriate series of isopleths.

Prevalence of both temperatures and salinities over large areas of the ocean surface does not appear to have been considered before Cochrane's (1956) work in the Pacific. Ideally, an estimate of the frequency distribution of characteristics for a selected period and region should be based on a long, uniform series of observations from many fixed points spaced in relation to average gradients. Such ideal data do not exist, and even approaching this standard with existing observations involves considerable difficulty. Consequently, as a method of obtaining a first approximation, the distributions used by Cochrane were based on available maps of average conditions. While this procedure has obvious limitations, it seems unlikely that the salient features of the distributions so derived are incorrect.

The temperature range (-2°C - 30°C) was divided by Cochrane (1958) into a series of 2°C intervals and the salinity range (29,2 - 37 ‰) into intervals of 0,4 ‰. Between 20° and 50° latitude, both north and south (regions with large horizontal gradient), the ocean surface was divided into areas 2,5° latitude by 5° longitude; and in other latitudes, into areas 5° latitude by 5° longitude. The area mean characteristics of each small area were estimated in terms of the centre values of the characteristic classes for February and August. The area distributions were obtained by summing the small areas within each characteristic class. These area distributions are used as approximations to the frequency distributions. Temperature-salinity diagrams showing the frequencies of surface-water characteristics were produced for winter (February in North Pacific, and August in South Pacific) and summer and for the whole year. Isopleths of specific volume anomaly were included as curves on the diagrams in preference to density or sigma-t for the reasons presented by Montgomery and Wooster (1954).

The first proper volumetric analysis was carried out by the related studies of Cochrane (1958), Pollak (1958) and Montgomery (1958) although none of them actually referred to their studies as such. Pollak and Cochrane referred to their results as frequency distributions of water characteristics though the frequency was expressed in terms of volume. It was Montgomery who placed the emphasis on volume.

Cochrane (1958) used both observed as well as interpolated values of selected hydrographic stations. Each pair of temperature and salinity values at a station was taken as typical of a volume surrounding the pair. In the cases where selected stations did not reach to sufficient depths, values from neighbouring stations were used. Boundaries between hydrographic stations were located partly for convenience and partly on the basis of established features in the fields of temperature and salinity. He also attempted to select boundaries in such a way as to keep the depth of each region (represented by a hydrographic station) fairly uniform. The volume, which a pair of temperature and salinity values was assumed to typify, was determined in the following way: The area of the region was obtained by planimetering an equiareal chart. The depth of a given pair extended between the midpoint to the next pair above and the midpoint below, or if the pair was at the top or the bottom of a station, between the top or the bottom and midpoint to the next pair. The volumes obtained in this way were summed to produce a

volume for the entire Pacific Ocean which compared very well with the more precise volume calculated by Kossina (1921).

The class intervals used for the bivariate distributions (Cochrane, 1958) represented a compromise between the detailed information of small intervals and the reliability of large intervals. Since the sample was relatively large at low potential temperatures, small intervals could be employed. These intervals were not suitable for the entire range so two sets of class interval were used, finer classes (0,5°C and 0,1 ‰) for water colder than 10°C and more saline than 32,5 ‰ and coarser classes (2°C and 0,5 ‰) for the rest of the range. The volumes for each particular class were summed and the results were presented as a diagram of a bivariate distribution of volume with salinity and potential temperature as co-ordinates. Potential specific volume anomaly was represented by a curve on the diagram. Classes comprising 50 per cent and 75 per cent of the volume of the entire Pacific Ocean were enclosed in heavy and light boundaries, respectively. Totals summing the distribution by potential temperature alone were given of at the bottom and by salinity alone at the right. (See figure 4.1).

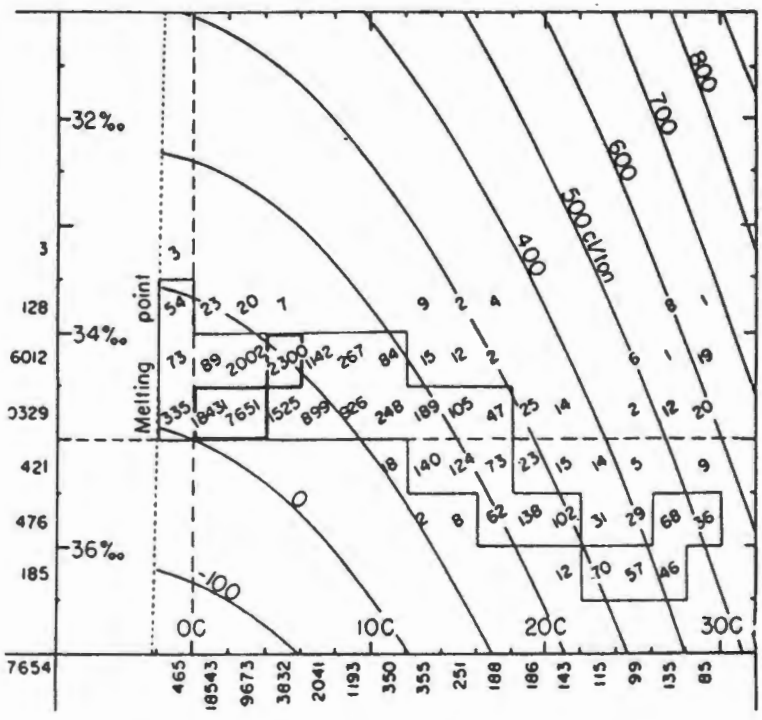

Figure 4.1 The bivariate distribution of volume in potential temperature and salinity co-ordinates for the Pacific Ocean. Sloping numbers give the volume of water in 10^4 km^3 units for each class of 2°C x 0,5 per mille. Sums at the bottom give the distribution by potential temperature alone, and sums at the left by salinity alone. The heavy boundary encloses classes comprising 75 % and the light boundary 99 % of the volume of the Pacific Ocean. Potential specific volume anomaly is represented by the curves (from Cochrane, 1958). Note the orientation of this diagram.

There are some specific differences between this method of Cochrane (1958) and the method applied by Montgomery (1958) in his volumetric analysis of the Atlantic Ocean. The volume which Montgomery considered, is the entire Atlantic Ocean and includes all tributary

seas. One hundred-and-five stations which were selected were distributed rather uniformly. The surface area of the Atlantic Ocean, taken as 106,2 x 10^6 km^2 (Stocks, 1938), was divided by the number of stations, so each station represented an area of about 10^6 km^2. Wherever possible, stations with gaps no greater than 500 m between samples or between the lowest sample and the sea bottom,were chosen.

Montgomery decided to adhere to values of potential temperature and salinity of actual samples (observations), thus avoiding all spatial and temporal interpolation of water characteristics. Because the sample-depths (observations) were not uniformly spaced in the vertical, each sample was weighted in proportion to the thickness of the layer represented. The layer was decided by midpoints between samples (the same as Cochrane's (1958) method). The volume assigned to each sample or temperature/salinity pair was the layer thickness to the nearest decametre (10 m) times 10^6 km^2, the horizontal area. This resulted in a volume unit of 10^4 km^3. The volume represented by each temperature/salinity pair (sample) is the weight or number of decametres times the volume unit.

This primary weighting resulted in a total Atlantic Ocean volume exceeding the actual volume considerably. This discrepancy mainly was due to the deliberate selection of deepest stations available. The weights were subsequently adjusted, where appropriate, so as to yield the correct volume of each tributary sea and of each 10° zone of the entire Atlantic. The volume of water in each bivariate class was determined by summation.

Like Cochrane (1958), Montgomery (1958) also presented his results by employing two sets of classes, a fine-scale class (0,5°C and 0,1 per mille) and a coarse-scale class (2°C and 1,0 per mille). The fine-scale class is the same in all three papers (Cochrane, 1958; Montgomery, 1958 and Pollak, 1958) as well as in Montgomery (1955). The coarse-scale class was applied to the entire range of potential temperature and salinity for the Atlantic Ocean. Thus, the densely populated area on the coarse-scale diagram is represented in greater detail by the fine scale class bivariate diagram. In a bivariate distribution a boundary to enclosing all classes of a certain and greater frequency (volume) can be drawn. Boundaries enclosing 50 percent, 75 percent and 99 percent respectively were drawn in the diagrams.

Pollak's (1958) study of the Indian Ocean is the third in the series of papers, the methodology of which is discussed here. In order to obtain results that would be comparable to those published for the other two oceans a sampling network of one station per 10^6 km^2 of surface area was selected in this instance. In some areas a denser network would have been possible while in other areas of the ocean even the minimum number of stations would have been unobtainable. Like the other two authors, Pollak (1958) selected as many stations as possible on the basis of reasonably uniform horizontal spacing and maximum depth. These were called primary stations and wherever an otherwise unused deeper station was located in the vicinity of such a primary station, its additional sampling depths were appended to the primary series. To compensate for the horizontal gaps in the data (network) it was assumed that any missing station could be represented by mean values of the nearest surrounding stations. Like

Montgomery (1958) in the Atlantic, vertically each observation (potential temperature/salinity pair) was weighted according to the half-distances to the next higher and lower sampling depths. The unit weight was 10 metres, making the volumetric unit $10^4 km^3$. A correction factor was applied to the weight of each observation on the basis of the average area enclosed by each depth zone (eg. 1000 - 2000 m) and on the number of stations providing observations in this zone. Consequently the sum of all weights (in volume units) equalled the total volume of the Indian Ocean (including the Red- and Andaman Seas and the Persian Gulf). As a result of the irregular geographical distribution and different depths attained, the station weights varied widely.

Two classes (with potential temperature (θ) and salinity co-ordinates) were employed by Pollak (1958). A fine-scale class (0,5°C and 0,1 per mille) in harmony with the other two papers and a coarse-scale class (0,5°C and 0,5 per mille). The weights of all observations in each class were summed thus giving the frequency of that class in terms of 10^4 km^3. Boundaries for 50 percent and 75 percent of the total volume were including on the fine-scale diagram as well as the customary potential specific volume anomaly curves. On the coarse-scale diagram Pollak included boundaries demarcating the major water masses (in these cases defined by depth, eg. surface water = surface to 200 m depth) which the others did not do.

There are a few important aspects of the analyses discussed above that have to be emphasized at this stage. All the above-mentioned authors discussed were emphatic that their results were only first approximations. Due to the paucity of stations, their work included data from all seasons. Cochrane's (1956) surface characteristic frequency distributions in the Pacific Ocean are exceptions. Although the surface layer is subject to seasonal changes, the upper 200 metres of the water column contains only about 5 percent of the total volume. Therefore this merging of all seasons does not do undue violence to the statistical results in their preliminary form. Furthermore, no attempt was made to take account of any other temporal variations. In the light of the total volume of the Indian-, Atlantic- and Pacific Oceans and the number of observations available at the time the magnitude of the unit volume (10^4 km^3) does not appear unduly large. Except for the total volume, all volumes presented are accurate to no better than a few percent. The insignificant digits were only retained for simplicity in accounting.

The results of all these authors were presented in diagrams with potential temperature and salinity as co-ordinates. The orientation of these diagrams (figure 4.1), which had potential temperature (θ) as abscissa and decreasing salinity as ordinate, meant a rotation of the usual potential temperature-salinity diagram through 90 degrees. This orientation is apparently advantageous for plotting station curves (Montgomery, 1954).

Wright and Worthington (1970) did a volumetric census of the North Atlantic using a much higher density of observations (a density not attained in any other ocean at that stage) than Montgomery (1958), Cochrane (1958) and Pollak (1958). An example of the effect the denser distribution has on the results is that in the latter authors' studies a station on average represented about 4 200 000 km^3 of volume whereas in the case of Wright and Worthington the

volume per station ranged from 85 000 km^3 (denser distribution of stations) to 300 000 km^3. A much finer class interval was possible in the frequency diagrams mainly due to the greater number of good deep stations and the introduction of the conductivity salinometer. The class intervals were 0,1°C (θ) and 0,01‰ compared with the finest scales of 0,5°C and 0,1‰ of Montgomery, Cochrane and Pollak. Wright and Worthington (1970) divided the North Atlantic into areas of 1 degree of latitude by 1 degree of longitude (called one-degree squares). A depth then was assigned to each one-degree square. The maximum depth of the deepest station within that square was usually taken and in the cases of squares with no stations, the depths were taken from bathymetric charts. Each one-degree square was then assigned to a station, usually the nearest station that was deep enough. The average was 6 squares per station.

For each station the depths between successive isotherms and isohalines were taken from temperature-depth and salinity-depth traces. Extrapolation was used where necessary to reach the greatest depth assigned to the station. Subsequently the volume of each interval was obtained by multiplying the depth first by the number of squares assigned to that station and then by the area of a degree square of the appropriate latitude. The resulting volume was rounded off to 0,1 x 10^3 km^3. A volumetric temperature-salinity diagram for each five-degree-square was prepared and these were summed to produce a grand total for the entire North Atlantic. Wright and Worthington (1970) also divided the North Atlantic into warm water and cold water provinces (4° θ being the dividing isotherm) and prepared volumetric diagrams for each. Boundaries containing 50 per cent, 75 per cent and 90 per cent of the frequency (volume) were drawn on the diagrams as well as specific volume anomalies represented as curves.

Wright and Worthington's method differs from that of Cochrane (1958) and his collaborators in that the latter used potential temperatures throughout while the former only used it in cold water. The use of interpolated values (temperature-depth and salinity-depth curves) instead of observed values only, gave smoother results and made the finer scale possible. Results were presented on diagrams with the more standard orientation of salinity as abscissa and temperature as ordinate. The data used for their analysis spanned 9 years.

Sayles, Aagaard and Coachman (1979) presented volumetric potential temperature-salinity diagrams for the Bering Sea basin for summer, winter and autumn in their Atlas of the Bering Sea Basin. These diagrams were modelled after those of Cochrane (1958), Pollak (1958) and Montgomery (1958), but on a finer scale. The class intervals were 0,1°C (θ) and 0,02 ‰ for potential temperature (θ) and salinity ranges of -2,0°C to 10°C and less than 32,12 ‰, respectively. The basin was divided into grid areas of 1° latitude by 2° longitude. Only stations executed after 1949 that extended deeper than 500 m (to provide continuity between upper and deeper waters) were selected. The stations were subjected to a quality screening (especially for salinity accuracy). This volumetric census was limited to the upper 1500 m of the water in the basin. Although modelled on Cochrane, Pollack and Montgomery's diagrams these diagrams were oriented according to the normal convention.

Sayles, Aagaard and Coachman (1979) were the first to display the results of their volumetric census not only as two-dimensional bivariate θ-S diagrams, but also as three-dimensional plots with the z-axis representing volume. The highest volume is represented by the biggest peak. Not only did this portrayal place the results in a new visual perspective, but Sayles, et al. also enhanced the usefulness of the three-dimensional diagram further by rotating it through 180 degrees. This allowed viewing from two perspectives (both being centered at the middle of the salinity range): one looked towards higher temperatures (view from cold side) and the other towards lower temperatures (see figure 4.2).

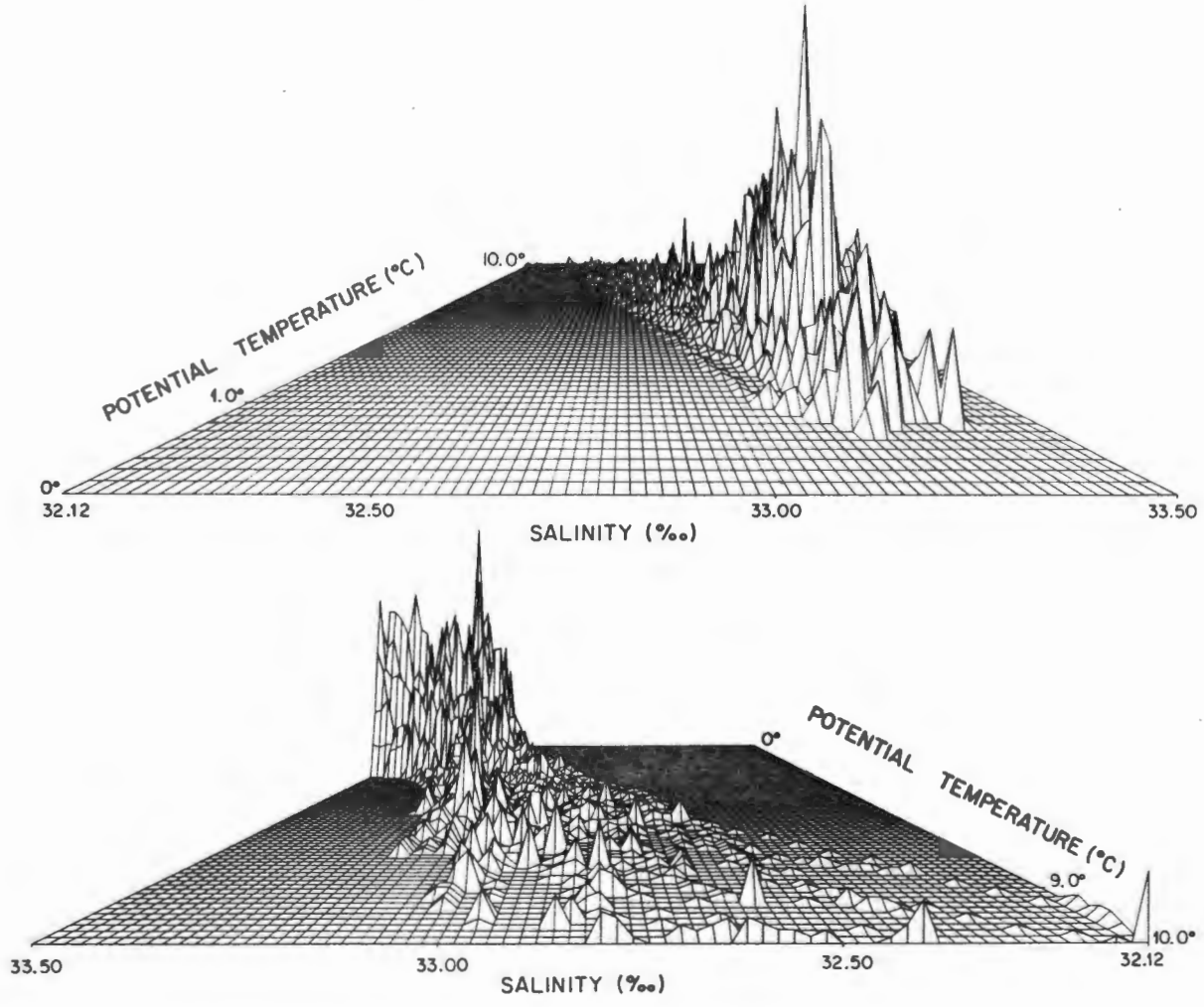

Figure 4.2 An example of a three-dimensional potential temperature/salinity volumetric diagram. Apparent elevation is proportional to volume. The top panel provides a perspective view towards higher temperatures of the volumetric distribution (of summer upper waters in the Bering Basin), while the lower panel provides a perspective view towards lower temperatures of the same distribution (after Sayles, Aagaard and Coachman, 1979).

Carmack and Aagaard (1977) applied the volumetric method to synoptic data in the upwelling region of the Benguela system. A weight factor system to determine the area represented by each station was used. In the vertical, parameters were interpolated at one metre intervals to determine the thickness of water in the specified bivariate class intervals. The class

intervals used for the temperature-salinity volumetric diagram was 1,0°C and 0,05 ‰. A very significant aspect of the above authors' work is that they employed parameters other than T/S in their volumetric study eg. phosphate and nitrate or temperature and phosphate were used as co-ordinates. This was possible because they used synoptic data. Any two characteristic parameters of sea water can be used to produce a volumetric diagram but since hydrographic data collected over several years are usually grouped together for this purpose, the two conservative characteristics of sea water (temperature and salinity) traditionally were used. Carmack and Aagaard (1977) emphasized the usefulness of volumetric calculations, apart from water mass description and quantification, in obtaining a spatial mean value of the strichiometric ratio, since the nutrients relationships were weighted by volume rather than by number of observations.

The most comprehensive volumetric analysis of the world ocean to date is probably that of Worthington (1981). He divided the ocean into areas of 5° latitude by 5° longitude (conveniently called 5°-squares). His data source was all the high quality hydrographic stations available from the National Oceanographic Data Centre (NODC) before June 1977. He selected one station per 5°-square. If no station was available for a particular square, that square was not included in the volumetric analysis. If a selected station did not pass Worthington's stringent quality control test it was rejected. For instance, potential temperature-salinity diagrams were plotted using only those deep hydrographic stations of the NODC that recorded salinity to three places. If the scatter of prints on any station in the deep water was more than about ±0,001 ‰, the station did not qualify. Deep stations were considered as stations that extended to 90 % of the water depth. Another, less stringent criterion was that bottle spacing be sufficiently close so that an unambiguous T/S curve could be drawn. Class intervals of 0,1°C and 0,01‰ were employed.

The following, very important, assumption of Worthington has to be born in mind when comparing results. If for example only 30 per cent of the 5°-squares of an ocean were represented by stations it was assumed that the remaining 70 % were divided into the same T/S classes. So totals of volume were calculated on the basis of the area (or number of 5° squares) of the ocean. Consequently a volume of 18 x 10^6 km^3 for a particular T/S class interval could be reported based on only 6 x 10^6 km^3 (30 per cent) actually observed.

4.2 Benguela Upwelling system

The geographic area, off the South African west coast, selected for the volumetric pilot study of this investigation stretches from 20° to 36° south and from 8° to 20°E. This area lies within the accepted boundaries of the South-East Atlantic upwelling system (Nelson and Hutchings, 1983, Van Foreest et al. 1984).

Hydrographic data from the South African Data Centre for Oceanography (SADCO) were used for this analysis. All the data (which were quality checked and stored by SADCO),

spanning the period 1921 - 1982 were used for the temperature/salinity (T/S) analysis, while a subset of selected stations was used for the volumetric analysis.

For the T/S relationship investigation, three generic areas relating to coastal upwelling (according to criteria set out by Lutjeharms and Stockton, 1987) were selected. These are: the area inshore of the 200 m isobath, which represents the area of consistent, contiguous upwelling; the open-ocean domain in which there is insignificant direct influence of coastal upwelling: and the mixing zone with filaments and mesoscale circulation features of the upwelling front, in between.

The volumetric analysis was carried out on an area stretching only to 12°E in the west. This was divided into 1 degree-squares (1 degree of latitude by 1 degree of longitude). One station per degree-square was selected as representative of that square. Criteria for this selection were: that all the measured parameters (including temperature and salinity) had to have been measured over the full depth range of the station; deepest stations were preferable, and vertical proximity and higher density of readings received preference. If by these criteria more than one suitable station was available per square, the one closest to the centre of that square was selected. If no suitable station in any particular square was available, that square was not represented and, therefore, not used in the calculations to determine the overall volume. The absolute area per square varies between 11 565 km^2 in the north to 10 053 km^2 in the south. For those stations closer to shore, where the square intersects the coastline, the actual surface area of ocean represented by the station was calculated.

Class intervals used for this study were 0,10‰ for salinity and 0,5°C for temperature. Bivariate diagrams with estimates of the volume of water in each class interval, were produced for the correlations of temperature and salinity to three different depths i.e. 100, 500 and 1000 metres. Observed and interpolated values were used. A Lagrangian 3-point method was used for the interpolation. In this case temperature and not potential temperature was used for the correlation diagrams.

4.3 Agulhas Retroflection Area

For this particular study the Retroflection area not only includes the geographical area generally associated with the retroflection of the Agulhas Current, but also the lower part of the Agulhas Current system. The area stretches from 33° to 45° south and 6° to 27° east. Only conductivity-temperature-depth (CTD) stations from the following cruises were considered for this analysis:

(i) AJAX Expedition (leg 1): October -November 1983 - R.V. Knorr

(ii) Agulhas Retroflection Cruise (ARC): November - December 1983 - R.V. Knorr

(iii) Marathon Cruise (legs 11 and 12): February - March 1985 - R.V. Thomas Washington

(iv) Agulhas Retroflection Zone (ARZ) cruise: February 1987 - R.V. Discovery

(v) Subtropical Convergence and Agulhas Retroflection Cruise (SCARC): February - March 1987 - R.V. S.A. Agulhas.

For a list of all the stations that were used for this analysis see table 4.1 in Addendum I.

The data were collected over a period of three and a half years, which represents the shortest time span ever employed for a general volumetric survey over a significant geographical area. All the data were also collected with a particular type of instrument, namely a Neil Brown Mark III CTD. The sensors on these instruments were calibrated (for details of the calibrations see the Data Reports of the mentioned cruises: Camp et al., 1987; Read et al., 1987; Valentine et al., 1988 and Anon, 1985) and the data were then adjusted accordingly.

These instruments are capable of very precise measurements. For example, temperature is theoretically accurate to three decimals; conductivity to four decimals and pressure to within 0,1 decibar of the desired levels. Salinities are calculated from the conductivity, pressure and temperature using UNESCO (1983) algorithms.

The CTD has considerable advantages over the Niskin and/or reversible bottles that were used to collect data for most of the volumetric analyses discussed above. A major advantage over the bottle data method is the determination of salinity. The requirement of this study was that salinity (conductivity) was recorded to at least three decimal places. These figures were then rounded off to two decimal places. This requirement was met easily by the CTD. Worthington (1981) who had the same requirement for salinity had to, on occasion, exclude whole cruises from his data set because a particular ship had measured salinity wrongly. He used the very tight potential temperature-salinity correlations of all deep masses in the world ocean as a standard in selecting station for his analysis. For earlier volumetric studies salinometers were not even in existence and salinity had to be determined by chemical titration.

Another big advantage of the CTD is the sampling rate. With bottle samples taken at discrete depths the boundaries between water masses and, therefore, the thickness of water masses could not be determined accurately. With the sampling rate of the CTD of 31 frames per second (= 31 sets of measurements) and the standard lowering rate of 1 metre per second, the thickness of different water masses can be determined very accurately.

One metre vertical intervals were selected for the volume calculations. Because of the extremely high sampling rate of these instruments, no interpolation between observed depths was necessary. Observed depths were rounded off to the nearest metre where necessary. Only observed values were considered and no attempt was made to extend the depth of shallower stations by either extrapolation or weighting factors. The above factors make this data set the most uniform yet employed in a volumetric analysis. Although the vertical resolution is the finest ever used in a volumetric analysis, the potential of this data set has not been exploited to the full. The vertical resolution could have been an order finer if so desired.

The selected data set was divided into two for the volume calculations. First, only bottom stations, i.e. only those stations that measured the entire water column, down to the ocean bed were used. The distance between the deepest and the bottom observation ranges from less than five metres to seventy metres. The station with the largest distance between the deepest observation and the bottom still sampled 93 per cent of the water column. Second, stations that sampled at least the upper 1 500 m of the water column were used for the other set of calculations.

One station per degree-square was selected as representative of that particular square. Because all the stations were virtually on a par as far as quality control was concerned, the station closest to the centre of the degree-square was selected. Since there were more stations that measured up to 1 500 m than bottom stations, the former represented a better coverage of the geographical area (see figures 5.10 and 5.11). The more dynamic part of the water column is sampled more intensively than the deep waters. Experience has shown that all the deep water masses of the world ocean have a very tight potential temperature-salinity correlation. Squares that were not represented by a station were not considered for this analysis.

A volumetric census or analysis estimates the amount of water in each class interval of a bivariate correlation diagram. I have chosen the two more conservative characteristics of seawater, namely temperature and salinity. Potential temperature instead of *in situ* temperature was used. Parameter values at one metre intervals were used to determine the thickness of water in specified bivariate class intervals. The size of the class intervals is an important consideration in volumetric analysis. Class intervals should be significantly larger than the accuracy of the measurements. They should be small enough to maintain the integrity of the water mass identification (provide the signal), yet large enough to filter spatial variability and yield a concise volumetric diagram (suppress the noise) (Carmack and Aagaard, 1977). Class intervals used for this study were 0,01 practical salinity units (psu) for salinity and 0,1°C for potential temperature.

The results of these analyses are presented and discussed in the next chapter.

CHAPTER 5

RESULTS AND DISCUSSION

5.1 The Benguela Upwelling System

Carmack and Aagaard (1977) have already demonstrated that a volumetric census is highly applicable to an upwelling region, enhancing the understanding of both the physical and biochemical aspects involved. This was therefore part of the motivation to choose the Benguela upwelling region as the subject of this pilot study (Lutjeharms and Valentine, 1987).

5.1.1. Temperature/salinity relationships

The T/S scattergrams based on historic hydrographic data for the three different oceanic regimes (figure 5.1; Lutjeharms and Stockton, 1987) show notably different distributions of data points (figure 5.2). The first diagram (figure 5.2a) represents stations well outside any influence of upwelled water and is taken as representative of the open ocean domain. The T/S curve show the classical distribution of water masses for this part of the Atlantic Ocean. Atlantic Subtropical Surface Water (35,30-35,70 ‰) makes up the upper part of the water column. This overlies the South Atlantic Central Water (SACW). The latter is represented by the linear section of the T/S plot; 7°-14°C and 35,50-35,30 ‰. This in turn overlies the Antarctic Intermediate Water (AAIW) at ~4°C and 34,35 ‰ which represents the salinity minimum section of the T/S curve. Underlying the intermediate waters, are the deep water masses, in this case North Atlantic Deep Water at ~2°C and 34,85 ‰, at the salinity maximum section of the T/S curve. At temperatures below about 2°C is the dense Antarctic Bottom Water. No Antarctic Bottom Water was present in the mixing domain (figure 5.2b) while in the upwelling domain only surface water and Central Water (though modified) were present. The latter is not unexpected because the core of the AAIW in the South East Atlantic Ocean is generally expected to be at about 750 m depth (Shannon and Hunter, 1988). The upwelling domain is more or less restricted to the continental shelf.

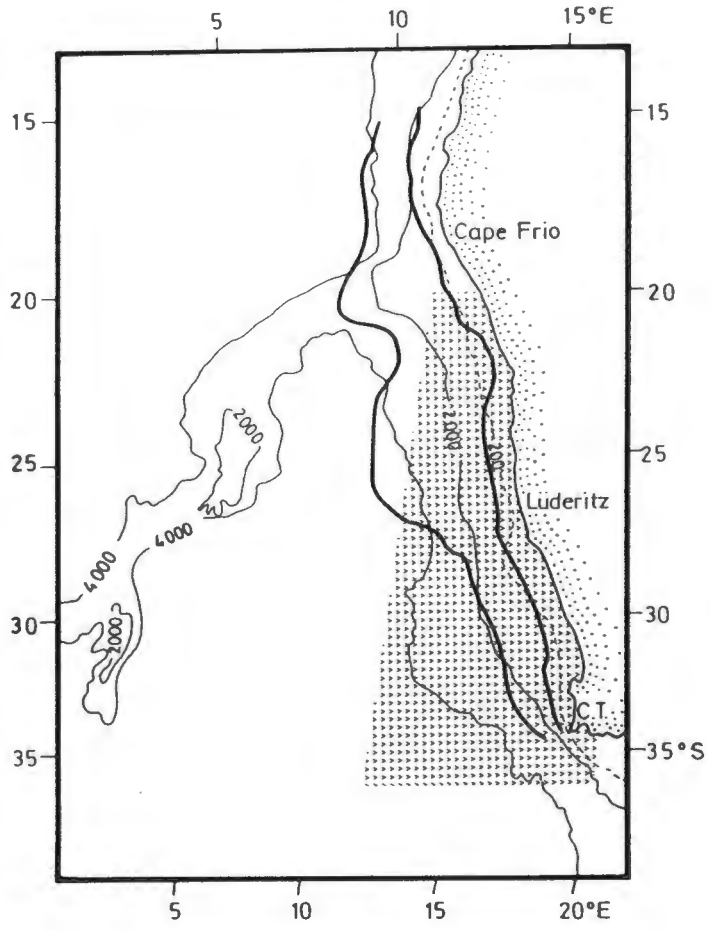

Figure 5.1 Geographic subdivision of the South-East Atlantic Ocean into an upwelling area adjacent to the coast, a pure oceanic regime in mid-ocean and a filamentous mixing domain between the former two (after Lutjeharms and Stockton, 1987). The shaded area represents the area of the volumetric pilot study. The bottom topography in metres are according to Simpson (1974).

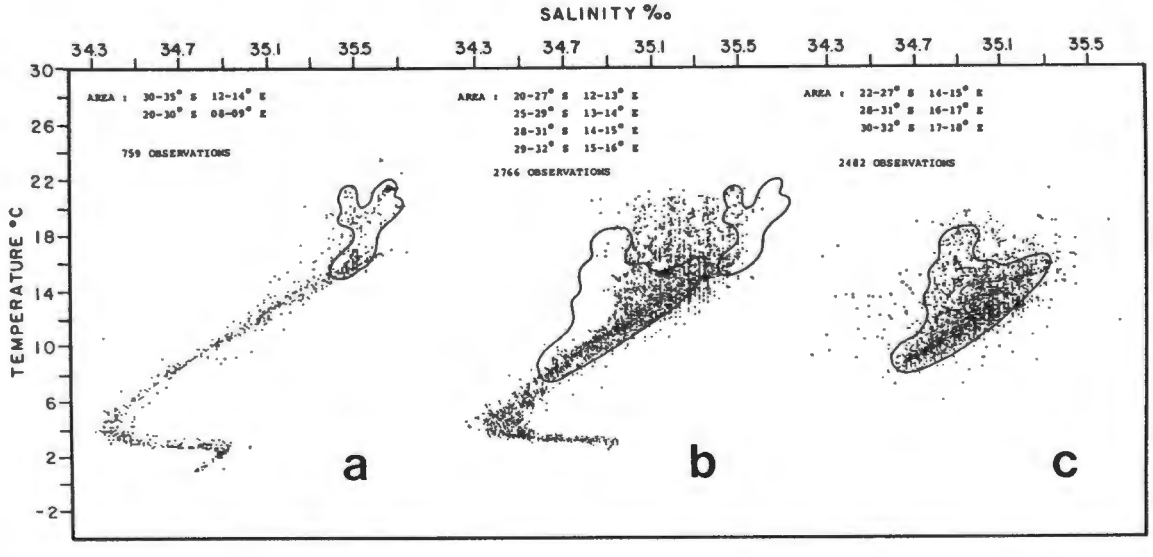

Figure 5.2 Temperature/salinity (T/S) scatter diagram for selected stations lying in (a) the oceanic, (b) the mixing and (c) the upwelling domains of the South-East Atlantic Ocean, as defined in figure 5.1. To facilitate comparison, outlines of the highest concentrations of data points in the upper 300 m of the oceanic and upwelling domains have been superimposed on (b) (from Lutjeharms and Valentine, 1987).

The water in the upper 300 meters of the water column, has on the whole temperatures higher than 15°C and salinities in excess of 35,30 ‰. The main concentration of points in T/S space of this water layer has been outlined in figure 5.2a. This demarcation may be subjective but this is insignificant, because it only serves to focus attention on concentrations in different T/S space. In contrast to the surface water of the South-East Atlantic open-ocean domain the waters involved in the full upwelling domain (basically the waters on the shelf) are considerably less saline (figure 5.2c). The main concentration of points is again outlined. It lies more or less between 34.60 ‰ and 35.30 ‰. The temperature of this water ranges between 8° and 18°C which implies that the greater part of the South Atlantic Central Water is involved in the upwelling and, that upwelled water observed may have been in various stages of warming. The broadening of the Central Water core in the upwelling regime is not only due to the larger number of observations (figure 5.2c) therefore picking up more outliers. This broadening has also been described previously by Stander (1964), Nelson and Hutchings (1983) and Shannon (1985) and is due to a noticeable salinity shift in the Central Water on moving equatorward.

By its nature, one would expect the mixing domain lying between the upwelling zone and the open ocean zone to exhibit T/S characteristics lying between those of the other two zones. This is indeed so (figure 5.2b). Since the stations used for this T/S plot covered the full meridional range of this mixing domain the width of the Central Water core which demonstrates the salinity shift is more obvious. (See section 5.2 for more details of the Central Water). Vertical offsets from the linear Central Water line in T/S space, which indicate warming of upwelled water are found between about 35,00 and 35,50 ‰. This fact demonstrates the considerable overlap between the mixing domain (figure 5.2b) and the open ocean (figure 5.2a) on the one side and the upwelling domain (figure 5.2c) on the other side. The warm most saline water of the open ocean domain is excluded from the upwelling process. This water may include inflow of Indian Ocean surface water via Agulhas filaments (Lutjeharms and Stockton 1987) or Agulhas rings and eddies (Lutjeharms and Gordon, 1987; Olson and Evans, 1986) (see section 5.2).

Also noteworthy is the fact that no upwelled water from the deeper parts of the Central Water i.e. below 12°C, 34,90 ‰, was found in the mixing domain. This implies that, although a substantial portion of the upwelled water may be advected out of the upwelling domain (into the mixing zone) as filaments of colder water driven by wind stress (Lutjeharms and Stockton, 1987), upwelled water from greater depths is not involved in this process. Another noteworthy observation from the T/S scattergram (figure 5.2b) is that all upwelled water present in the mixing domain, no matter from what part of the Central Water it is derived from, is eventually heated to a maximum of 23°C and no more. This could be an upper thermal boundary dependant on a dynamic interaction between insolation and average ocean-air interaction.

T/S scattergrams thus demonstrate that distinct and recognizable oceanic regimes do exist in the South-East Atlantic ocean, regimes which may be dominated by different driving forces.

5.1.2 Volumetric relationships

The volumetric analysis was carried out on a smaller geographic area than described above due to a lack of suitable stations. This analysis is also not divided into three geographic areas to coincide with the oceanic domains of Lutjeharms and Stockton (1987) (referred to above), but into three depth ranges namely 0-100 metres, 0-500 m and 0-1000 m and are portrayed in figures 5.3, 5.4 and 5.5.

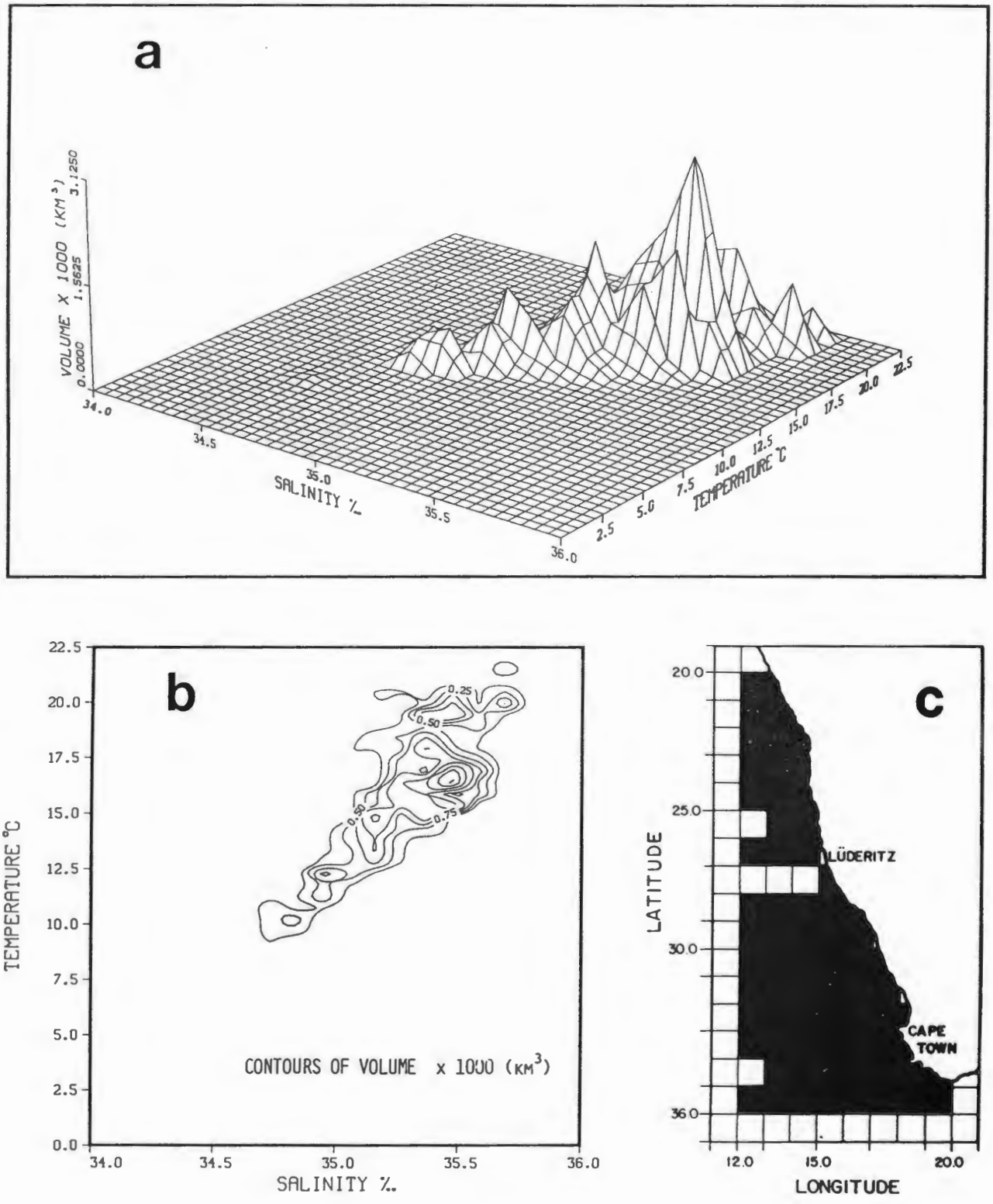

Figure 5.3 Volumetric analysis of water masses in the upper 100 m of the South-East Atlantic Ocean - (a) three-dimensional volumetric portrayal, (b) volume contours in T/S space, (c) 1° x 1° geographic areas (black) from which, in each case, one station was used (from Lutjeharms and Valentine, 1987).

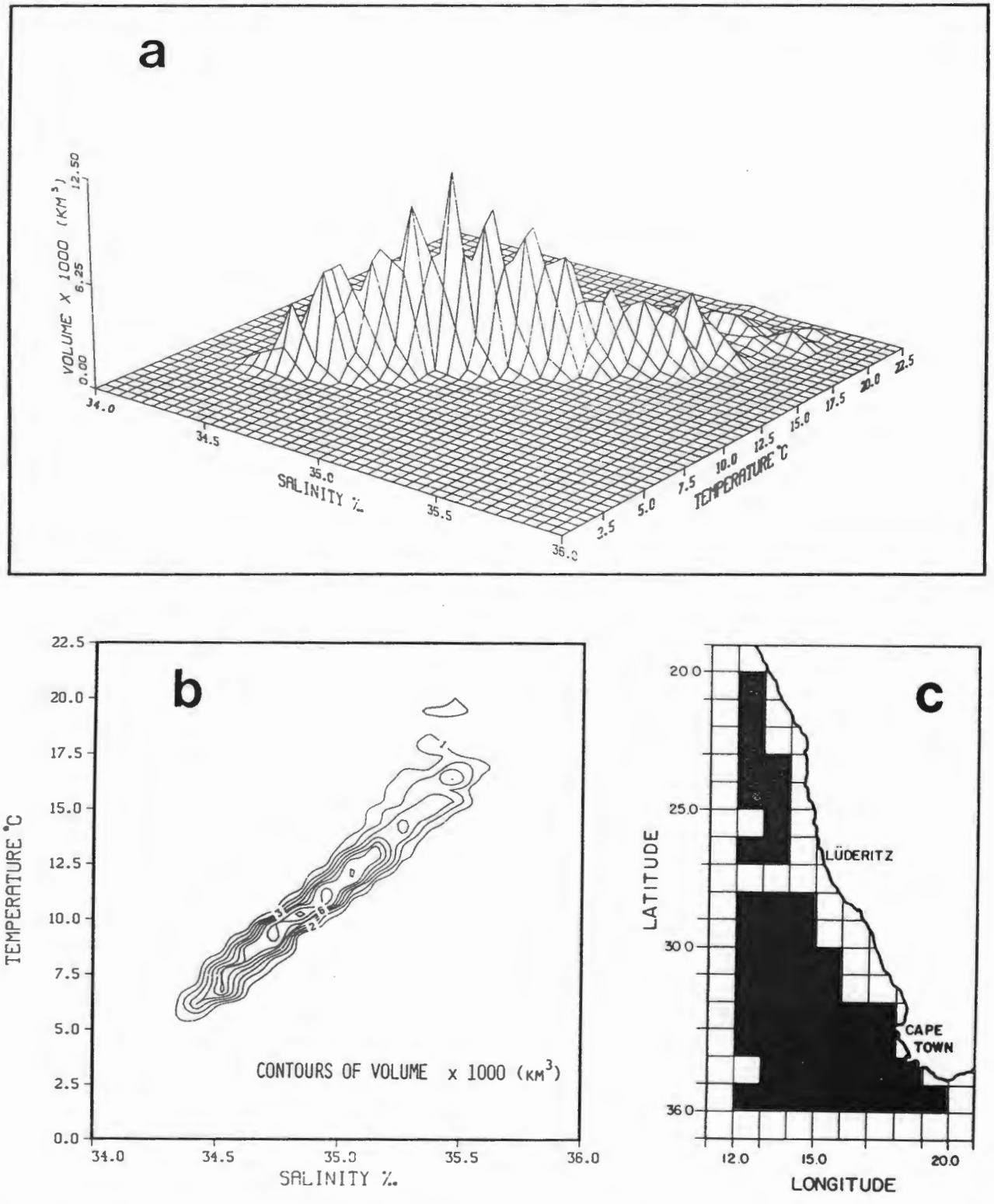

Figure 5.4 Volumetric analysis of water masses in the upper 500 m of the South-East Atlantic Ocean - (a) three-dimensional volumetric portrayal, (b) volume contours in T/S space, (c) 1° x 1° geographic areas (black) from which, in each case, one station was used (from Lutjeharms and Valentine, 1987).

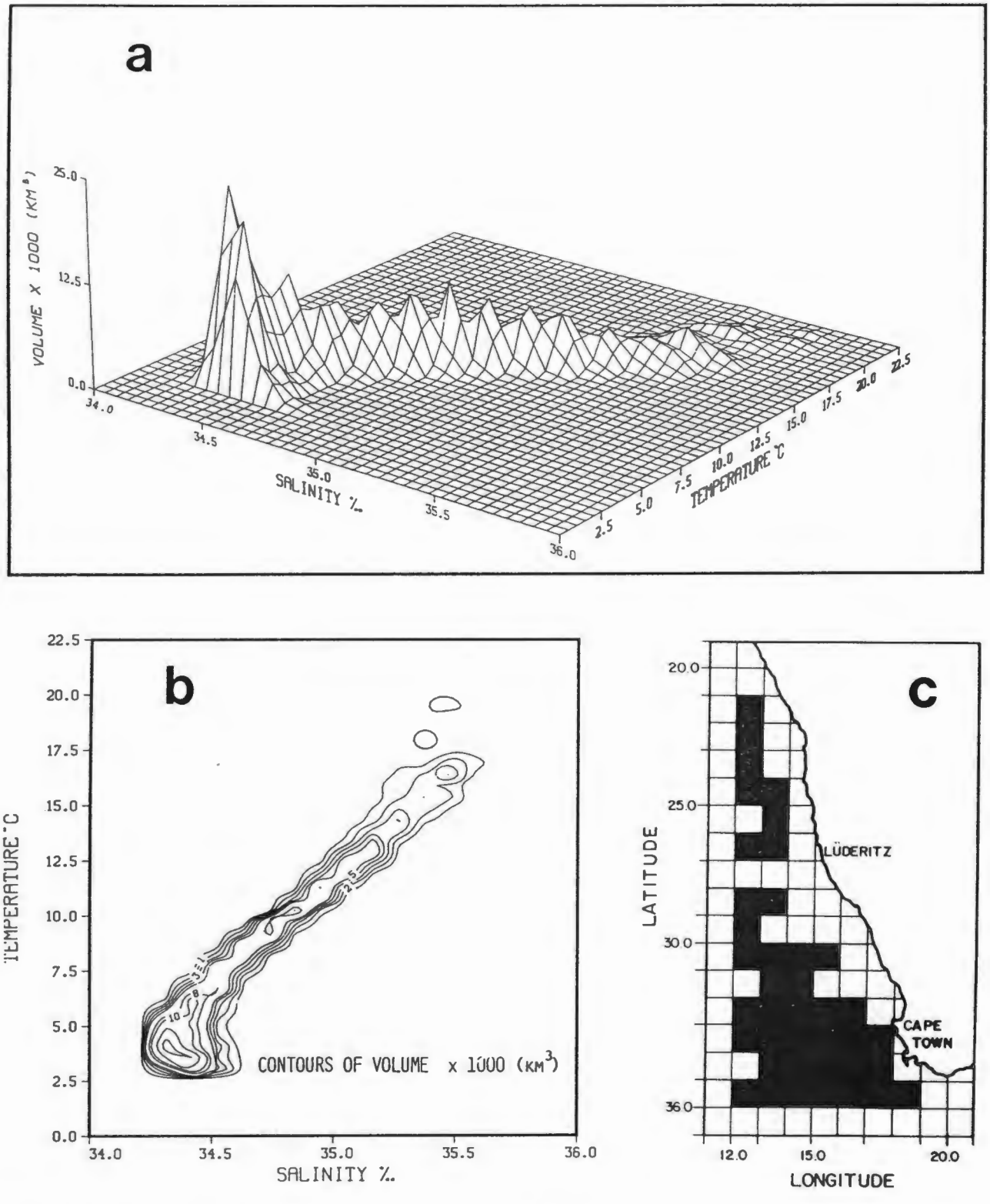

Figure 5.5 Volumetric analysis of water masses in the upper 1000 m of the South-East Atlantic Ocean - (a) three-dimensional volumetric portrayal, (b) volume contours in T/S space, (c) 1° x 1° geographic areas (black) from which, in each case, one station was used (from Lutjeharms and Valentine, 1987).

With the exception of only five one-degree-of-latitude by one-degree-of-longitude squares, the stations selected for the volumetric analysis of the upper 100 m covered the full geographic area from 20° to 36°S and from 12° to 20°E. No suitable stations could be found in those five one-degree-squares. The highest volume or volumetric core of the water lies between 15° and 21°C and 35,20 and 35,60 ‰ (figures 5.3b, 5.7). This area in T/S space overlaps both the South Atlantic Subtropical Surface Water (figure 5.2a) and the surface water present in the mixing domain (figure 5.2b). The peak in the three dimensional bivariate diagram (figure 5.3a), however, indicates that the greatest volume of water has salinities in excess of 35,40 ‰ and that it is therefore pure South Atlantic Subtropical Surface Water. This is not entirely unexpected because the major part of the geographic area used (figure 5.3c) is presumed to experience no influence of upwelled water at the sea surface. Two smaller peaks are evident at temperatures in excess of 19°C (figure 5.3b). The larger of these peaks is partially obscured in figure 5.3a. The smaller of these two peaks lies at 35,70 ‰ and may represent Agulhas Current water penetration into the South-East Atlantic Ocean.

The only other volumetric study in the upwelling area with which these results can be compared is that of Carmack and Aagaard (1977). Their information is derived from one cruise only on the continental shelf. They show (figure 5.6) that the primary mode in the upwelling regime represented water from the depth of upwelling, i.e. 10-11°C and 34,90 - 34,95 ‰. Such water forms a very minor part of the overall volume in the upper 100 m of the South East Atlantic Ocean as a whole (figures 5.3b and 5.7), but it falls well within the core of the water type involved in upwelling (figure 5.2c). The distribution of all water observed on this occasion (Carmack and Aagaard, 1977) (figure 5.6) is therefore in good agreement with that observed with the historical data and shown here (figure 5.2c).

Because the depths of the Argo stations used by Carmack and Aagaard (1977) ranged from less than 50 metres to more than 300 metres a direct comparison between their volumetric results and those of any one of the three depth ranges employed in this study is not straight forward. Furthermore they used a smaller salinity class interval (0,05 ‰) than this study (0,10 ‰) but a larger temperature interval (1,0°C) than this study (0,5°C). The results from the first depth range (0-100 m) (figures 5.3a and 5.7) should logically be the best to be compared to Carmack and Aagaard's (1977) results as both studies include the water on the shelf. (Bearing in mind though, that the Carmack and Aagaard study only include stations on the shelf while this study also include stations off the shelf and from the open domain). Carmack and Aagaard's primary mode water on the volumetric T/S diagram made up 11% of the total volume (figure 5.6). The primary mode on the volumetric T/S diagram (figure 5.7) for the upper 100 m of the water column (figure 5.3) makes up, in comparison, only 5% of the total volume (bearing in mind the difference in class intervals). It is also much warmer and more saline (16,0 - 16,5°C and 35,4-35,5 ‰) and less dense than the mode of Carmack and Aagaard because it include warm, saline surface water of the South East Atlantic. The water falling within the 45 % frequency boundary is without exception less dense than 26,50 σ t (figure 5.7) while in the Carmack and Aagaard study it is exclusively more dense than 26,50 σ t (figure 5.6). This may

be attributed to the fact that the pilot study area extends much further south (20-36°S) compared to that of Carmack and Aagaard (20-26°S) and is therefore much closer to the influence of the Agulhas Current (filaments, eddies and rings leaking into the South Atlantic). Surface water from Agulhas Current origin is warmer (~16-26°C) and more saline (>35.50 ‰) than the Atlantic Subtropical Surface Water. Another factor can be the data used. This study included stations done over several years with no bias towards a particular season, while Carmack and Aagaard's stations were done in October which fall well within the active upwelling season.

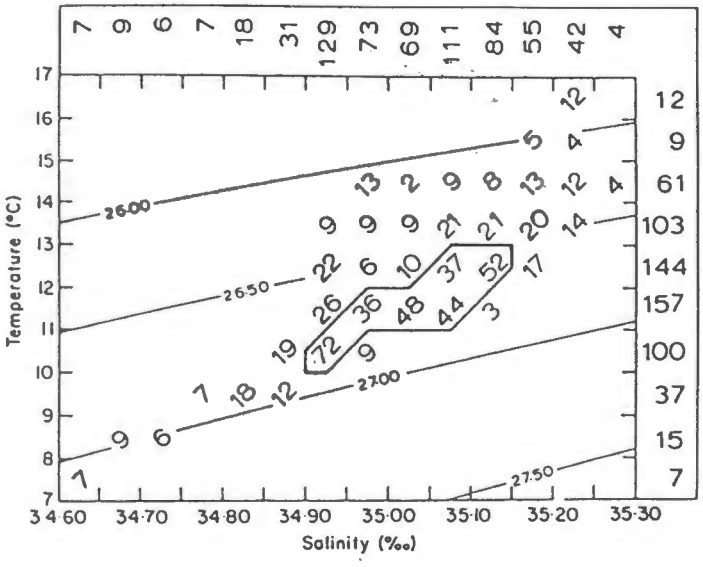

Figure 5.6 Temperature-salinity bivariate volumetric diagram for the stations occupied by the R.V. Argo (October 1968). Volumes are in 10 x km^3 units. Univariate distributions are given by the sums at the top (salinity) and the right (temperature) of the diagram. The 45 % frequency boundary is denoted by the heavy border (from Carmack and Aagaard, 1977).

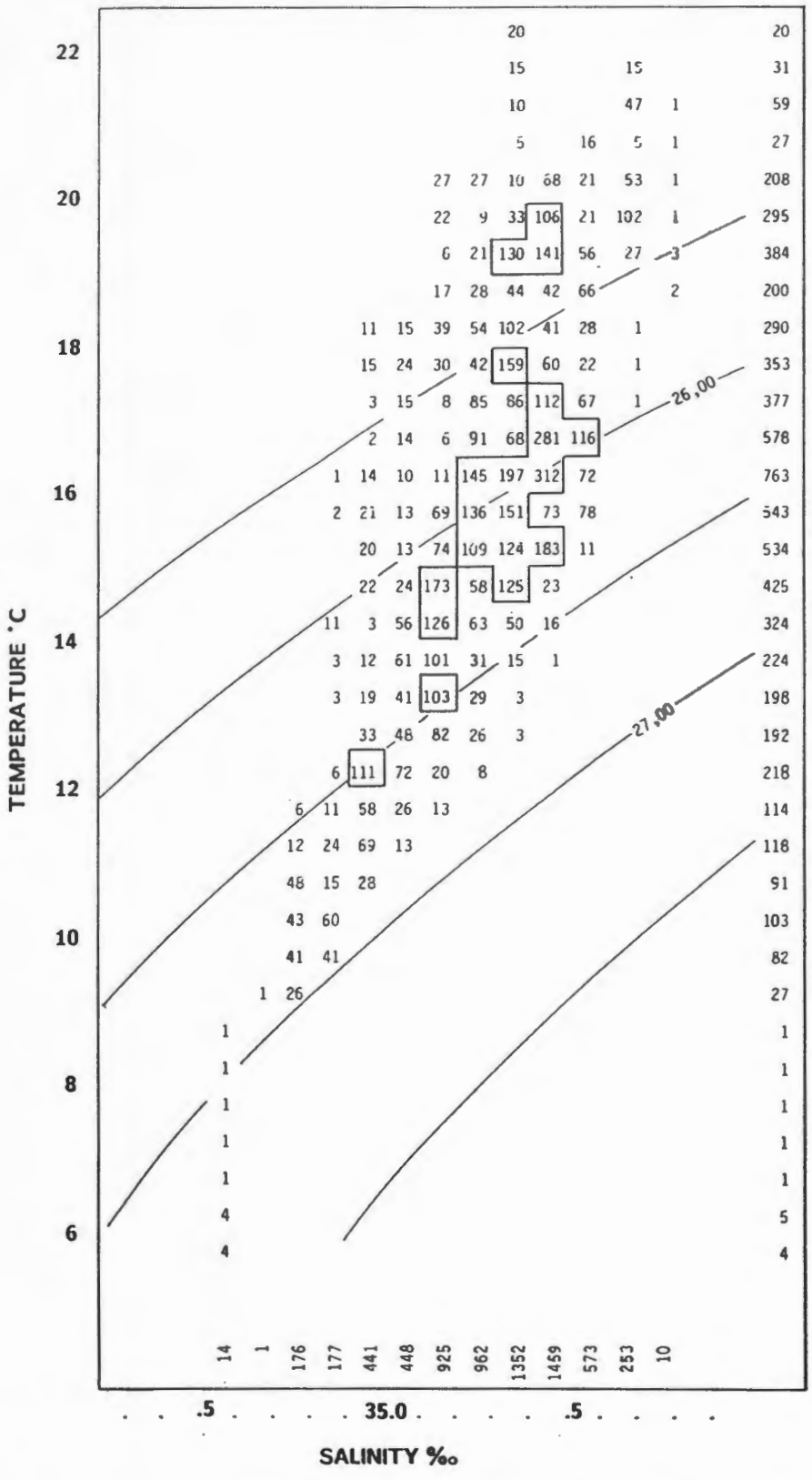

Figure 5.7 Bivariate volumetric diagram for the upper 100 m of the water of the pilot study area. Volumes are in 10 x km^3 units. Univariate distributions are given by the sums at the bottom (salinity) and the right (temperature) of the diagram. The heavy border denotes the 45 % frequency boundary.

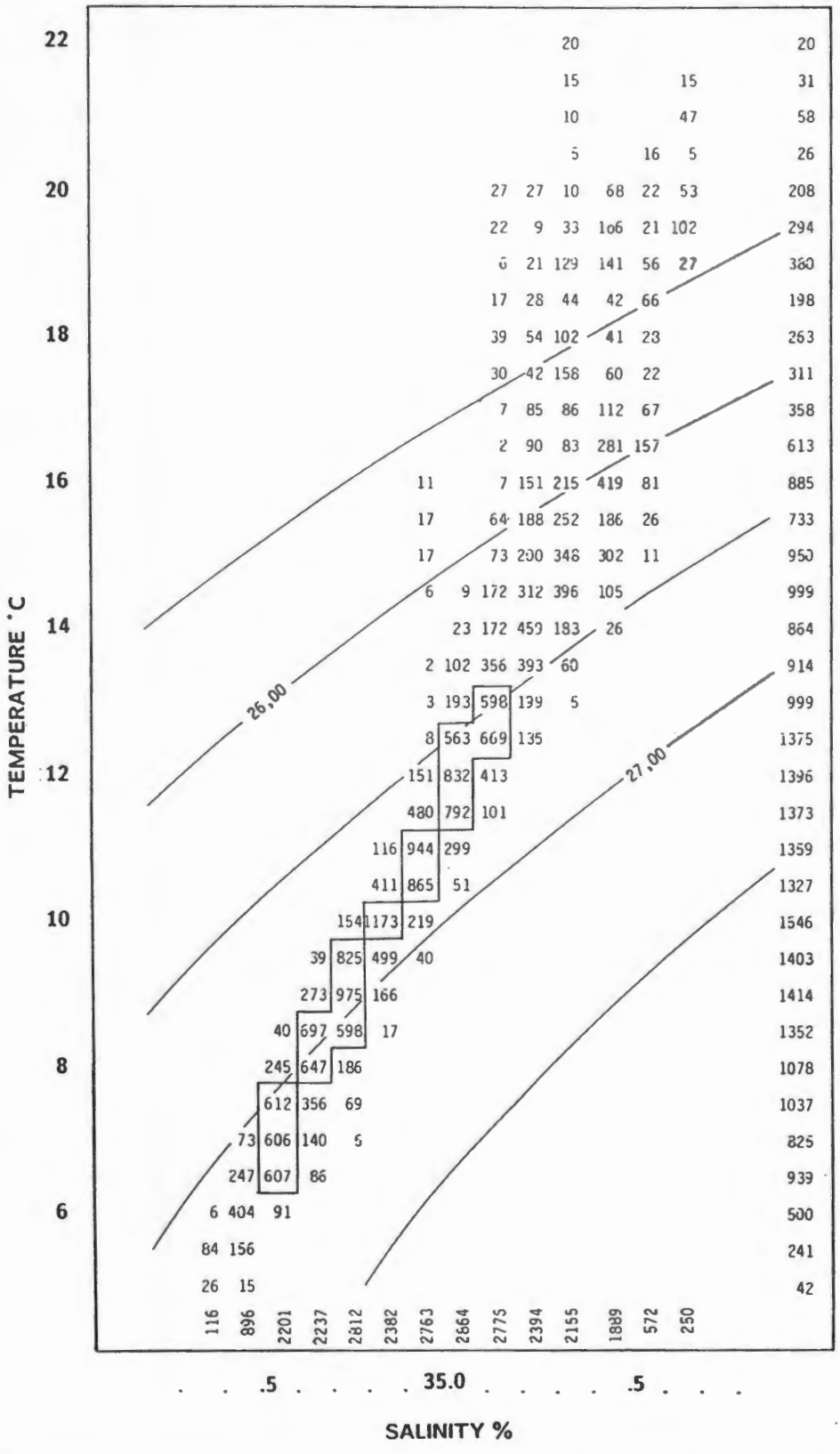

Figure 5.8 Bivariate volumetric diagram for the upper 500 m of the water of the pilot study area. Volumes are in 10 x km^3 units. Univariate distributions are given by the sums at the bottom and the right of the diagram. The heavy border denotes the 45 % frequency boundary.

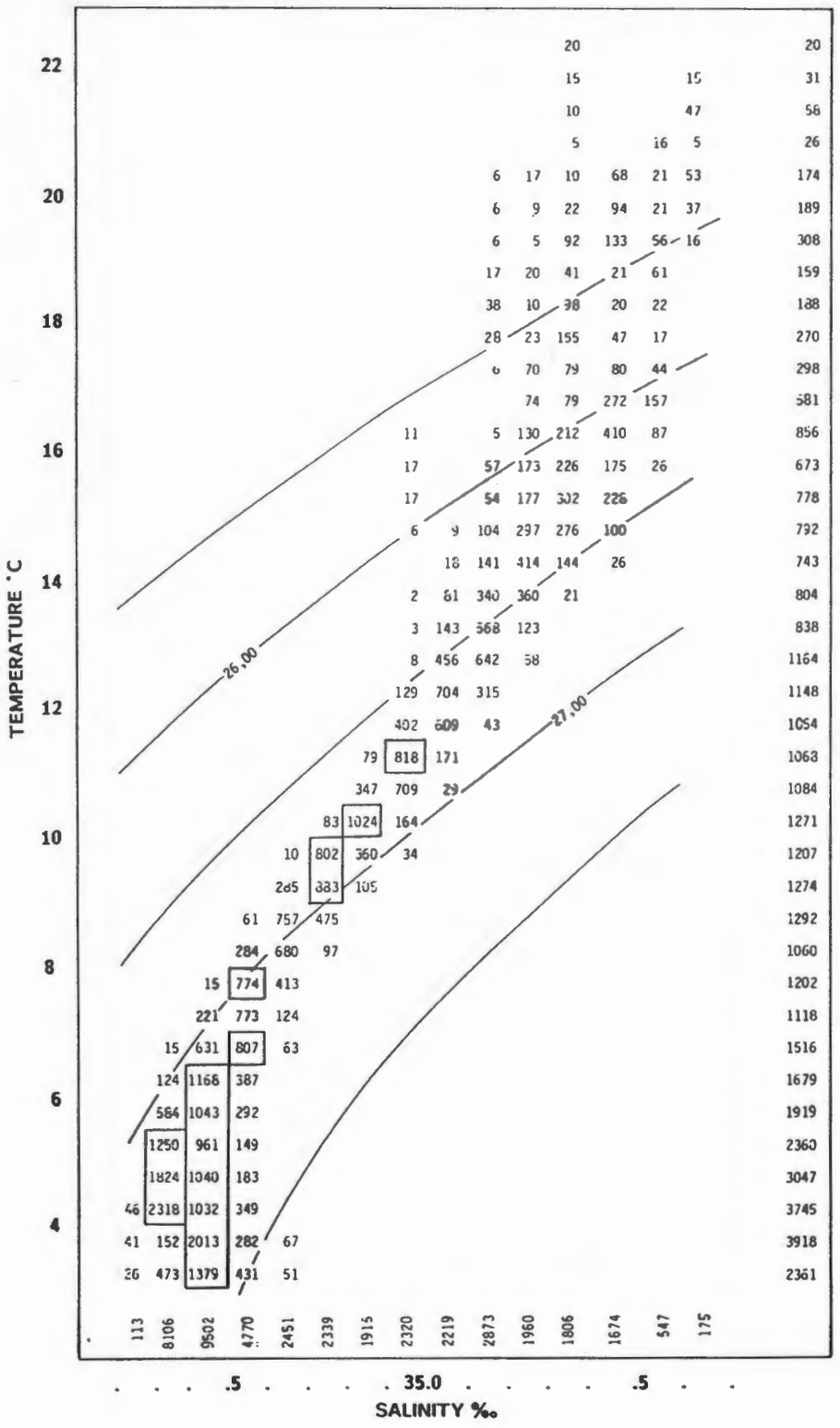

Figure 5.9 Bivariate volumetric diagram for the upper 1000 m of the water of the pilot study area. Volumes are in 10 x km^3 units. Univariate distributions are given by the sums at the bottom and the right of the diagram. The heavy border denotes the 45 % frequency boundary.

Investigating the volumetric characteristics of oceanic areas based only on stations up to 500 m deep excludes the continental shelf area and therefore, according to the definition of Lutjeharms and Stockton (1987), also the main upwelling domain (figure 5.4c). These characteristics (figures 5.4 and 5.8) seem to correspond much better (see later) with those presented by Carmack and Aagaard (figure 5.6). The volume distribution over this depth (500 m) closely follows the Central Water axis (figure 5.4b), demonstrating that, between about 34,50 and 35,20 ‰, the volume of water available to upwelling processes shows a linear relationship to both salinity and temperature (figure 5.4a). The above-mentioned salinity range also forms the boundary for the 45 % volume frequency (figure 5.8). This linear relationship is further brought home by analysing the full vertical extent of the Central Water (figures 5.5 and 5.9). The volume of the (South-East Atlantic) Antarctic Intermediate Water (2,0 - 6,0°C and 33,80 - 34,80 ‰) starts to dominate at the lower depths of the 1000 m depth interval (figures 5.5a, b and 5.9). The primary mode water for this 1000 m depth analysis (4,0 - 4,5°C and 34,30 - 34,40 ‰) falls within the core of the Intermediate Water and makes up 5 % of the total volume of water over this depth (figure 5.9). The full range of Atlantic Central Water shows a linear relationship between volume of water and either salinity or temperature.

This set of linear relationships has some potentially important consequences. Because all the upwelled water is derived from the Central Water (figure 5.2b, c) and because it can be assumed that, on a macroscale, salinity is a conservative property in the upwelling process, it is in principle possible to pinpoint the degree of warming of a particular mass of upwelled water by reference to the T/S diagram. As the volume of Central Water available in each salinity interval is relatively constant, the intensity of upwelling may be directly related to that part of the Central Water from which its constituent water masses are derived. It is noteworthy that the identification of the water column structure during active and passive phases of the upwelling cycle has already been attempted using some of the tenets set out above (Waldron 1985). If a rough estimate of heating rate over the upwelling regime could be established and found to be generally applicable, the intensity of upwelling could be estimated from the T/S relationships. Furthermore, the time-history at each cell could in principle be established.

Although the stations included in the 0-500 m depth analysis excluded most of the water on the continental shelf and the stations used by Carmack and Aagaard (1977) were almost exclusively on the shelf there are a few similarities in the volumetric results of the two sets of data. Both contain Central Water. The primary mode water in both instances occupies more or less the same T/S space (10-11°C and 34,90-34,95 ‰ - figure 5.6 and 10,0-10,5°C and 34,80 - 34,90 ‰ - figure 5.8). The 45 % frequency boundary in both cases only include water more dense than 26,50 σt. In the case of the 500 m depth analysis the 45 % frequency also include water denser than 27,00 σt though. This is to be expected due to the greater depth of the stations used. These similarities are not entirely unexpected, due to the considerable overlap in T/S characteristics of the water on the shelf and off the shelf (figures 5.2b and c). Carmack and Aagaard (1977) showed that during their cruise about half the water on the continental shelf displayed the T/S properties of water derived from the offshore depth of upwelling. Since

the source water for upwelling is Central Water it is therefore Central Water (though modified) that Carmack and Aagaard refer to here.

In the 0-1000 m depth analysis the primary mode water (4,0-4,5°C and 34,30-34,40 ‰) is well within the Antarctic Intermediate Water mass, while most of the 45 % frequency is found on the denser side of 27,00 σ t (figure 5.9). It is interesting to note that over the three depth ranges the primary mode water has shifted almost linearly from 16,0-16,5°C and 35,40-35,50 ‰ (100 m) to 10,0-10,5°C and 34,80-34,90 ‰ (500 m) to 4,0-4,5°C and 34,30-34,40 ‰ (1000 m).

5.1.3 Conclusions

This preliminary investigation into the temperature-salinity relationships and volumetric characteristics of various domains of upwelling in the South-East Atlantic Ocean describes a few of the dominant macroscale characteristics of the general area.

i) The T/S characteristics of the upwelling and open-ocean domains are significantly different and show no overlap. Upwelled water is derived from different parts of the South Atlantic Central Water mass.

ii) The filamentous mixing domain between the true upwelling and pure oceanic regimes falls in an intermediate part of T/S space.

iii) No water from the deeper part of the Central Water, and therefore involved in intense upwelling events only, is observed in the mixing domain.

iv) Upwelled water, no matter from what part of the Central Water mass, is all eventually heated to a limit of 23°C.

v) The greater part of the South-East Atlantic Ocean surface layer is dominated by South Atlantic Subtropical Surface Water.

vi) The volumes of water in each bivariate T/S class of Central Water available to upwelling are constant. This implies that intensity of upwelling may possibly be estimated from the salinity of the upwelled water only.

Further studies are required to refine these conclusions, to establish the average heating rates and to establish more precisely the geographic boundaries of the different domains and of the various water types.

Due to: (i) the lack of high resolution (geographical and vertical), high quality data in this area in general and, (ii) the availability of high quality data in the Agulhas Retroflection area and (iii) the serious gap that the area south of Africa represented in the volumetric census of the world ocean, it was decided to select the Agulhas Retroflection area for a more detailed fine-scale volumetric analysis.

5.2 The Agulhas Retroflection Area

The volumetric analysis in the Agulhas Retrofelction region was done for two depth ranges i.e. for the upper 1500 m of the water column and for the full water depth which is from the surface down to the ocean floor. The one degree of latitude by one degree of longitude 'squares' that are represented by the selected stations are shaded in figures 5.10 (1500 m stations) and 5.11 (bottom stations). Since there were more stations available that measured down to 1500 m than to the bottom, the former (figure 5.10) represented a better coverage of the geographic area of 33°-45°S and 6°-27°E than the latter (figure 5.11). On the other hand experience has taught us that deep water masses are less variable than the surface layers and that they have very tight potential temperature-salinity correlations. So in both cases (shallow and deep stations) the geographical area is well represented by the selected stations. The geographical area was so chosen to specifically also include stations that were obviously outside the Agulhas-Current-Agulhas Return Current-system's direct influence such as the ones far west and those south of the Subtropical Convergence. Lutjeharms and Valentine's (1984) location of the thermal fronts and Lutjeharms and van Ballegooyen's (1988) description of the Agulhas Retroflection have been used to determine the study area.

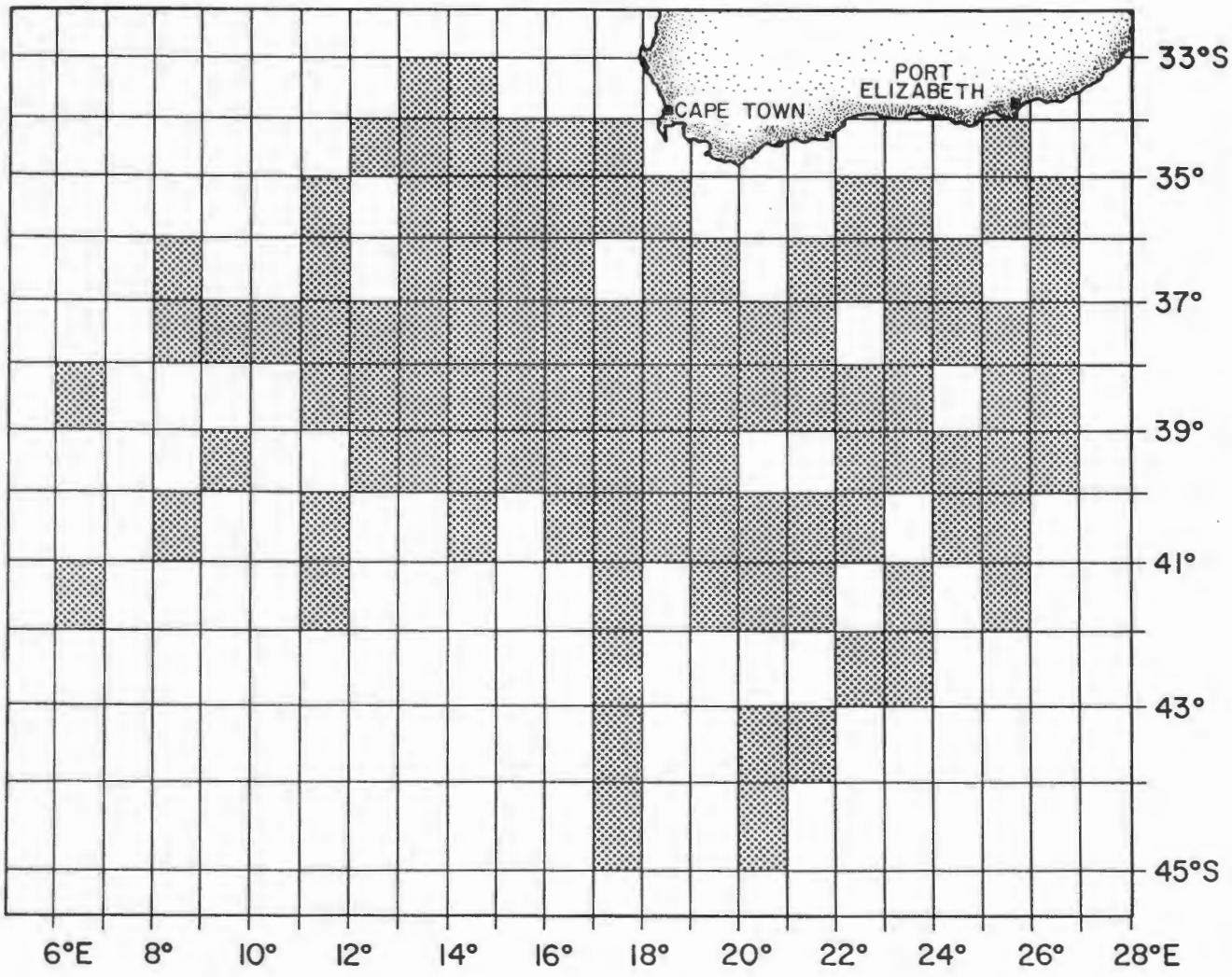

Figure 5.10 The distribution of 1° x 1°-squares (shaded) that are represented by stations, measuring to at least 1500 m depth, for the volumetric census of the water masses of the Agulhas Retroflection area.

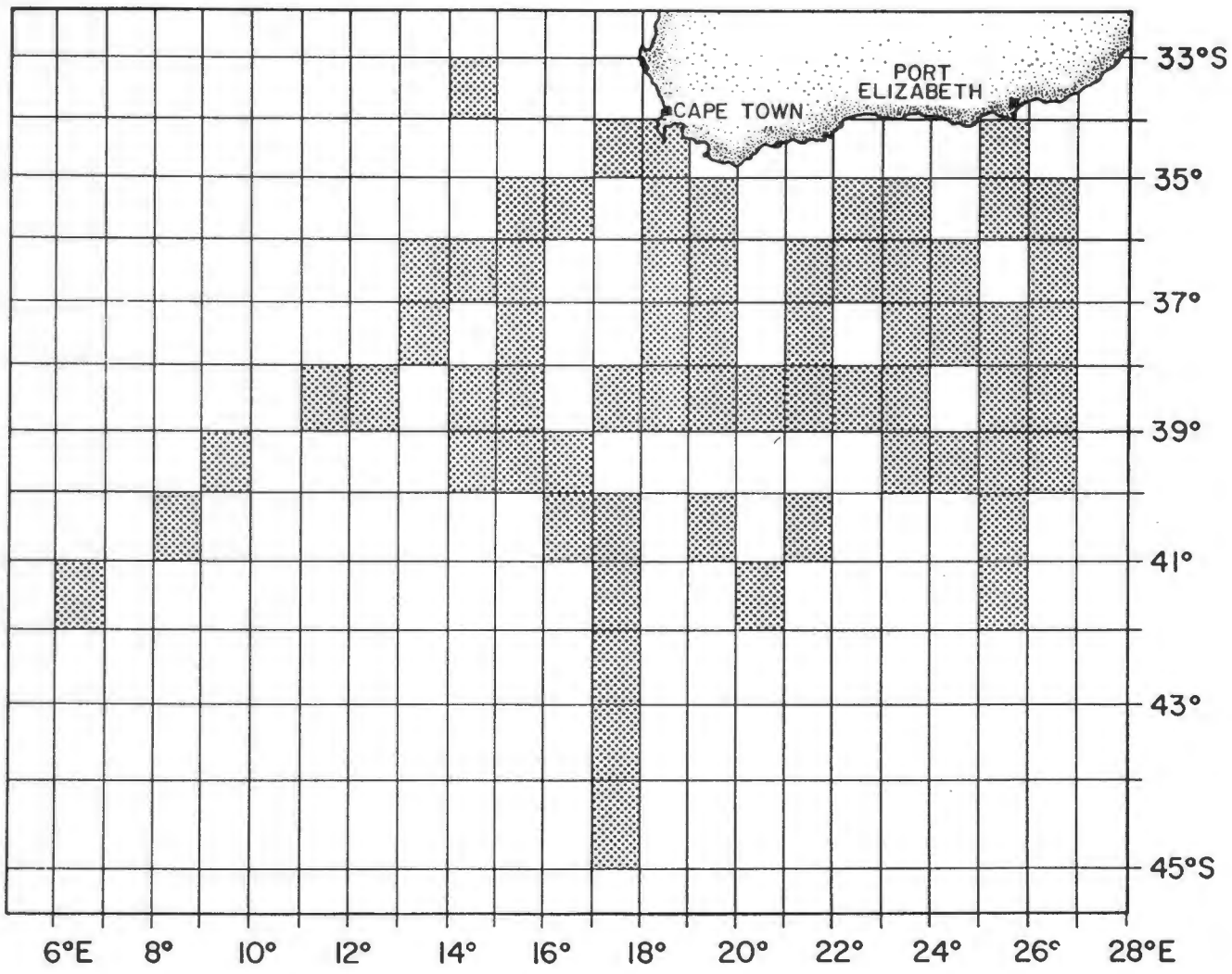

Figure 5.11 The distribution of 1° x 1°-squares (shaded) that are represented by bottom stations for the volumetric census of the Agulhas Retroflection area.

5.2.1 Temperature-Salinity relationships

The vertical structure of the Retroflection area is composed of several recognizable layers of water, each of them originally derived from surface water in a particular area of the world ocean. The conditioning of water at the surface, the sinking to equilibrium depths and the spreading along appropriate density surfaces is a continuous or repetitive process that eventually leads to large volumes of water having relative uniform values of temperatures and salinities.

Water masses are traditionally identified by a core property i.e. that part of a layer where some oceanographic characteristic reaches an extreme value. This method assumes that the core represents both the main axis of spreading and the maximum percentage of a particular water type within a layer. Water masses may also stand out as densely patterned areas or modes on a T/S correlation diagram. Boundaries between water masses, on the other hand, are more difficult to define. Divisions may be based on slope changes in the T/S curve, volumetric considerations, or simply taken as the mid-point between two cores (Carmack, 1977). Reid, Nowlin and Patzert (1977) demonstrated that stability maxima surfaces, extending over wide geographical areas, often interlie core properties, and thus may represent true water mass boundaries between layers from different sources.

A limitation of volumetric analysis is, that, water mass identification must be based solely on absolute position in potential temperature-salinity space, rather than the primary identification characteristics discussed above. The aim of this section is thus to review the T/S characteristics of the Retroflection water masses so that a comparison to the volumetric census can later be made. This analysis of T/S relationships is intended to be simple, for comparison to the volumetric diagrams, and is not intended to reveal the complexities of the Retroflection water mass structure.

The background or general temperature/salinity (T/S) characteristics of the area as represented by the historic data from the South African Data Centre for Oceanography (SADCO) are portrayed in figure 5.12. Obviously this diagram contain a lot of noise but other than SADCO's routine quality control checks there was no way for them to verify the data. Almost all of the data points are from bottle stations of which most were rather shallow, usually down to the 1% light level. *In situ* temperatures and not potential temperatures were used for the SADCO T/S plot. This diagram (figure 5.12) is based on more than 80 thousand observations so the diverse distribution of T/S values is not unexpected. The T/S points at about 23-26°C and 35,2 - 35,6 ‰ are probably from stations in the Agulhas Current core. There seems to be a dramatic broadening of the Central Water (6-16°C and 34,5 - 35,5 ‰) core, especially above 8°C. Most of the scatter of points (T/S values) on the fresh side of the Central Water can be attributed to stations south of the Subtropical Convergence. The scatter of points on the saline side of the Central Water core is not so easily explained. At the salinity minimum section of this scatter diagram (AAIW) there is a strong Red Sea Water signal on the saline side of the AAIW. The salinity spread at about 2°C and colder (Deep Water to Antarctic

Bottom Water section of the diagram) seems unrealistic and is probably a reflection on the quality of the historic data.

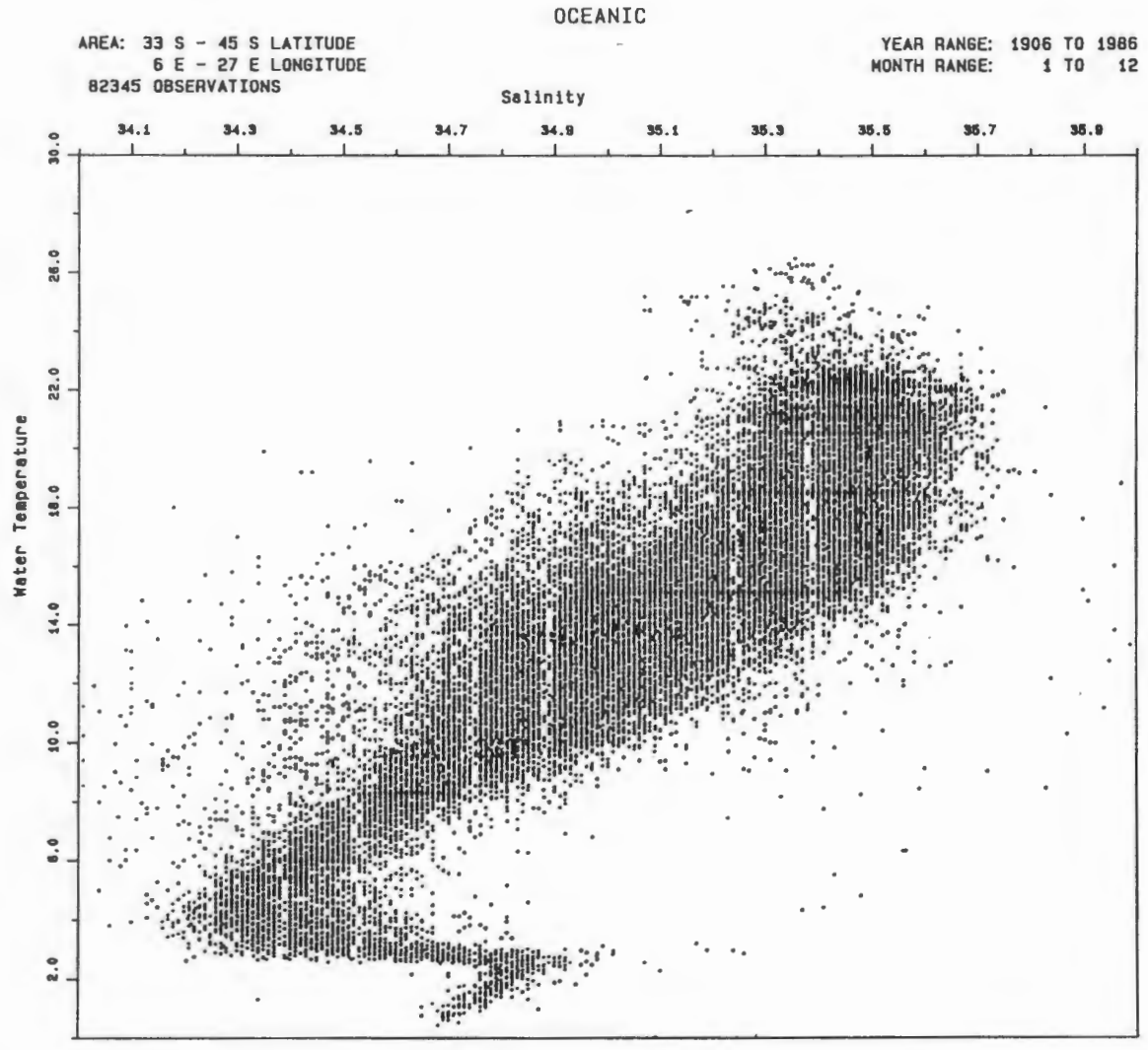

Figure 5.12 A temperature/salinity scatter diagram representing all the historic data of the geographic area selected for the fine-scale volumetric census.

The potential temperature-salinity (θ -S) correlation for the shallow stations (1500 m) selected for the volumetric census and taken as representative of the Agulhas Retroflection area, is portrayed in the combined θ -S plot (scattergram) (figure 5.13) and that for the bottom stations in figure 5.14. The measurements of the upper 1500 m of all the bottom stations (figure 5.14) are included in the shallow station analysis except for the few bottom stations on the continental shelf that were less than 1500 m deep.

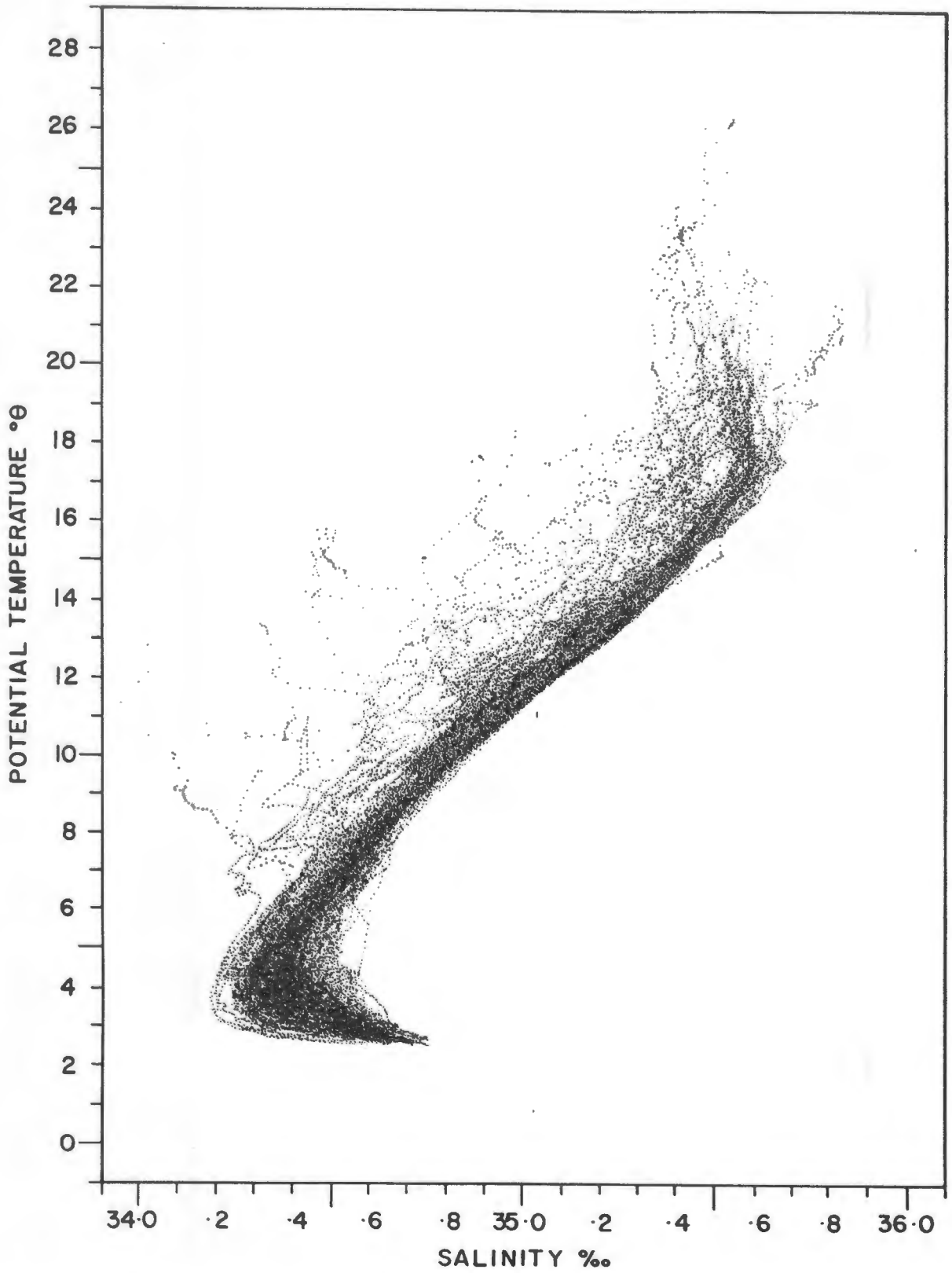

Figure 5.13 A potential temperature/salinity (θ /S) scatter diagram representing all the high-quality CTD stations (0-1500 m) used for the fine-scale volumetric census of the Retroflection area.

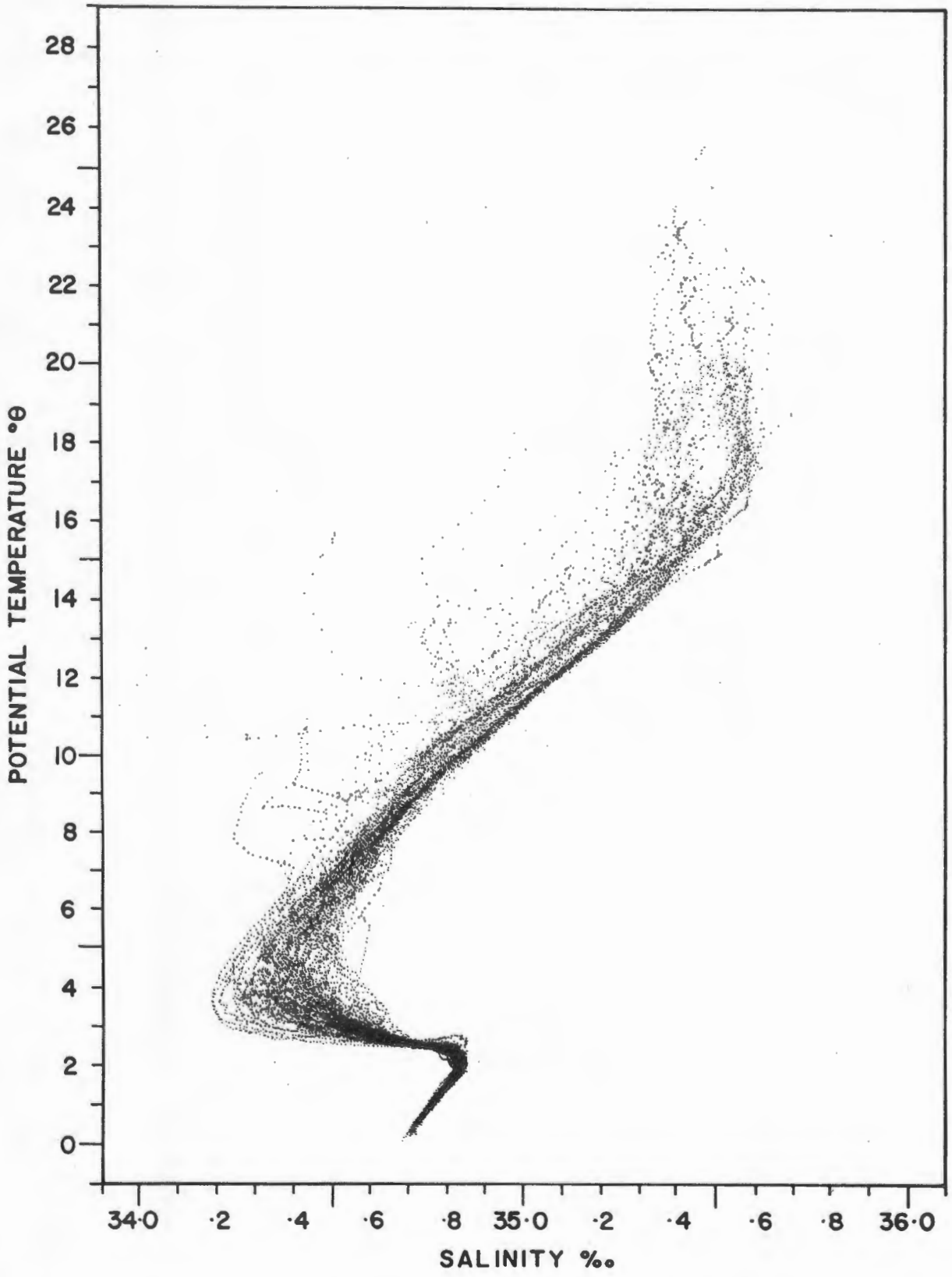

Figure 5.14 A θ/S scatter diagram representing all the high-quality CTD bottom stations used for the fine-scale volumetric census of the Retroflection area.

What is immediately clear from the scattergram of the shallow stations (figure 5.13) is that the deep water masses (North Atlantic Deep Water, Circumpolar Deep Water and Antarctic Bottom Water) are not represented in the θ-S space. So one can conclude that in the Retroflection area one should expect the deep water masses generally to be below 1500 m depth. Another obvious aspect is the scatter of points to the lower salinity side of the section of the curve that represents the Central Water. Most of those points are from stations south of the Subtropical Convergence. Gordon et. al. (1987) stated that the Atlantic Ocean south of 30°S is the source of low salinity water mixing into the Retroflection. These waters are transported form the South Atlantic Ocean and are found predominantly south of the Subtropical Convergence in the Agulhas Retroflection region. At a given density, these waters are characteristically the freshest found in the Retroflection area. In general the upper waters from the South Indian Ocean are warmer and saltier than those of the South Atlantic. The linear part of the θ-S curve (6-16°C) which in this case forms a broad band of points, represents the Central Water. The South West Indian Central Water and the South-East Atlantic Central Water are very similar in potential temperature-salinity (θ-S) properties between 7°-15°C (Gordon et. al., 1987). At lower temperatures the South Atlantic waters are slightly fresher. It is, however, possible to distinguish between the Central Waters from the different oceans (see later).

The Central Water overlies the Antarctic Intermediate Water. The latter has a potential density ($\sigma\theta$) of about 27,20 in the Retroflection region and represents the salinity minimum section of the θ-S plot. It has quite a large salinity range i.e. from about 34,20 to 34,55 practical salinity units (psu) at 4°C. There is a bigger concentration of points towards the middle of this salinity range. This concentration is more obvious in figure 5.14. This concentration (~34,30-34,45 psu) can be seen as Antarctic Intermediate Core Water, while the low salinity water from south of the Subtropical Convergence (mentioned above) is responsible for the points to the fresh side of the Intermediate Water. Of course some mixing between the two different water masses has occurred. To the more saline side of the Intermediate Water, Red Sea Water (RSW) mixes with the Antarctic Intermediate Water (AAIW) and provide the high salinity component for the AAIW observed here in the Retroflection region (Jacobs and Georgi, 1977). Gründlingh (1985) has traced Red Sea Water at densities of 27,20-27,50 $\sigma\theta$, and showed that the AAIW was occasionally interrupted by water from Red Sea origin. Gordon et al. (1987) have discussed the presence of Red Sea Water between 4° and 6°C in the Retroflection area during October-December 1983. On this combined θ-S plot (figure 5.13) the RSW signal actually continues to below 4°C (to almost 3°C). So the spread (range) at the salinity minimum section of the curve is caused by basically three water masses, namely low salinity water from south of the Subtropical Convergence, Antarctic Intermediate Water and Red Sea Water and of coarse products of their mixing.

The high temperature points (up to 26°C) of this θ-S plot (figure 5.13) come from stations that were done in the core of the Agulhas Current (for e.g. SCARC station 56 and Thomas Washington stations 259 and 274, Valentine et al., 1988).

The very saline, high temperature water (~35,80 psu and 20-22°C) was detected in the upper ~ 75 meters of eddies of Agulhas Current origin drifting in a north-westerly direction (e.g. SCARC stations 8, 11 and 22 and ARC stations 77 and 79 amongst others). These eddies reflected higher salinities in the surface mixed layer than their source. Gordon and Haxby (submitted) believed that evaporation is responsible for the increase in salinity. Evaporation within the confines of the warm eddies would be larger than the regional mean, as warm water drives larger evaporation. Olson et al. (1989) found that Agulhas eddies behave like the Agulhas Retroflection regime and lose heat to the atmosphere even during the summer months at a rate of well over $100W/m^2$. So the surface mixed layer of these eddies has lost some heat but experienced an increase in salinity.

The most obvious difference between the θ-S scattergram for the shallow stations (figure 5.13) and that for the bottom stations (figure 5.14) is the extension (at the lower end of the θ-S plot) into the Deep and Bottom Water (figure 5.14). The very tight θ-S correlation of the Antarctic Bottom Water (AABW) colder than 1,7°C and also the, to a lesser extent, Deep Water (North Atlantic Deep Water - NADW) and Circumpolar Deep Water (CDW) is clear. This could be due to the smaller number of bottom stations (compared to shallow stations) used, but from experience it is known that *all* the deep water masses of the world have a very tight potential temperature-salinity correlation. The deviation from this tight correlation at the Deep Water density is represented by ARC station 2 and I can offer no obvious explanation for this. The same large salinity range exists at the Intermediate Water depth. The higher concentration of points in the middle of this range (representing AAIW) is much more obvious in this case.

Gordon (1985) has stated that from 7°-15°C (Central Water) the South Atlantic and Indian thermoclines are similar in θ-S properties. The usefulness of T/S analysis per se around Southern Africa is limited by the very small differences that occur between the Central Waters of the South Indian and South Atlantic oceans (Clowes, 1950). Any small error or uncertainty in the measurement of salinity and/or temperature will prevent one from differentiating between water derived from different origins. Nutrients may also be used to distinguish between water of different origins. Nutrient/salinity plots have been used by Chapman et al. (1987) south of Africa to distinguish between Agulhas and Atlantic waters. This method is however less precise than a T/S (θ-S) plot, because of the larger errors involved in nutrient determinations, namely 2-3% for nitrate, phosphate and silicate (Mostert, 1983) compared to less than 0,1 % for salinity and temperature.

Clowes (1950) had some success in showing real differences between Atlantic Central Water and Indian Central Water from combinations of several oceanic cruise data. All the hydrographic data since 1950 from the South African Data Centre for Oceanography (SADCO) have been used to plot T/S scattergrams (figure 5.15) for two geographic areas. These areas are, one in the southeast Atlantic (32-35°S and 13-15°E (figure 5.15a) and one in the South West Indian ocean (34-40°S and 22°-26°E) (figure 5.15b). It is not suggested that these areas are absolutely representative of the Southwest Indian Ocean and South East Atlantic Ocean respectively. These areas were selected merely on the basis of lying obviously within the direct

influence of the Agulhas Current input (figure 5.15b) and outside the direct Agulhas Current input (figure 5.15a) respectively. These areas are also not the same in size, but the number of observations represented by each, compare very well. Plotting a linear regression through the linear section or Central Water section of the T/S diagrams for the two areas, the line of regression for the South-East Atlantic lies slightly more to the fresher side of the plot (figure 5.15c). Towards the lower temperature section of the Central Water the shift to the fresher side becomes more pronounced. Gordon (1985) first suggested this when he stated that below 7°C the South Atlantic waters are slightly fresher. Although the difference in the T/S character (Central Water section) for the two geographic areas is small it is nevertheless significant especially if one bears in mind that, by far the largest portion of the data used for these T/S plots came from bottle stations. The considerable overlap in the plots for the two areas is not unexpected. With all the eddies and Agulhas rings that move through the area (Gordon and Haxby, submitted; Lutjeharms and Van Ballegooyen, 1988) it will be difficult to find 'pure' South Atlantic Water in this part of the Atlantic Ocean. Pure, meaning water that has not at one time or another been part of an Agulhas eddy or ring or filament.

Chapman and Largier (1989) have found that combining data from several cruises for the purpose of distinguishing between Central Water from Atlantic or Indian Ocean origin is not successful on the Agulhas Bank. Temporal variations in the T/S character of the water on the bottom of the Bank (which is basically Central Water) and possible variations in instrument calibration smudged the subtle differences in T/S character which would indicate spatial differences in this bottom water composition. They used three individual cruises on the Bank. They found in their T/S analyses that stations west of 20°30'E (Alphard Banks) at temperatures below 10°C have consistently less saline water compared to the stations east of 20°30'E. This difference in salinity amounts to about 0,03-0,05 psu at 8°C, well within the discriminatory performance of the CTD (conductivity-temperature-depth) instrument. These differences, although small, are statistically significant and these trends are confirmed by nitrate/salinity plots.

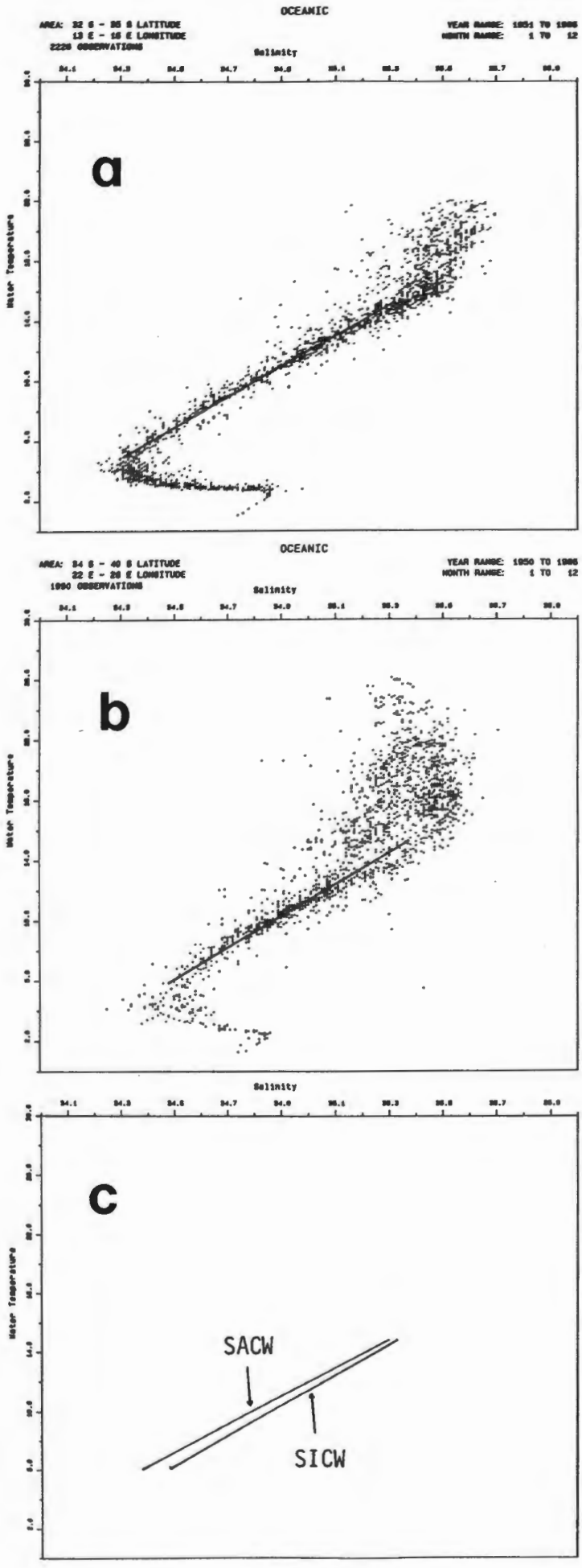

Figure 5.15 T/S scatter diagrams of historic data representing an area (a) in the South-East Atlantic and (b) in the South West Indian Ocean. Lines that represent linear regressions through the section of the T/S curve that represents Central Water are indicated. These lines are compared to each other in panel (c).

On the θ -S scattergram for the bottom stations (figure 5.14) there are two distinct bands of points (T/S values) at temperatures of about 6-15°C. This temperature range is typical of Central Water (Sverdrup et al., 1942; Gordon et al., 1987). These bands or concentrations of data points might represent Central Water from the two different oceans. If the distinction (using historic data) between the Central Water of the two oceans (South Atlantic and South Indian) discussed above is accepted and incorporated here, then the less saline band would be South-East Atlantic Ocean Central Water and the saline one, South West Indian Ocean Central Water. Bearing in mind that this θ -S plot consists of data collected over a period of 3,5 years the differences in the T/S character of the Central Water become significant. The difference ranges from about 0,04 to 0,07 psu depending on the temperature used as reference for example at 8°C it is about 0,04 psu while at 13°C it is almost 0,08 psu.

The stations responsible for the two bands of points in the Central Water section of the curve have been separated into either of the two possible groups namely South-East Atlantic - or South West Indian Central Water. There were quite a number of stations that display T/S characteristics of both types of Central Water. Fine et. al. (1988) concluded that almost all the Agulhas Retroflection Cruise (ARC) stations had layers from both the South Indian and South Atlantic oceans. About one third of the stations used for this θ -S analysis as well as the volumetric analysis are ARC stations. The stations that display both types of Central Water and also those with a T/S character in between the two bands of points were not included in the two groupings. So only stations that 'fall' definitely in one of the two groups were plotted geographically (figure 5.16). It is immediately clear that there is not a distinct east-west orientation (separation) of the two groups, unlike Chapman and Largier's (1989) findings on the Agulhas Bank. Their east-west separation is topographically controlled which one does not find in the open ocean. Some of the stations with South Atlantic Central Water are found as far east as 26°E and some South Indian Central Water stations as far west as 14°E. The latter is not surprising taken into account that the Agulhas Current on occasion extends quite far into the South Atlantic, and the north-northwestern drift of eddies and rings (Gordon and Haxby, submitted).

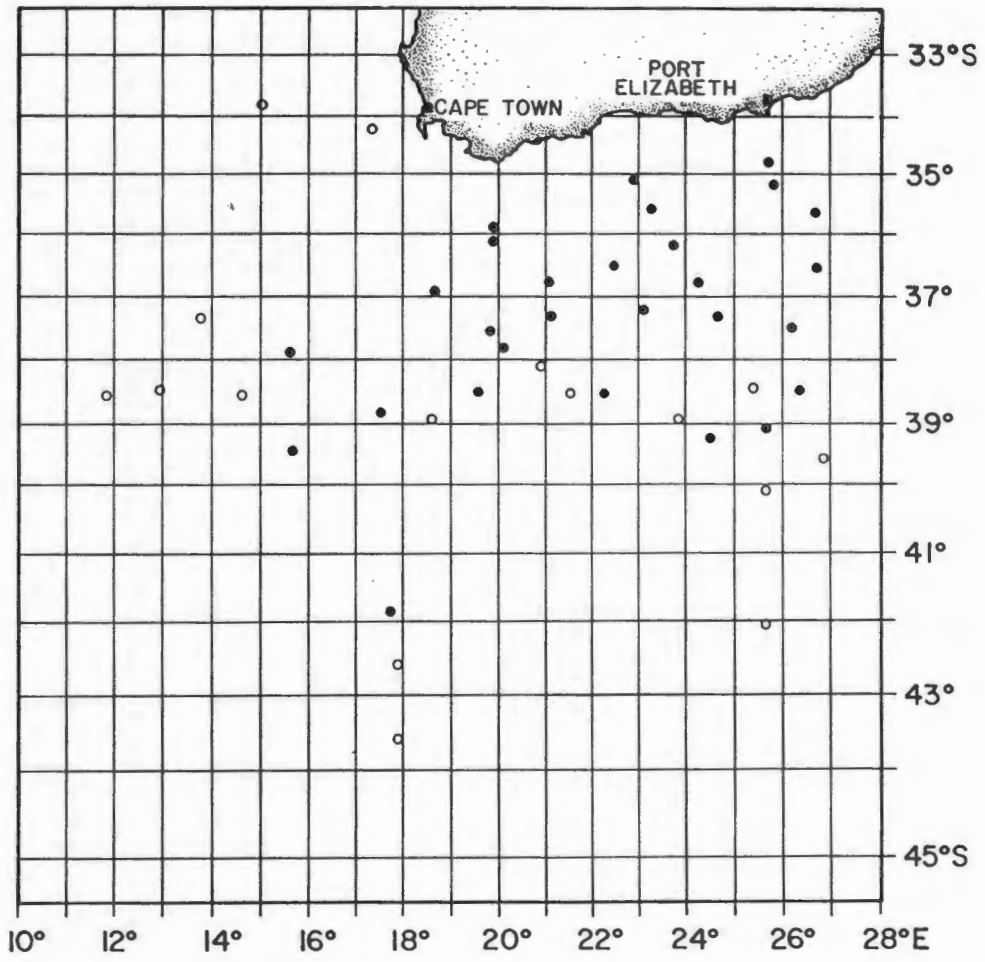

Figure 5.16 The distribution of high-quality CTD stations that display θ /S characteristics that are typical of South Atlantic Central Water (open circles) and South Indian Central Water (filled circles).

To try and find an explanation for the easterly location of some South Atlantic Central Water (SACW) stations (figure 5.16), individual cruises were analysed. For two of the cruises, namely the ARC and the *Thomas Washington* Marathon Leg Cruise declouded thermal infrared imagery from the Meteosat satellite was available. Plotting the surface isotherms from the ARC hydrographic data and enhancing them with the aid of the satellite imagery Lutjeharms and Gordon (1987) produced a composite diagram (figure 5.17) of the surface temperatures of the Retroflection region for the duration of the ARC cruise. Superimposing the two groups of stations (for the ARC) onto this diagram it became clear that all the SACW-stations clearly fall outside the Agulhas Current proper, the Agulhas Return Current and any observed rings, eddies and Agulhas water filaments (figure 5.17). A possible exception could be the station at about 39°S and 18°30'E which seems to lie inside a possible Agulhas ring. The same result was obtained using *Thomas Washington* cruise data. The fact that some stations that are geographically far east but display typical SACW characteristics does not necessarily imply that the Central Water circulates from the west to the east. This is not unlikely, however, since Fine et al. (1988) stated that according to their calculations substantial quantities of the Agulhas

water inflow into the Atlantic are replaced by water from the South Atlantic subantarctic zone at least between 15° and 4°C (which are more or less Central Water temperatures).

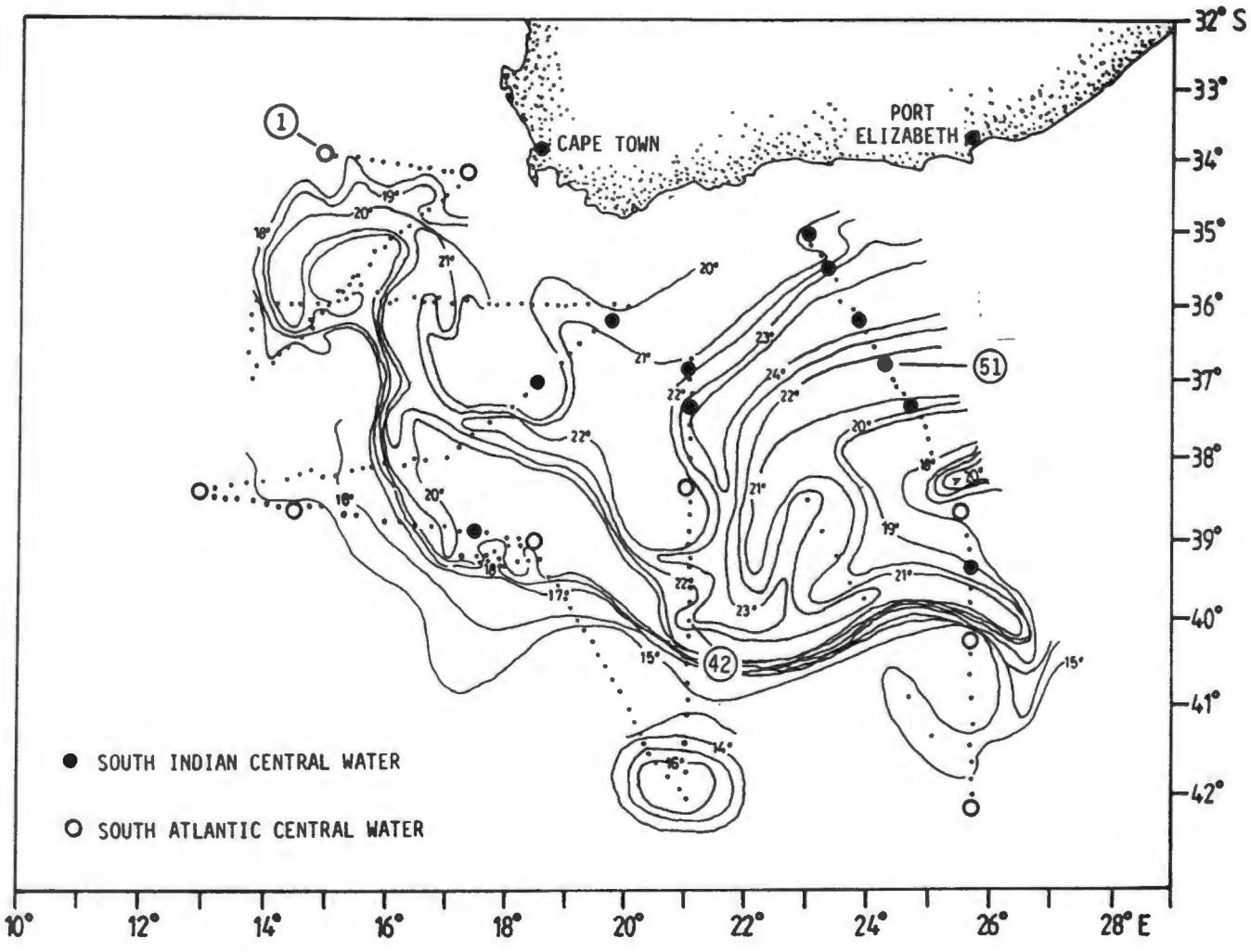

Figure 5.17 A composite picture of the surface isotherms based on the hydrographic data of the *R.V. Knorr* (Nov/Dec 1983) and declouded METEOSAT infra-red imagery. The small black dots denote the cruise track. The *Knorr* stations that show South Atlantic Central Water (open circles) and South Indian Central Water (open circles) characteristics are indicated.

Central Water is formed at the Subtropical Convergence region by the sinking and northward spreading of mixed subtropical and subantarctic water masses. Shannon and Hunter (1988) inferred the circulation of Central Water from the Antarctic Intermediate Water (AAIW) circulation. Part of this northward moving Central water would be exposed to an input of warmer more saline water from the tropics (via the Agulhas Current system). The water to the west of the Retroflection region will have a lesser chance of being exposed to the warm saline input. I conclude therefore that those eastern stations with SACW characteristics have the same Central Water as those in the west of the area and that they just escaped the warm, saline input. The stations inside the Agulhas current loop or eddies and rings obviously did not escape this saline warmer input. In other words the Central Water in this region would have theoretically all be similar had it not been for the Agulhas input.

On comparing individual stations the difference between the two types of Central Water are even more pronounced (figure 5.18) than by combining data from several cruises. The geographic positions of these stations are indicated in figure 5.17 and their co-ordinates are given in Addendum I. Using potential density ($\sigma\theta$) levels as reference instead of temperature or depth, enhances the difference even more. An example is at 12°C where the salinity difference is just over 0,06 psu while at the potential density ($\sigma\theta$) level of 26,50 (relative to the surface or 31,10 relative to 1000 decibar) which cuts the θ-S curve at about the same level, the difference is just below 0,10 psu (figure 5.18). Although this comparison of individual stations may be less significant from a statistical point of view it is nevertheless much more dramatic.

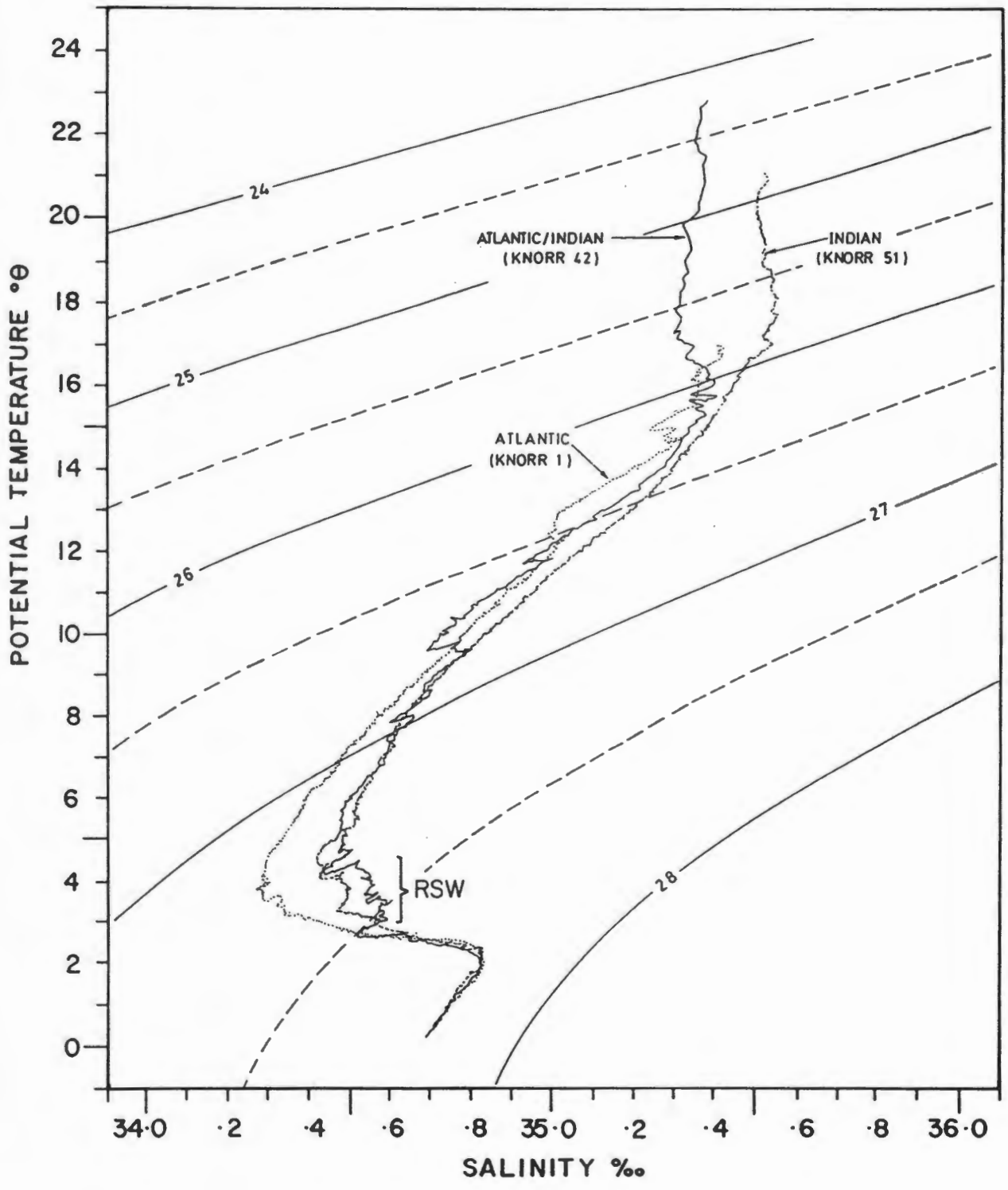

Figure 5.18 Three θ /S traces of *R.V. Knorr* stations. The dotted line (station 1) display θ /S characteristics typical of South Atlantic Central Water (SACW); the dashed line (station 51) display typical South Indian Central Water (SICW) characteristics. The solid line (station 42) display typical SACW characteristics above 10°C but at this temperature it clearly enters a different water mass and the θ /S cure shifts to typical SICW characteristics. The same curve also displays a very strong Red Sea Water (RSW) signal between about 4° and 2,5°C. Sloping lines denote potential density (referenced to the surface).

The differences between the Central Water from the South-East Atlantic Ocean and that from South West Indian Ocean are therefore real. This has been demonstrated in several ways. Clowes (1950) and Valentine (this thesis) combined historical data, mostly discrete bottle casts from different cruises and show small but significant differences. Chapman et al. (1987) used nutrients to distinguish between waters from Agulhas and Atlantic origin. Chapman and Largier (1989) using high quality (accurate) data from individual cruises to show differences in Central Water on the bottom of the Agulhas Bank. Valentine (this thesis), using high quality CTD data also distinguished between the two types of Central Water by combining data from several cruises and by using individual cruises. One could therefore conclude then that with calibrated CTD data it should in many instances be possible to distinguish between South Atlantic Central Water and South Indian Central Water.

5.2.2 Volumetric considerations

The volumetric distributions in θ-S space of the water in the Agulhas Retroflection area are portrayed in figures 5.19 to 5.22. These three-dimensional (3-D) bivariate diagrams are produced from both the shallow stations (1500 m) as well as the bottom stations data sets. Figures 5.19 and 5.20 represent the shallow stations and are essentially the same diagram but viewed from different angles namely from the high salinity side (figure 5.19) and from the high temperature side (figure 5.20). The same applies to figures 5.21 and 5.22 respectively which represent the bottom stations. The fine-scale classes of these biviarate diagrams have been ranked in decreasing volume order. For the shallow stations the top 150 classes were ranked which represent 35% of the total volume of the upper 1500 m of the water column (see Addendum II). The top 200 classes of the bottom station diagram (Addendum III) were ranked which make up 69 % of the total volume of the water of the Retroflection area. To extend the process of ranking the fine-scale classes till 90 % of the water in the Agulhas Retroflection area is classified, would be excessively time consuming (as also pointed out by Worthington, 1981) and have limited justification due to the relatively small volumes involved.

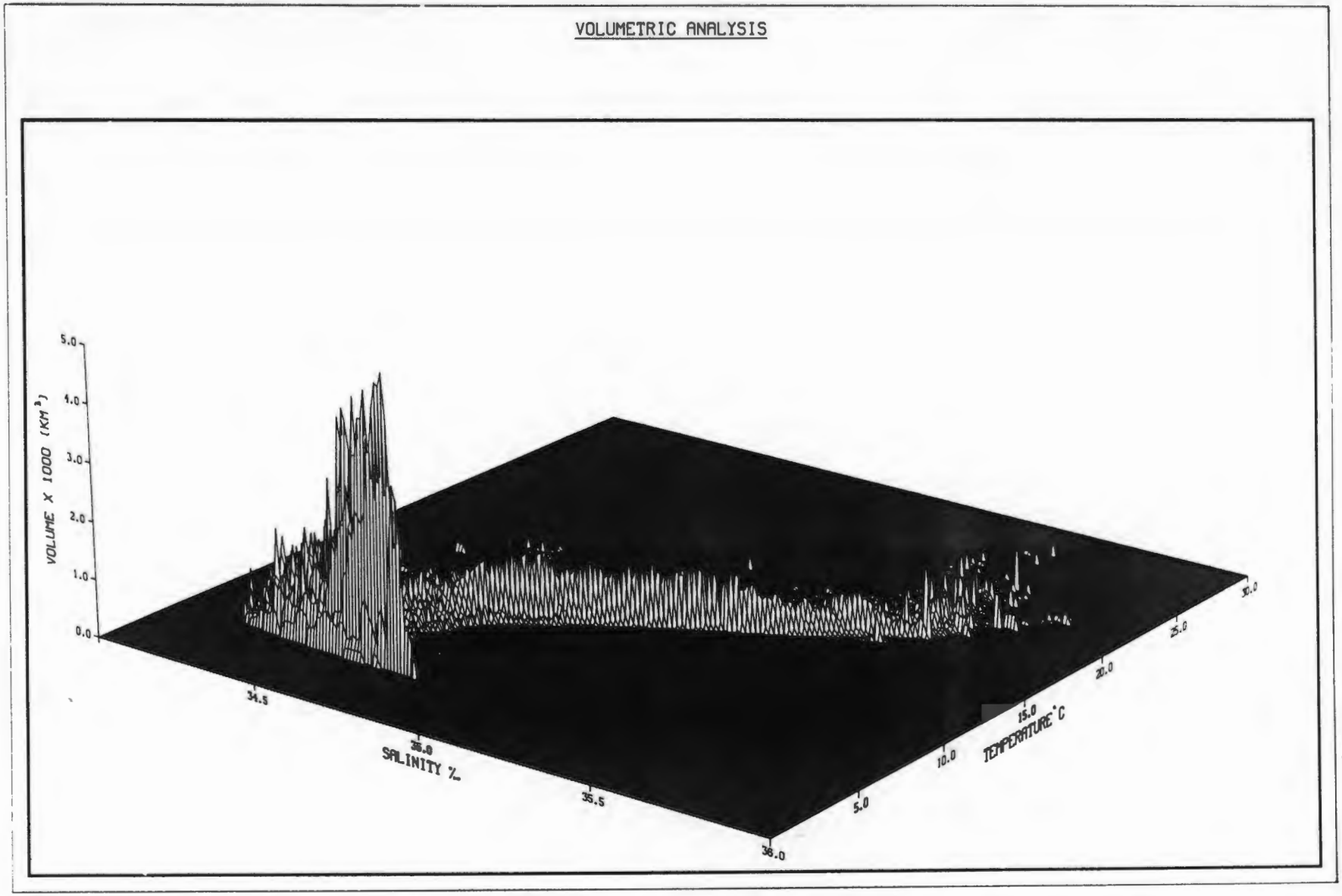

Figure 5.19 A three-dimensional volumetric diagram of the water masses of the upper 1500 m of the Retroflection area. Apparent elevation is proportional to volume. This is a perspective view towards higher temperature and lower salinity.

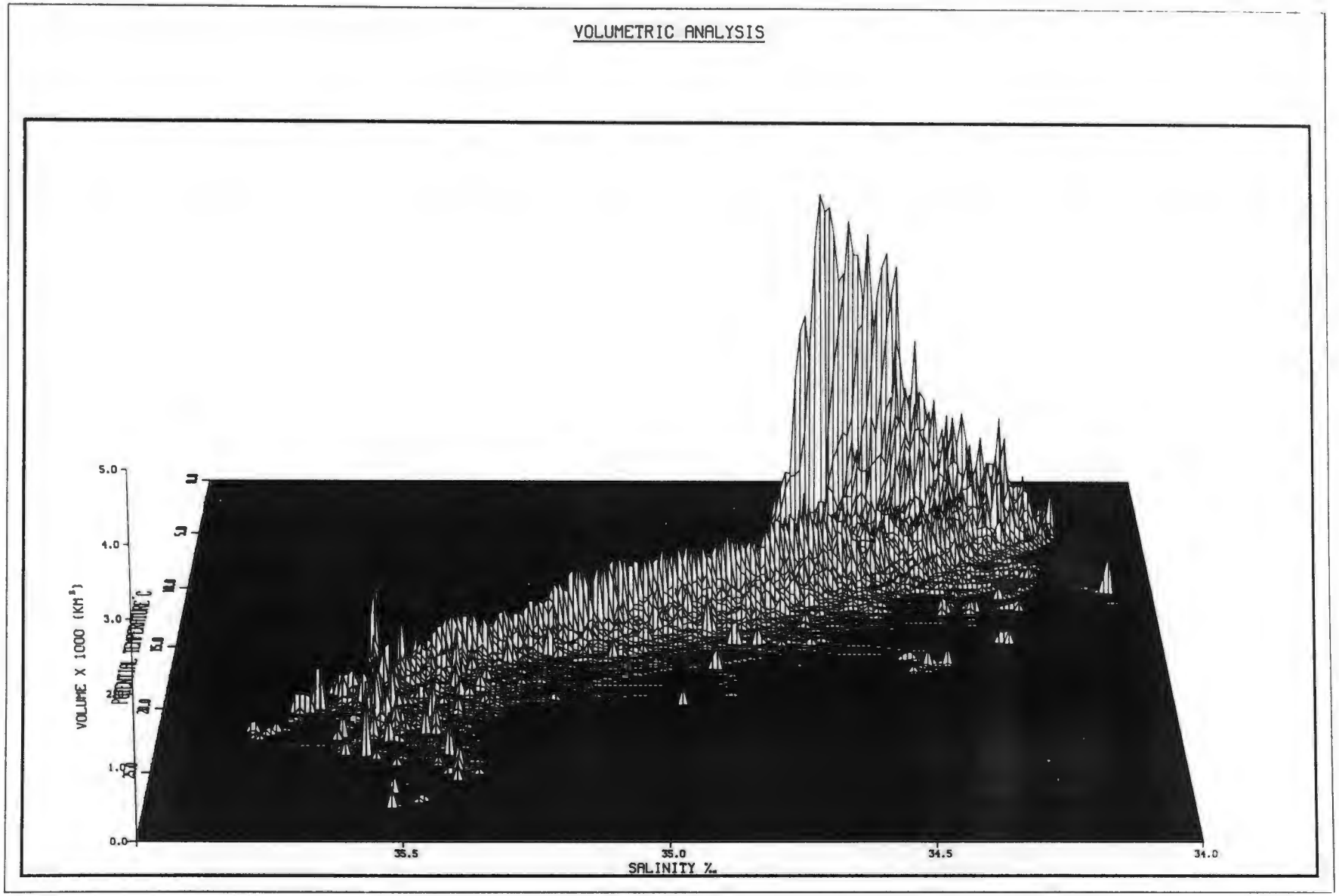

Figure 5.20 As for figure 5.19 but rotated to provide a perspective view towards lower temperatures.

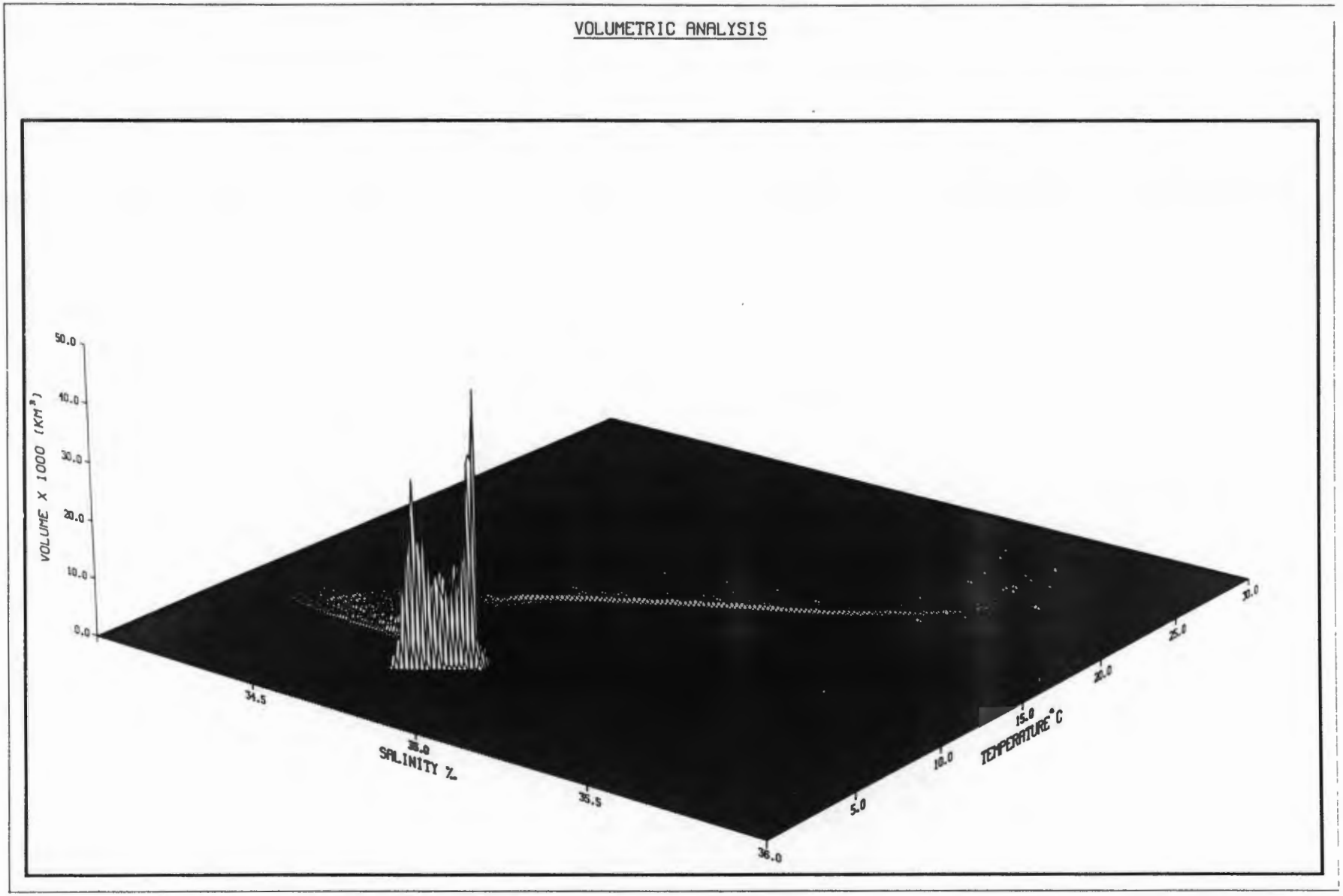

Figure 5.21 A three-dimensional volumetric diagram of the water masses (surface to ocean floor) of the Retroflection area. Apparent elevation is proportional to volume. This is a perspective view towards higher temperature and lower salinities.

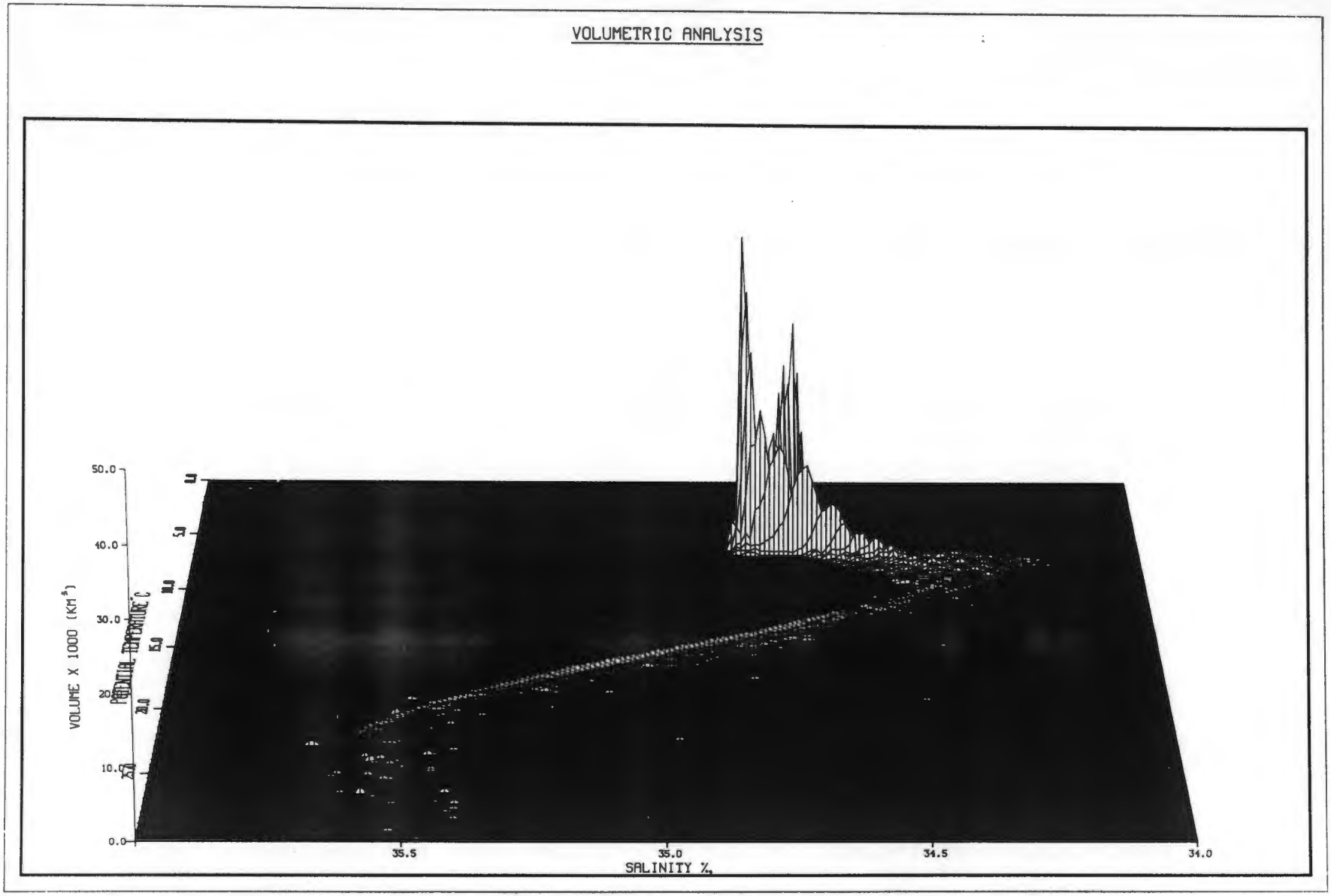

Figure 5.22 As for figure 5.21 but rotated to provide a perspective view towards lower temperatures.

Several factors are responsible for the fact that in some cases more than one class can have the same ranking. First, the contribution of the difference in latitude towards calculating the actual area of the degree-squares is relatively small. Second, the vertical resolution is very small and the thickness of the water column that fall within a certain θ-S class is rounded off to the nearest metre. Third, the volume per class interval is rounded off to the nearest one-tenth of a cubic kilometre.

5.2.2.1 The shallow stations (0-1500 m)-data set

The obvious difference between the θ-S plots and the bivariate diagrams is the apparent elevation which in these cases are proportional to volume. Several obvious conclusions can be drawn from a visual inspection of the three-dimensional (3-D) diagrams of the shallow stations (figures 5.19 and 5.20). (i) The warm saline surface water contributes very little to the overall volume of the upper 1500 m of the water column. (ii) The contribution of the low salinity water that originates south of the Subtropical Convergence (STC) and found on the low salinity side of the linear section of the diagram (see section 5.2.1) is even less. (iii) Central Water contributes considerably more and the volume is rather uniformly distributed over the full θ-S range of Central Water. (iv) Antarctic Intermediate Water (AAIW) is by far the biggest contributor to the overall volume of the upper 1500 m of the water column and the volume per fine-scale class increase dramatically towards the deeper side of the AAIW especially at its transition into the Deep Water masses.

The surface water is rather diverse and contain no high volume classes. Only six classes have enough volume to be included in the top 150 highest volume classes or ranks (90, 127, 127, 144, 145, 145). The low salinity water from south of the STC is widely spread on the less saline side of the 3-D diagrams and has very little volume (see figure 5.20). Even at AAIW depth where it contributes towards the salinity minimum (~34,20 ‰) part of the AAIW, the volume per fine-scale class is not enough to qualify for ranking.

The volume of the Central Water is rather evenly distributed along its θ-S range. This is more noticeable in figure 5.19. The same uniform distribution was observed in the volumetric analysis of South African west coast data (figure 5.5a). Comparable volumetric studies (Worthington, 1981; Cochrane, 1958; Pollak, 1958 and Montgomery, 1958) concentrated on the larger (volume-wise) water masses so this rather uniform distribution of Central Water cannot be directly compared or straight forwardly verified. A possible explanation could be that the supply at the source of Central Water (at the Subtropical Convergence) and the rate of mixing between the AAIW below the Central Water and the surface water on top of it have reached an equilibrium over an extensive period. This equilibrium is maintained. Although the Central water forms part of what is termed thermocline water, seasonal variations will not have any noticeable effect on the T/S structure of Central Water. Because the θ-S characteristics of stations distributed over a relatively large area, and spread over a 3,5 year period, are combined, it is doubtful whether more extreme (than seasonal) variations will have a marked

effect on Central Water as far as the distribution of volume is concerned. Worthington (1981) stated that we have no idea about the time scales of the mixing processes of the water masses and suggested that for the deep water masses (which would be considerably longer than for Central Water) it could be in the order of centuries or even conceivably millenia.

On the basis of volume (elevation) the Central Water section of the bivariate 3-D plots can be divided into two parts. The one part is towards the lower salinity side of the linear section of the plot, is slightly more diverse and does not contain any high volume classes. The other part (on the more saline side) seems more concentrated in a narrower band and has noticeably higher volumes. This is more obvious in figure 5.20. This division roughly fits our distinguishing of the two types of Central Water according to source or origin (see section 5.2.1). The concentrated, more saline, higher volume part corresponds to South West Indian Central Water, while the lower volume, more diverse part corresponds to the South-East Atlantic Central Water. Eighty three of the fine-scale classes within the section of the diagram that represent the Central Water are ranked, ranging form the high volume class 83 (rank number) to the low of 150. All of these ranked classes fall exclusively in the South West Indian Ocean Central Water band (warmer, more saline) of the Central Water.

The Antarctic Intermediate Water (AAIW) is quite diverse in T/S space and has a salinity range from about 34,20 psu to about 34,50 psu (figures 5.13 and 5.14). Although it is obviously the largest water mass in the upper 1500 m of the water column as confirmed in the diagrams in figures 5.19 and 5.20, the really high volume classes only begin to occur at the bottom (deeper) end of the AAIW where it has a tighter θ -S relationship due to mixing with the Deep Water. It is therefore not surprising that the class with the highest volume (rank number 1) in the upper 1500 m of water occurs at this transitional (to the Deep Water) depth. In fact, the ten highest volume classes are all found in this area of the diagram ranging from 5,0 x $10^3 km^3$ (number 1) to 4,1 x 10^3 km^3 (number 10). The dramatic increase in volume of the fine scale classes is largely brought about by the fact that the AAIW mass is condensed (restricted) to a very limited T/S range at the transition into the Deep Water compared to the rest of the Intermediate Water mass just above it (see figures 5.13 and 5.14). Worthington (1981) referred to this transitional water as a separate water mass. He called it an unnamed water mass of considerable volume found between the AAIW and the North Atlantic Deep Water (NADW) in the South Atlantic Ocean, and between the AAIW and the Antarctic Bottom Water (AABW) in the South Pacific and Indian Oceans. It is also found south of the southern limit of NADW, and in the North Pacific it is found between the North Pacific Intermediate Water and the bottom water. This unnamed water mass presumably originates south of the Antarctic Polar Front. According to Worthington's census 31 % of this water is found in the North Pacific; 31 % in the South Pacific; 17 % in the Indian Ocean; and 21 % in the South Atlantic Ocean. In this analysis no distinction is made between the AAIW and the transitional (unnamed) water or between the latter and the NADW or Circumpolar Deep Water (CDW). Only between the AAIW and the Deep Water (NADW and CDW) is distinguished in this study.

The definitions of the water masses of the Agulhas Retroflection Area, as discussed in Chapter 2 and summarized in Table 2.1, and the volumetric calculations were merged to give some idea of how much of each of the water masses there is in this area. The upper 1500 m of the water column has a total volume (sampled one-degree-squares only) of 1537,0 x 10^3 km^3. The surface water has a volume of 130,0 x 10^3 km^3 which is 8,46 per cent of the total volume (upper 1500 m) in the Retroflection area. The Central Water makes up about one third of the total, namely 525,8 x 10^3 km^3 or 34,21 per cent. The Antarctic Intermediate Water being the dominant water mass (volume wise) represents more than fifty per cent of the total namely 805,4 x 10^3 km^3, or 52,40 per cent. The rest of the volume (4,93 per cent) is made up by the low salinity water from south of the Subtropical Convergence (less than one per cent) and water that either does not fall within a specific definition or is at the boundary or transition of the different water masses. These results are summarized in table 5.1.

Table 5.1. Volumes of the water masses of the upper 1500 m of the water column in the Agulhas Retroflection Area.

Water mass	Volume	Percentage of total
Surface Water	130,0 x 10^3 km^3	8,46
Central Water	525,8 x 10^3 km^3	34,21
Antarctic Intermediate Water	805,4 x 10^3 km^3	52,40
Others	75,8 x 10^3 km^3	4,93
TOTAL	1 537,0 x 10^3 km^3	100,00

Unfortunately no really reliable quantitative estimates of the volumes of the thermocline and warm water masses exist in the world (Worthington, 1981). So these results could not really be put into perspective as far as the world ocean is concerned.

5.2.2.2 Bottom stations - data set

The results of the volumetric analysis of the bottom station data are portrayed in figures 5.21 and 5.22. These two figures look dramatically different, as far as elevation (volume) is concerned, from figures 5.19 and 5.20. Note that the scale of the Z-axis has changed from 0-5 x 1000 km^3 to 0-50 x 1000 km^3. Surface Water, Central Water and to a large extend AAIW have very little elevation (volume) compared to the Deep Water and Bottom Water. This is not uncommon and is in fact a good reflection of the situation in the world ocean. Worthington (1981) observed that such well-known masses like the AAIW and Mediterranean Outflow Water are barely perceptible in the 3-D diagrams. These mid-depth water masses have little volume relative to the deep water masses (even more so for a shallower water mass like Central Water) and moreover, their T/S characteristics are diverse, so that their volumes are spread over a wide area (T/S space) with little elevation.

High volumes on these (figures 5.21 and 5.22) diagrams are basically limited to the area (T/S space) colder than 3°C. There are two peaks in the volume. The bigger one corresponds to the θ-S of the Deep Water (North Atlantic Deep Water) while the other peak corresponds to the θ-S of Antarctic Bottom Water/Circumpolar Deep Water (AABW/CDW). The ten highest volume, fine-scale classes have a volume of 311,1 x 10^3 km^3 which is 13,00 percent of the total volume of the water in the Agulhas Retroflection Area. Nine of these fine-scale classes are in the NADW and only one in the Circumpolar Deep Water/Antarctic Bottom Water (figure 5.23). Only 21 of these fine-scale classes make up 25 percent of the total volume of the water (593,1 x 10^3 km^3 or 24,78 %). Of these classes 13 contain NADW while the rest (eight classes) contain CDW/AABW. The top seventy one highest ranked (in order of volume) classes add up to 50 percent of the total volume of the water in the Retroflection area. All (except five) of these seventy one classed contain water whose θ-S characteristics correspond to Deep or Bottom Water (figure 5.23). The other five classes fall within the AAIW θ-S space, more specifically transitional or 'unnamed' water mass (Worthington, 1981) space. All of these 71 classes (and therefor 50 % of the water) have temperatures below 3°C. In fact if one were to add the lower volume non-ranked classes almost seventy percent (67,26%) of all the water in the Retroflection Area is colder than 3°C.

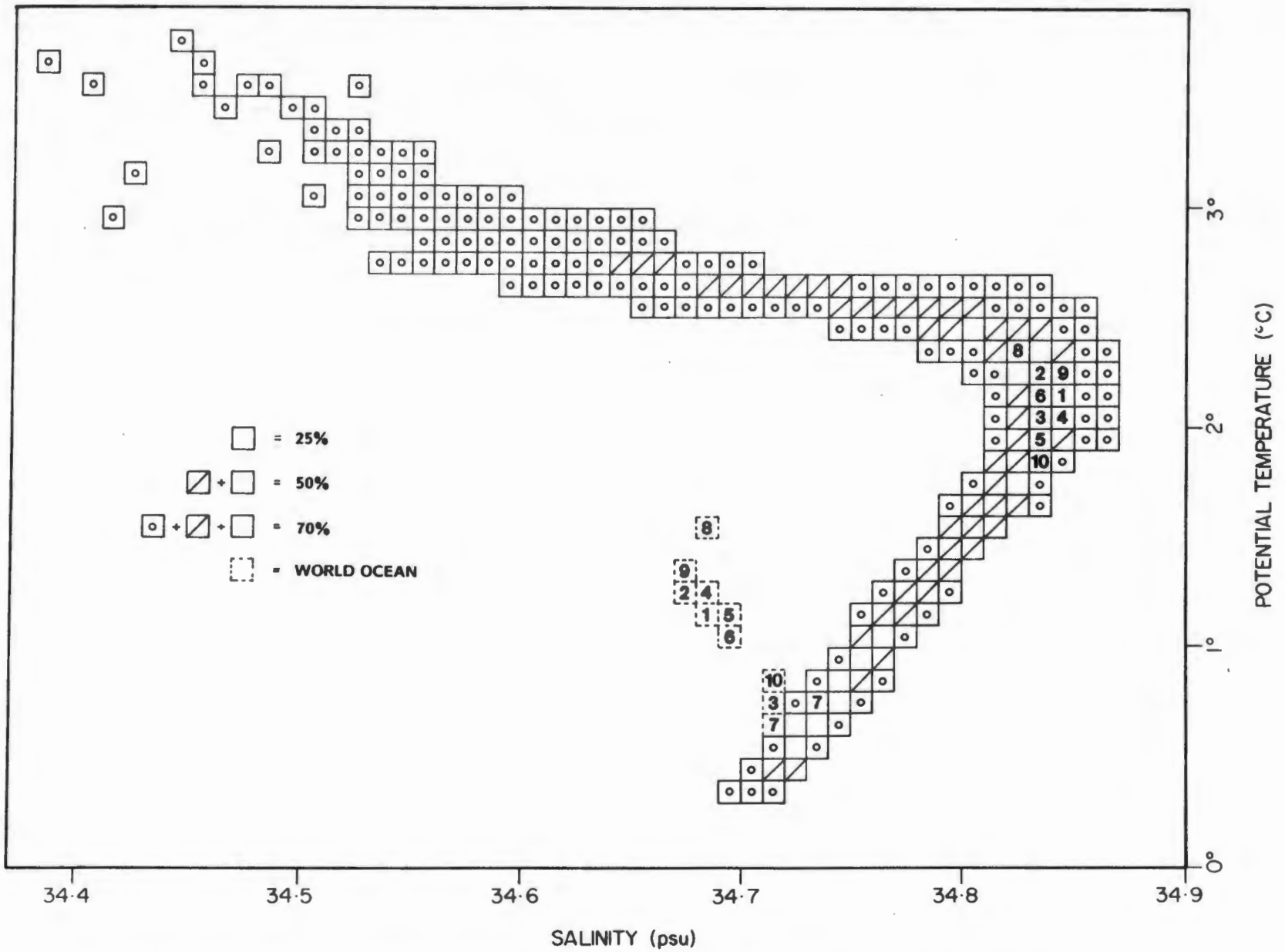

Figure 5.23 The 226 highest volume fine-scale classes that contain almost seventy percent (67,26 %) of the water in the Retroflection area. The ten highest ranked classes are numbered (1-10). The ten highest volume classes of the world ocean are also indicated to facilitate comparison.

It is obvious from the above that the Deep Water and more spesifically the North Atlantic Deep Water is the dominant water mass in this geographical area. It represents 40 percent of the total volume of the water of the Retroflection area. If one should add Worthington's so called 'unnamed' water mass and the Circumpolar Deep Water, the Deep Water would then represent more than 60 percent of the total volume (Table 5.2). Very little AABW is present in the Retroflection area.

The contributions from the upper layers of the water column (Surface-, Central- and Intermediate Water) to the total volume of the whole water column compared to their contributions to the upper 1500 m of the water column are decreased by more than 50 %. Surface Water's total has decreased from 8,46 percent (1500 m) to 3,43 percent (whole water column) of the total (tables 5.1 and 5.2). The Central Water showed a similar decrease from 34,21 percent to 12,99 percent and the Antarctic Intermediate Water from 52,40 percent to 22,93 percent. The totals for the different water masses are given in table 5.2.

Table 5.2. Volumes of the Water Masses of the Agulhas Retroflection Area.

Water mass	Volume	Percentage of total
Surface Water	82,1 x 10^3 km^3	3,43
Central Water	310,9 x 10^3 km^3	12,99
Antarctic Intermediate Water	548,8 x 10^3 km^3	22,93
North Atlantic Deep Water	954,1 x 10^3 km^3	39,86
Circumpolar Deep Water/ Antarctic Bottom Water	457,9 x 10^3 km^3	19,13
Others	39,7 x 10^3 km^3	1,66
TOTAL	2 393,5 x 10^3 km^3	100,00

It should be stressed here that the actual volumes mentioned are for the sampled one-degree-squares only (figures 5.10 and 5.11). The assumption is made that the distribution of the sampled squares is such that sampled squares are representative of the whole Retroflection area. It is assumed that the T/S characteristics and therefore volumetrics of the unsampled squares are unlikely to be significantly different from that of the sampled ones. It is therefore more reliable to use the percentages rather than the actual volumes. In comparable studies (Cochrane, 1958; Montgomery, 1958; Pollak, 1958; Wright and Worthington, 1970 and Worthington, 1981) the sample size is calculated as a percentage of the total volume of the whole ocean or basin or sea. The calculated volumes are then subsequently adjusted to make up the total volume of a specific ocean or basin. This was not done in this case. So the only sensible way to compare the results of this analysis with other comparable studies is to use percentages.

The thermocline (> 4°C) and warm (> 16°C) water masses of the world ocean are dwarfed by the great volumes of the Deep Water masses. This is also the case in the Retroflection area, as shown above (see figures 5.21) and 5.22). A logarithmic volume scale for the results as

presented in figures 5.21 and 5.22 has been suggested so that the warm and thermocline waters could be made to stand out more clearly, but one of the principal virtues of the volumetric T/S diagram (according to Worthington, 1981) is that it displays the relative abundances of the water masses as they actually exist. Hence the decision rather to split the volumetric analysis of the Retroflection area into two (shallow or/1500 m stations and bottom stations).

For the first time a really reliable quantitative estimate of the volumes of the thermocline and warm water masses for an extended area is presented (figures 5.19 and 5.20 and table 5.1). Worthington (1981) has acknowledged the lack of any reliable estimates for the thermocline and warm water masses of the world ocean at the time, but could contribute little to amend the situation. He produced a contoured volumetric diagram representing the upper layers but warned that it is merely a sketch. Other than this there are only Wyrtki's (1971) volumetric diagrams for the Indian Ocean and those of Wright and Worthington (1970) for the North Atlantic that can be referred to. For the other oceans, the warm-water diagrams (coarse-scale) of Montgomery (1958), Cochrane (1958) and Pollak (1958) still stand. Their classes were too large though. If the fine-scale classes of this study were to be merged into divisions as large as 0,5 ‰ of salinity, as Cochrane and Pollak have done, or 1,0 ‰ as Montgomery has done, most of the detail of figures 5.19 and 5.20 would be lost and the high volume peaks would be artificially blurred.

Worthington (1981) produced a simulated three-dimensional T/S diagram of the water masses of the world ocean (figure 5.24). The apparent elevation is proportional to volume. This makes it a very useful diagram. Not only does it provide one with a summary, at a glance, of the distribution of the water masses according to their T/S characteristics but also of the proportional volumes of the water masses. Most of the elevation (volume) is restricted to a very limited space in T/S co-ordinates (T = 1,0 - 3,0°C and Salinity = 34,60 - 34,75 ‰). By far the largest part of the volume of the world ocean water is fresher than 34,75 ‰. The highest peak on this diagram corresponds to the highest volume per bivariate class of 0,1°C and 0,01 ‰. This particular class (defined by temperature = 1,1 - 1,2°C and salinity = 34,68 - 34,69 ‰) contain 25 973,0 x 10^3 km^3 water compared to the 46,7 x 10^3 km^3 water of the highest volume class (T = 2,1 - 2,2°C and S = 34,84 - 34,85 psu) in the Retroflection area. This high volume class (world ocean) contains more water (26 x 10^6 km^3) than all the water in the world ocean warmer than 19°C (21,9 x 10^6 km^3) according to Worthington (1981). In fact it contains more than ten times the total of all the water in the Retroflection area (sampled squares only). If one, however, considers what percentage of the total these highest volume classes represent, a good comparison is revealed. The highest volume class of the world ocean represents 1,97 percent of the total volume of the world ocean compared to 1,95 percent of the total volume of the Retroflection area presented by the highest volume class of this analysis.

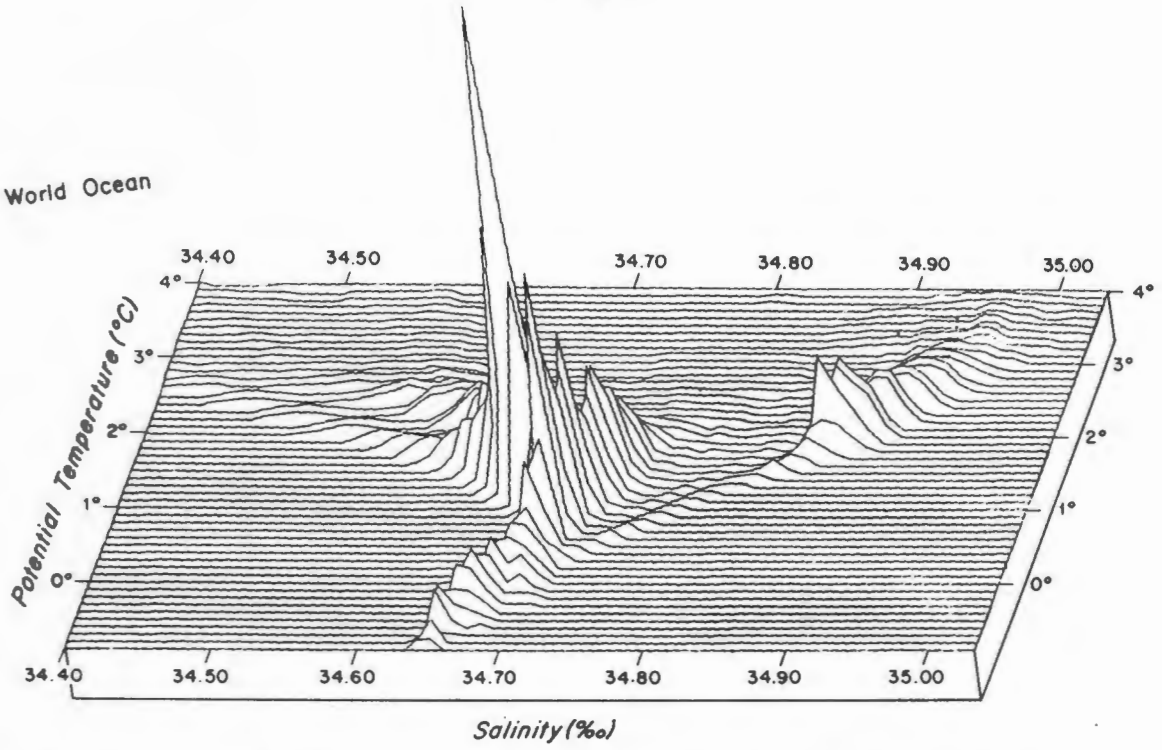

Figure 5.24 Simulated three-dimension T/S diagram of the water masses of the world ocean. Apparent elevation is proportion to volume. The elevation of the highest peak corresponds to 26,0 x $10^6 km^3$ per bivariate class 0,1°C x 0,01 ‰ (from Worthington, 1981).

All the water in this high volume class (world ocean) is exclusive to the Pacific Ocean. In fact most of the top ten volume classes (except rank numbers 3, 7 and 10) which represent 7,5% of the total, contain water that is exclusive to the Pacific Ocean (figure 5.23). Worthington divided his composite three-dimensional T/S-diagram (figure 5.24) into the different oceans (figure 5.25). From these it is obvious that the Pacific not only contains the highest volume classes (figure 5.25a) but has also the largest volume compared to the other oceans (see also table 5.3).

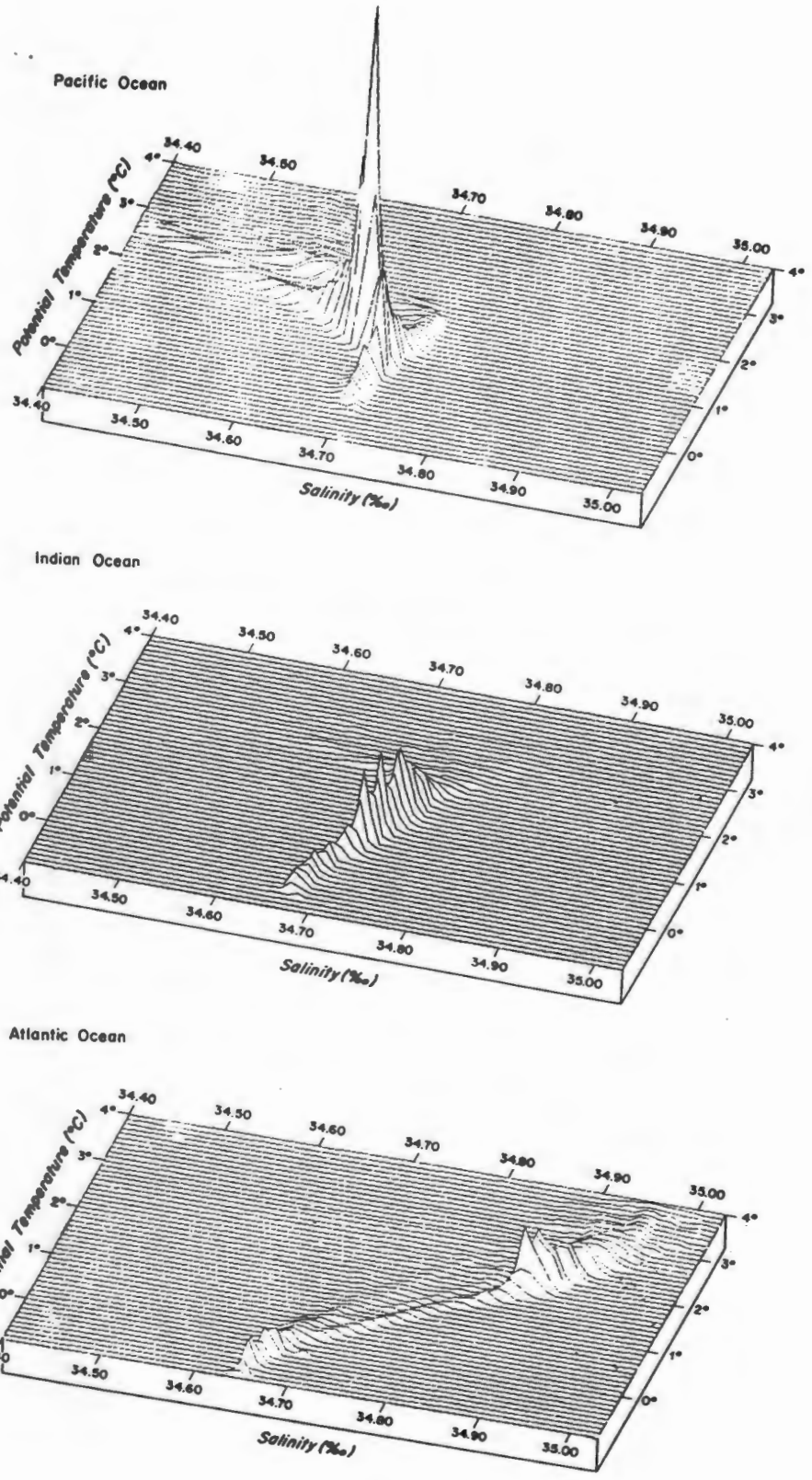

Figure 5.25 Simulated three-dimensional T/S diagrams of the water masses of the world oceans - (a) Pacific Ocean, (b) Indian Ocean and (c) Atlantic Ocean. Apparent elevation is proportional to volume (from Worthington, 1981).

Table 5.3. Volumes of the different oceans of the world, excluding adjacent seas. Volumes are given in $km^3 \times 10^3$. Volumes in brackets ( ) are for the different sectors of the Southern Ocean while percentage are given in square brackets [ ].

	Pacific	Atlantic	Indian	Southern
Volume:	656 173 [50]	295 460 [22]	245 974 [19]	
	(55 413) [4]	(30 738) [2]	(36 730) [3]	122 881 [9]
	711 586 [54]	326 198 [24]	282 704 [22]	
Total:	**1 320 488 x 10^3 km^3**			

(Adapted from Worthington, 1981)

The boundary of the Southern Ocean in this particular case is taken as 55°S.

According to Worthington's (1981) census (table 5.3) the Pacific contains about 50 percent of the total volume of the world ocean. The Pacific is also the freshest of the oceans of the world. Most of the water in the Pacific has a salinity of less than 34,70 ‰. Worthington calculated a mean salinity of 34,60 ‰ and a mean potential temperature (θ) of 3,14°C for the Pacific. He warned against the indiscriminate use of these means, though. The accuracy of these means depends on the percentage of the ocean that has been sampled (surveyed). It is assumed that the water in the unsurveyed areas of each ocean is divided into the same T/S classes as that of the surveyed areas and in the same proportion. This assumption has the effect of assigning artificially large volumes of water to classes that are found where coverage is good.

The Southern Ocean (defined in this case as south of 55°S) is the coldest (mean θ = 0,71°C) and after the Pacific the next freshest (figure 5.25b and c). The Indian Ocean (figure 5.25b) has a mean salinity of about 34,78 ‰. Although each ocean has bivariate classes that are exclusive to that ocean (e.g. of the 34 highest volume classes 18 are exclusive to the Pacific) the Pacific and Indian Oceans are much more similar to each other than to the Atlantic. The latter is the most eccentric of the oceans, standing aloof on the saline side of the diagram (figure 5.25c, connected to the Southern Ocean only by a narrow umbilicus that contains little water. Three of the top ten highest volume classes namely 3, 7 and 10 (rank number in order of volume) are circumpolar classes (figure 5.23). They contain a cosmopolitan type of water that is found in all the oceans except the North Pacific and the North Atlantic. If the distribution of the bulk of the water (colder than 3°C) of the Retroflection area is fitted onto Worthington's simulated 3-D diagram (figure 5.24) it would slot in between the two peaks that represent the Indian Ocean and the Atlantic Ocean respectively. This is as expected taking into account the geographical position of the Retroflection Area. The highest peak on figures 5.21 and 5.22 that corresponds more or less with T = 2,0 - 2,3°C and S = 34,80 - 34,83 psu would fit in right next to (fresh side of) the highest peak of the Atlantic Ocean (figure 5.25c).

The most abundant classes, those that together contain 50 percent of the volume of the world ocean (according to Worthington's 1981 census) all fall into numbered (ranked by volume) classes 1 to 186 (figure 5.26). In his analysis they all fall below 3°C. There are two groupings of numbers. On the fresh side are the high volume classes of the Pacific-, Indian- and Southern Ocean and on the saline side the high volume classes of the Atlantic Ocean. There are no high volume classes that connect the Atlantic Ocean to the circumpolar oceans, but there is a thin group of relatively small-volume classes that does make the connection (according to Worthington, 1981, figure 5.25c). Positioning the classes ranked 1-71 that represent 50 percent of the water of the Retroflection area onto Worthington's diagram (figure 5.26) it becomes clear that most of these classes form part of the small-volume classes that makes the connection between the Atlantic and the circumpolar ocean. The connection is made at the cosmopolitan classes ~ 0,5°C and 34,71 ‰. Above ~ 2,0°C the classes of the Retroflection Area lie between the high volume classes of the Atlantic and Indian Oceans. They are probably products of the mixing of the waters of the two oceans.

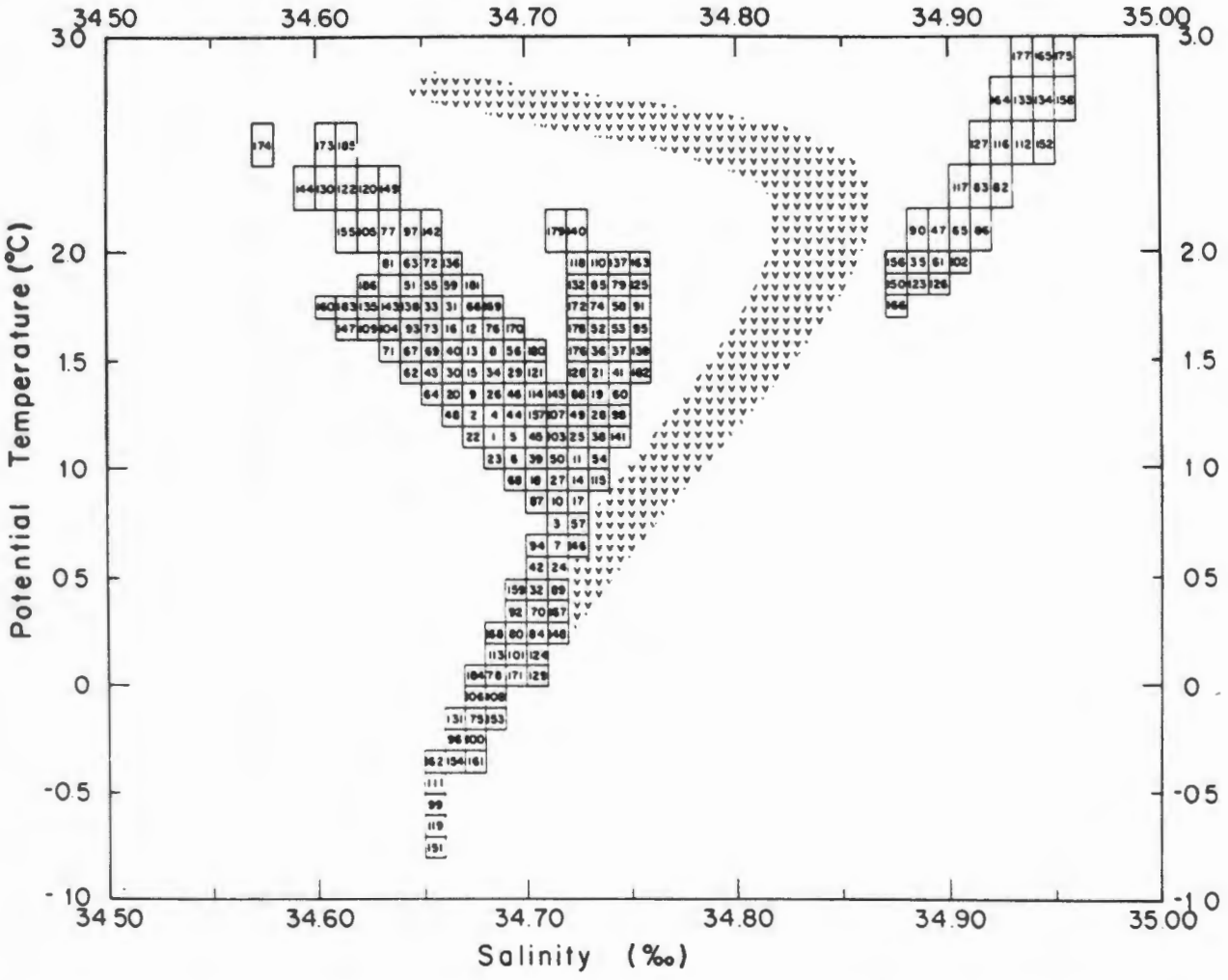

Figure 5.26 Catalogue of the 186 most abundant fine-scale bivariate classes in the world ocean (adapted from Worthington, 1981). These classes contain 50 % of the world-ocean volume. The number in each bivariate class represents its ranking according to volume. The most abundant classes (ranked 1-71) that contain 50 % of the water of the Retroflection area are represented by the hatched area.

The water masses that embrace 50 percent of the volume of the world ocean are diverse, owing to the widely different locations in which they have been formed and, presumably, to slow changes that have taken place in these water masses since their formation as the result of mixing with the water masses that they are in contact with. In contrast to the world ocean the Atlantic is far less diverse. Wright and Worthington (1970) have shown that compared to the 186 fine-scale classes that make up 50 percent of the total of the world ocean, 50 percent of the total of the North Atlantic is contained in only 43 classes, despite the fact that they identified five separate sources of deep water for the North Atlantic. The relatively smaller area (North Atlantic) sampled, compared to the world ocean, is probably also contributing to the smaller diversity of classes. The same is most likely true for the Retroflection area. The top ten (ranked 1 to 10) highest volume classes (figure 5.23) contain 14,3 percent of the total compared to only 10,1 percent of the total of the world ocean contained in the top ten classes. Like-wise 21 classes (Retroflection) contain 25 percent while 21 classes (world ocean) only contain 16 percent of the total. In fact more than double the number of classes (45) are 'needed' to embrace 25 percent of the total. Classes 1-71 contain 50 percent of the total in the Retroflection area compared to classes 1-186 for 50 percent of the total of the world ocean. As the volume of these fine-scale bivariate classes diminishes, their diversity increases; 50 percent of the world ocean's volume is contained in only 186 classes, while the next 25 percent requires 507 classes. In the same way 50 percent of the Retroflection area is contained in 71 classes while the next 20 percent requires 269 classes. The Retroflection area is very small and therefore expected to be less diverse. Its geographic position in relation to the oceans of the world, the influence of the Agulhas Current and the fact that it is considered to be a crossroads for water masses from several different geographical regions, on the other, hand would favour diversity.

In general, expanding the description from 50 percent to 75 percent or to 69 % (in the case of the Retroflection Area) results in the addition of a few deeper classes, compared to the greater number of warmer classes.

The conclusions and a summary of the results are presented in the following chapter.

CHAPTER 6

CONCLUSIONS

There is little doubt about the significant and crucial role that the Agulhas Retroflection area plays in global as well as local weather and climate. It has received fair recognition, judging by the substantial number of studies and publications on this area, as one of the most important oceanic areas of its size in the world. With the recent emphasis on the predicted global warming and subsequent climate change, and the launching of large scale international projects such as the World Ocean Circulation Experiment (WOCE), the area will probably continue to receive the attention of many researchers and observers. Therefore, it is important that one of the serious gaps in our understanding of this area, namely that of water mass identification and description be addressed. After describing the water masses briefly (Chapter 2), I became more convinced that a thorough detailed description of the water masses of the Retroflection area could enhance considerably our understanding of this very dynamic area and lay the foundation for more dynamic studies (using synoptic data), such as water mass modifications and interrelations. The excellent data set used for this volumetric analysis supplemented by historic data, could be employed for such a study.

The subtle differences between Central Water of South Atlantic Ocean origin and that of South Indian Ocean origin have been addressed in this thesis. I have shown, using historic data (like Clowes, 1950) and high quality, high resolution CTD data (with combined cruises as well as individual stations), that the differences are real and distinguishable. Chapman et. al. (1987) used nutrients to distinguish between waters of Agulhas and Atlantic origin and Chapman and Largier (1989) used CTD data from individual cruises to distinguish between the two types of Central Water on the Agulhas Bank. I conclude, therefore, that using the quality of data acquired with a CTD it should be possible to distinguish between Central Water of different origins. Furthermore, it should be possible to make the distinction using synoptic data, by substituting either temperature or salinity with a parameter such as nutrients or dissolved oxygen.

Significant volumetric results are possible even with large bivariate classes and poor horizontal and vertical resolution data. Most of the earlier work (e.g. Montgomery, 1958; Cochrane, 1958 and Pollak, 1958) is still valid today as a first approximation. In an upwelling environment the results could be even more significant, as shown by Carmack and Aagaard (1977) and by the pilot study conducted in the Benguela upwelling regime (this thesis). For example, the volumes of water available for upwelling in each bivariate T/S class of Central Water seem to be constant. This implies that the intensity of upwelling may be estimated from the salinity of the upwelled water only.

The serious gap that existed in the fine-scale census of the world ocean (Worthington, 1981) is amended by this thesis to a large extent. In the process, new standards are set as far as the data are concerned. All the data used were acquired with the same type of instrument (CTD), which makes this the most uniform data set ever to be employed for a volumetric census over an extensive area. The data were also collected over only 3,5 years which makes it the shortest time span (excluding synoptic data) ever employed for a general volumetric survey. The vertical resolution of the data are incredibly fine. One meter intervals have been used for this analysis, but the quality of the data is such that an even smaller interval could have been used.

Although the high volume classes of the Retroflection area are not of the same order as those of the world ocean, these classes compare remarkably well percentage-wise. The warm and thermocline water masses and even the intermediate waters are dwarfed by the greater volumes of the deep water masses. About 70 percent of all the water in the Agulhas Retroflection area is colder than 3°C. The water in the Retroflection area is less diverse than that of the world ocean, mainly due to the restricted geographical area of the region. Fifty percent of Retroflection water is contained in 71 fine-scale classes compared to the 186 classes 'needed' to contain 50% of the world ocean. Only 21 fine-scale classes make up 25 % of the total volume of the water in the Retroflection area.

By dividing the volumetric analysis into two parts (upper 1500 m and bottom stations), a reliable quantitative estimate for the thermocline (> 4°C) and warm water (> 16°C) masses was produced for the first time. The warm, saline surface water contributes very little to the overall volume of the upper 1500 m of the water column in the Retroflection area. The low salinity water from south of the Subtropical Convergence is widely spread on the less saline side of the three-dimensional diagrams and has very little volume (less than 1 % of the total). The more saline, higher volume section of the Central Water in this area corresponds to South West Indian Central Water. Because the deep water masses of the world ocean and those of the Retroflection compare so favourably, one is tempted to extrapolate the results of the thermocline and warm water, but I would advise strongly against this.

As the volume of the fine-scale classes diminishes they become more diverse e.g. 50% of the water in the world ocean is contained in 186 classes while the next 25% requires 507 classes. I share Worthington's belief that if perfect observations of temperature and salinity were available the number of classes that contain the greater part of the volume of the world ocean would be fewer. Even the number of deep classes could be fewer. The ocean is probably more finely stratified than we can observe (with the available data) at the present time.

Worthington (1981) expressed dismay at the decrease in the rate of acquisition of new high-quality data. This is due, in part, to trends in modern physical oceanography in which the dramatic improvements in direct current measurements have taken priority over routine measurements of water properties on a large scale. This may not be true entirely for the Agulhas Retroflection area. We may see an increase in data acquisition owing to large

international projects like WOCE. Be that as it may, the recent excellent data set is far from fully utilized. The volumetric method as employed in this thesis, could be applied to the same data set, but instead of combining cruises quasi-synoptic data could be used. One could concentrate on specific water masses and dynamic processes such as mixing and water mass interrelations. Either nutrients or dissolved oxygen could be substituted for one of the parameters (θ or salinity) and volumetric diagrammes produced for them. This could yield exciting results as demonstrated to some extent by Carmack and Aagaard (1977), and enhance our knowledge and understanding of the area.

REFERENCES

Anon, 1985: Physical, chemical and *in-situ* CTD data from the AJAX Expedition aboard *R.V. Knorr*, University of California, Scripps Institution of Oceanography SIO-85-24 and Texas A & M University, Department of Oceanography TAMU-85-4-D, 275 pp.

Bang, N.D., 1970: Dynamic interpretations of a detailed surface temperature chart of the Agulhas Current retroflexion and fragmentation area, *South African Geographical Journal*, **52**, 67-76.

Bang, N.D. and F.C. Pearse, 1970: Hydrological data, Agulhas Current Project, March 1969, *Data Report 4*, 26 pp., Institute of Oceanography, University of Cape Town, South Africa.

Bennett, S.L., 1988: Where three oceans meet: the Agulhas Retroflection region, *PhD Thesis, Massachusetts Institute of Technology/Woods Hole Oceanographic Institution*, Woods Hole, Massachusetts, 367 pp.

Boudra, D.B. and W.P.M. de Ruijter, 1986: The wind-driven circulation in the South Atlantic-Indian Ocean-II. Experiments using a multi-layer numerical model, *Deep-Sea Research*, **33**, 447-482.

Broecker, W.S. and T. Takahashi, 1985: Sources and flow patterns of deep-ocean waters as deduced from potential temperature, salinity and initial phosphate concentration, *Journal of Geophysical Research*, **90**, 6925-6939.

Brundrit, G.B., L.G. Underhill and L.V. Shannon, 1990: Linear stochastic models of hake recruitment incorporating environmental change: representation and forecasting, *Selected Papers ICSEAF*, in press.

Bunker, A.F. 1980: Trends of variables and energy fluxes over the Atlantic Ocean from 1948 to 1972, *Monthly Weather Review*, **108**, 720-728.

Camp, D.B., W.E. Haines, B.A. Huber, S.E. Rennie and A.L. Gordon, 1986: Agulhas Retroflection Cruise (ARC), November-December 1983, Hydrographic (CTD) data, Lamont-Doherty Geological Observatory of Columbia University *Technical Report*, LDGO-86-1, 390 pp.

Carmack, E.C., 1977: Water characteristics of the Southern Ocean south of the Polar Front, In *A Voyage of Discovery: George Deacon 70th Anniversary Volume*, M.Angle (Ed.), supplement to *Deep-Sea Research*, Pergamon Press, Oxford, 15-41.

Carmack, E.C. and K. Aagaard, 1977: A note on volumetric considerations of upwelling in the Benguela Current, *Estuarine and Coastal Marine Science*, **5**, 135-142.

Catzel, R. and J.R.E. Lutjeharms, 1987: Agulhas Current border phenomena along the Agulhas Bank south of Africa, *CSIR Research Report*, **635**, 22 pp. + 30 pp. of figures + 43 pp. appendix.

Chapman, P., 1988: On the occurrence of oxygen-depleted water south of Africa and its implications for Agulhas-Atlantic mixing, *South African Journal of Marine Science*, 7, 267-294.

Chapman, P. and J.L. Largier, 1989: On the origin of Agulhas Bank bottom water, *South African Journal of Science*, **85**, 515-519.

Chapman, P., C. Duncombe Rae and B.R. Allanson, 1987: Nutrient, chlorophyll and oxygen relationships in the surface layers at the Agulhas retroflection, *Deep-Sea Research*, **34**, 1399-1416.

Cheney, R.E., J.G. Marsh and B.D. Beckley, 1983: Global mesoscale variability from collinear tracks of SEASAT altimeter data, *Journal of Geophysical Research*, **88**, 4343-4354.

Clowes, A.J., 1950: An introduction to the hydrology of South African waters, *Investigational Report of the Fisheries and Marine Biological Survey Division of South Africa*, **12**, 42 pp. + 20 pp. of charts.

Clowes, A.J. and G.E.R. Deacon, 1935: The deep-water circulation of the Indian Ocean, *Nature*, London, **136**, 936-938.

Cochrane, J.D., 1956: The frequency distribution of surface-water characteristics in the Pacific Ocean, *Deep-Sea Research*, **4**, 45-53.

Cochrane, J.D., 1958: The frequency distribution of water characteristics in the Pacific Ocean, *Deep-Sea Research*, **5**, 111-127.

Colton, M.T. and R.R.P. Chase, 1983: Interaction of the Antarctic Circumpolar Current with bottom topography: An investigation using satellite altimetry, *Journal of Geophysical Research*, **88**, 1825-1843.

Darbyshire, J., 1964: A hydrological investigation of the Agulhas Current area, *Deep-Sea Research*, **11**, 781-815.

De Ruijter, W.P.M., 1982: Asymptotic analysis of the Agulhas Current, *Review of Pure and Applied Geophysics*, **12**, 361-373.

De Ruijter, W.P.M. and D.B. Boudra, 1985: The wind-driven circulation in the South Atlantic-Indian Ocean - I. Numerical experiments in a one-layer model, *Deep-Sea Research*, **32**, 557-574.

Dietrich, G., 1935: Aufbau und Dynamik des südlichen Agulhasstromgebietes, *Veröffentlichungen des Institut für Meereskunde*, University of Berlin, 80 pp.

Dietrich, G., 1936: Aufbau und Bewegung von Golfstrom und Agulhasstrom, eine vergleichende Betrachtung, *Naturwissenschaft*, **24**, 225-230.

Dietrich, G., 1964: *General Oceanography*, Wiley, New York.

Duncan, C.P., 1968: An eddy in the Subtropical Convergence southwest of South Africa, *Journal of Geophysical Research*, **73**, 531-534.

Duncan, C.P., 1970: The Agulhas Current, *PhD Thesis, University of Hawaii*, 76pp.

Eagle, G.A. and M.J. Orren, 1985: A seasonal investigation of the nutrients and dissolved oxygen in the water column along two lines of stations south and west of South Africa, *CSIR Research Report 567*, 52pp.

Emery, W.J. and J.S. Dewar, 1982: Mean Temperature-Salinity, Salinity-Depth and Temperature-Depth curves for the North Atlantic and the North Pacific, *Progress in Oceanography*, **11**, 219-305.

Emery, W.J. and J. Meincke, 1986: Global water masses: Summary and Review, *Oceanologia Acta*, **9**, 383-391.

Fine, R.A., M.J. Warner and R.F. Weiss, 1988: Water mass modification at the Agulhas Retroflection: chlorofluoromethane studies, *Deep-Sea Research*, **35**, 311-332.

Fu, L., 1986: Mass, heat and freshwater fluxes in the South Indian Ocean, *Journal of Physical Oceanography*, **16**, 1683-1693.

Fuglister, F.C., 1960: Atlantic Ocean Atlas of temperature and salinity profiles and data from the International Geophysical Year of 1957-1958. *Woods Hole Oceanographic Institution Atlas Series*, **1**, 209 pp.

Garrett, J., 1981: Oceanographic features revealed by the FGGE drifting buoy array, In *Oceanography from Space*, J.F.R. Gower (Ed.), Plenum Press, New York, pp. 61-69.

Gill, A.E. and E.H. Schumann, 1979: Topographically induced changes in the structure of an inertial coastal jet : application to the Agulhas Current, *Journal of Physical Oceanography*, **9**, 975-991.

Gordon, A.L., 1981: South Atlantic thermocline ventilation, *Deep-Sea Research*, **28**, 1239-1264.

Gordon, A.L., 1985: Indian-Atlantic transfer of thermocline water of the Agulhas retroflection, *Science*, **227**: 1030-1033.

Gordon, A.L., 1986: Inter-ocean exchange of thermocline water, *Journal of Geophysical Research*, **91**, 5037-5046.

Gordon, A.L. and W.F. Haxby, 1990: Agulhas eddies invade the South Atlantic - Evidence from GEOSAT altimeter and shipboard CTD, *Journal of Geophysical Research, Special GEOSAT edition*, submitted.

Gordon, A.L., J.R.E. Lutjeharms and M.L. Gründlingh, 1987: Stratification and circulation at the Agulhas Retroflection, *Deep-Sea Research*, **34**, 565-599.

Gründlingh, M.L., 1977: Drift observations from Nimbus VI satellite-tracked buoys in the southwestern Indian Ocean, *Deep-Sea Research*, **24**, 903-913.

Gründlingh, M.L., 1978: Drift of a satellite-tracked buoy in the southern Agulhas Current and Agulhas Return Current, *Deep-Sea Research*, **25**, 1209-1224.

Gründlingh, M.L., 1979: Observation of a large meander in the Agulhas Current, *Journal of Geophysical Research*, **84**, 3776-3778.

Gründlingh, M.L., 1980: On the volume transport of the Agulhas Current, *Deep-Sea Research*, **27**, 557-563.

Gründlingh, M.L., 1983: On the course of the Agulhas Current, *South African Geographical Journal*, **65**, 49-57.

Gründlingh, M.L., 1985: Occurrence of Red Sea Water in the southwestern Indian Ocean, 1981, *Journal of Physical Oceanography*, **15**, 207-212.

Gründlingh, M.L., 1986: Features of the northern Agulhas Current in spring, 1983, *South African Journal of Science*, **82**, 18-20.

Gründlingh, M.L. and J.R.E. Lutjeharms, 1979: Large scale flow patterns of the Agulhas Current system, *South African Journal of Science*, **75**, 269-270.

Harris, T.F.W., 1972: Sources of the Agulhas Current in the spring of 1964, *Deep-Sea Research*, **19**, 633-650.

Harris, T.F.W. and N.D. Bang, 1974: Topographic Rossby waves in the Agulhas Current, *South African Journal of Science*, **70**, 212-214.

Harris, T.F.W. and D. van Foreest, 1978: The Agulhas Current in March 1969, *Deep-Sea Research*, **25**, 549-561.

Harris, T.F.W., R. Legeckis and D. van Foreest, 1978: Satellite infra-red images in the Agulhas Current system, *Deep-Sea Research*, **25**, 543-548.

Harrison, M.S.J., S.R. Juhnke and N.D. Walker, 1990: Circulation differences between one wet and one dry month of October and January over the interior of South Africa, *Journal of Climatology*, submitted.

Harvey, J., 1982: θ-S relationships and water masses in the eastern North Atlantic, *Deep-Sea Research*, **29**, 1021-1033.

Hastenrath, S., 1982: On meridional heat transports in the world ocean, *Journal of Physical Oceanography*, **12**, 922-927.

Helland-Hansen, B., 1916: Nogen hydrografiske metoder, In *Forhandlinger ved de 16 Skandinaviske Naturforskerermøte*, 357-359.

Helland-Hansen, B., 1918: Nogen hydrografiske metoder. *Forhandlinger ved de Skandinaviske Naturforsketesmøte*, **Kristiania, 10-15 July 1916**.

Helland-Hansen, B., 1930: Physical oceanography and meteorology. Bergen Museum, *Report on the scientific results of the "Michael Sars" North Atlantic Deep-Sea Expedition 1910*, **1**, 115 + 102 pp.

Helland-Hansen, B. and F. Nansen, 1926: The eastern North Atlantic, *Geofysiske Publikasjoner*, **4**, 76 pp. + 71 plates.

Hellerman, S. and M. Rosenstein, 1983: Normal monthly wind stress over the world ocean with error estimates, *Journal of Physical Oceanography*, **13**, 1093-1104.

Hsueh, Y. and J.J. O'Brien, 1971: Steady coastal upwelling induced by an alongshore current, *Journal of Physical Oceanography*, **6**, 238-242.

Jacobs, S.S. and D.T. Georgi, 1977: Observations on the South-west Indian/Antarctic Ocean, In *A voyage of discovery: George Deacon 70th anniversary volume*, **24**, M. Angel (Ed.) Supplement to *Deep-Sea Research*, Pergamon Press, Oxford, pp. 43-84.

Jury, M.R. and N.D. Walker, 1988: Marine boundary layer modification across the edge of the Agulhas Current, *Journal of Geophysical Research*, **93**, 647-654.

Kossina, E., 1921: Die Tiefen des Weltmeeres. Berlin University, Institut für Meereskunde, N.F. A *Geographische-naturwissenschaftliche Reihe*, **9**, 70 pp.

Lutjeharms, J.R.E., 1972: A quantitative assessment of year-to-year variability in water movement in the southwest Indian Ocean, *Nature*, London, **239**, 59-60.

Lutjeharms, J.R.E., 1976: The Agulhas Current system during the northeast monsoon season, *Journal of Physical Oceanography*, **6**, 665-670.

Lutjeharms, J.R.E., 1979: Interaction between the Agulhas Current and the Subtropical Convergence, *CSIR Research Report*, **384**.

Lutjeharms, J.R.E. 1981a: Spatial scales and intensities of circulation in the ocean areas adjacent to South Africa, *Deep-Sea Research*, **28**, 1289-1302.

Lutjeharms, J.R.E. 1981b: Features of the Southern Agulhas Current Circulation from satellite remote sensing, *South African Journal of Science*, 77, 231-236.

Lutjeharms, J.R.E., 1988a: Examples of extreme circulation events at the Agulhas retroflection, *South African Journal of Science*, **84**, 584-586.

Lutjeharms, J.R.E., 1988b: Meridional heat transport across the Subtropical Convergence by a warm eddy, *Nature*, **331**, 251-253.

Lutjeharms, J.R.E. and D.J. Baker, 1980: A statistical analysis of the meso-scale dynamics of the Southern Ocean, *Deep-Sea Research*, **27**, 145-150.

Lutjeharms, J.R.E. and A.D. Connell, 1989: The Natal Pulse and inshore counter-currents off the South African east coast, *South African Journal of Science*, **85**, 533-535.

Lutjeharms, J.R.E. and A.L. Gordon, 1987: Shedding of an Agulhas Ring observed at sea. *Nature*, London, **325**, 138-140.

Lutjeharms, J.R.E. and H.R. Roberts, 1988: The Natal Pulse: An extreme transient on the Agulhas Current, *Journal of Geophysical Research*, **93**, 631-645.

Lutjeharms, J.R.E. and P. Stockton, 1987: Kinematics of the upwelling front off southern Africa. In *The Benguela and Comparable Ecosystems*, Payne, A.I.L., J.A. Gulland and K.H. Brink (Eds), *South African Journal of Marine Science*, **5**, 51-62.

Lutjeharms, J.R.E. and H.R. Valentine, 1981: Ocean circulation studies in the vicinity of southern Africa : Preliminary results using FGGE drifters and remote sensing, *Advances in Space Research*, **1**, 211-223.

Lutjeharms, J.R.E. and H.R. Valentine, 1987: Water types and volumetric considerations of the South-East Atlantic upwelling regime. In *The Benguela and Comparable Ecosystems*, Payne, A.I.L., J.A. Gulland and K.H. Brink (Eds.), *South African Journal of Marine Science*, **5**, 63-71.

Lutjeharms, J.R.E. and H.R. Valentine, 1988: Eddies at the Subtropical Convergence south of Africa, *Journal of Physical Oceanography*, **18**, 761-774.

Lutjeharms, J.R.E. and R.C. van Ballegooyen, 1984: Topographic control in the Agulhas Current system, *Deep-Sea Research*, **31**, 1321-1337.

Lutjeharms, J.R.E. and R.C. van Ballegooyen, 1988: The Retroflection of the Agulhas Current, *Journal of Physical Oceanography*, **18**, 1570-1583.

Lutjeharms, J.R.E., N.D. Bang and C.P. Duncan, 1981: Characteristics of the currents east and south of Madagascar, *Deep-Sea Research*, **28**, 879-899.

Lutjeharms, J.R.E., R. Catzel and H.R. Valentine, 1989: Eddies and other boundary phenomena of the Agulhas Current, *Continental Shelf Research*, **9**, 597-616.

Mamayev, O. I., 1975: *Temperature-salinity analysis of World Ocean Waters*, Elsevier, Amsterdam, 374 pp.

McCartney, M.S., 1977: Subantantarctic mode water. In *A voyage of discovery : George Deacon 70th anniversary volume*, **24**, M. Angel (Ed.), Supplement to *Deep-Sea Research*, Pergamon Press, New York, 103-119 .

Montgomery, R.B., 1954: Analysis of a Hugh M. Smith oceanographic section from Honolulu southward across the equator, *Journal of Marine Research*, **13**, 67-75.

Montgomery, R.B., 1955: Characteristics of surface water at Weather Ship J, *Deep-Sea Research*, **3**, supplement, Papers in marine biology and oceanography dedicated to Henry Bryant Bigelow, 331-334.

Montgomery, R.B., 1958: Water characteristics of Atlantic Ocean and of world ocean, *Deep-Sea Research*, **5**, 134-148.

Montgomery, R.B. and W.S. Wooster, 1954: Thermosteric anomaly and the analysis of serial oceanographic data, *Deep-Sea Research*, **2**, 63-70.

Mostert, S.A., 1983: Procedures used in South Africa for the automatic photometric determination of micronutrients in seawater, *South African Journal of Marine Science*, **1**, 189-198.

Murray, J., 1899: The temperature of the floor of the ocean and of the surface waters of the ocean, *Geographical Journal*, **14**, 34-51 + 3 maps.

Nelson, G., and L. Hutchings, 1983: The Benguela upwelling area, *Progress in Oceanography*, **12**, 333-356.

Olson D.B. and R.H. Evans, 1986: Rings of the Agulhas Current, *Deep-Sea Research*, **33**, 27-42.

Olson, D.B., R.A. Fine and A.L. Gordon, 1989: Convective modification of water masses in the Agulhas, *Deep-Sea Research*, in press.

Orren, M.J., 1963: Hydrological observations in the southwest Indian Ocean, *Investigational Report of the Division for Sea Fisheries of South Africa*, **45**, 1-61.

Orren, M.J., 1966: Hydrology of the South West Indian Ocean, *Investigational Report of the Division for Sea Fisheries of South Africa*, **55**, 1-35.

Ou, H.W. and W.P.M. de Ruijter, 1986: Separation of an inertial boundary current from an irregular coastline, *Journal of Physical Oceanography*, **16**, 280-289.

Patterson, S.L., 1985: Surface circulation and kinetic energy distributions in the Southern Hemisphere oceans from FGGE drifting buoys, *Journal of Physical Oceanography*, **15**, 865-884.

Pearce, A.F., 1977: Some features of the upper 500 m of the Agulhas Current, *Journal of Marine Research*, **35**, 731-751.

Pearce, A.F., 1980: Early observations and historical notes on the Agulhas Current Circulation, *Transactions of the Royal Society of South Africa*, **44**, 205-212.

Pearce, A.F. and M.L. Gründlingh, 1982: Is there a seasonal variation in the Agulhas Current?, *Journal of Marine Research*, **40**, 177-184.

Pearce, A.F., E.H. Schumann and G.S.H. Lundie, 1978: Features of the shelf circulation off the Natal coast, *South African Journal of Science*, **74**, 328-331.

Piola, A. and D.T. Georgi, 1982: Circumpolar properties of Antarctic Intermediate Water and Subantarctic Mode Water, *Deep-Sea Research*, **29**, 687-711.

Pollak, M.J., 1958: Frequency distribution of potential temperatures and salinities in the Indian Ocean, *Deep-Sea Research*, **5**, 128-133.

Pollard, R.T. and S. Pu, 1985: Structure and circulation of the upper Atlantic Ocean northeast of the Azores, *Progress in Oceanography*, **14**, 443-462.

Read, J.F., R.T. Pollard and J. Smithers, 1987: CTD and Seasoar data from the Agulhas Retroflection Zone, Institute of Oceanographic Sciences Deacon Laboratory *Report* no. 245, 91 pp.

Reid, J.L., 1965: Intermediate waters of the Pacific Ocean, *The Johns Hopkins Oceanographic Studies*, **2**, 85 pp.

Reid, J.L., 1973: Northwest Pacific Ocean Waters in winter, *The Johns Hopkins Oceanographic Studies*, **5**, 96 pp.

Reid, J.L., D. Nowlin and W.C. Patzert, 1977: On the characteristics and circulation of the Southwestern Atlantic Ocean, *Journal of Physical Oceanography*, **7**, 62-91.

Saetre, R. and A. Jorge da Silva, 1984: The circulation of the Mozambique Channel, *Deep-Sea Research*, **31**, 485-508.

Sayles, M.A., K. Aagaard and L.K. Coachman, 1979: *Oceanographic Atlas of the Bering Sea Basin*, University of Washington Press, Seattle and London, 158 pp.

Schleicher, K.E. and A. Bradshaw, 1956: A conductivity bridge for measurement of the salinity of sea water, *Journal du Conseil*, **22**, 9-20.

Schumann, E.H., 1981: Low frequency fluctuations off the Natal coast, *Journal of Geophysical Research*, **86**, 6499-6508.

Schumann, E.H., 1982: Inshore circulation of the Agulhas Current off Natal, *Journal of Marine Research*, **40**, 43-55.

Schumann, E.H., 1986: The bottom boundary layer inshore of the Agulhas Current off Natal in August 1975, *South African Journal of Marine Science*, **4**, 93-102.

Shannon, L.V., 1966: Hydrology of the south and west coasts of South Africa, *Investigational Report of the Division for Sea Fisheries of South Africa*, **58**, 22 pp. + 30 pp. of figures.

Shannon, L.V. 1985: The Benguela Ecosystem Part I. Evolution of the Benguela, Physical Features and Processes. In *Oceanography and Marine Biology. An Annual Review*, **23**, Barnes, M. (Ed.). Aberdeen, University Press, 105-182.

Shannon, L.V. and D. Hunter, 1988: Notes on Antarctic Intermediate Water around Southern Africa, *South African Journal of Marine Science*, **6**, 107-117.

Shannon, L.V., R.J.M. Crawford, G.B. Brundrit and L. Underhill, 1988: Responses of fish populations in the Benguela ecosystem to environmental change, *Journal du Conseil International Exploration de la Mer*, **45**, 5-12.

Simpson, E.S.W., 1974: Southeast Atlantic and Southwest Indian Oceans. Chart **125A** *Bathymetry*, 1st Edition (National Research Institute of Oceanology).

Stander, G.H., 1964: The Benguela Current off South West Africa, *Investigational Report of the Marine Research Laboratory of South West Africa*, **12**, 43 pp. + plates 5-81.

Stavropoulos, C.C. and C.P. Duncan, 1974: A satellite-tracked buoy in the Agulhas Current, *Journal of Geophysical Research*, **79**, 2744-2746.

Stocks, T., 1938: Statistik der Tiefenstufen des Atlantischen Ozeans. Berlin. Verlag von Walter de Gruyter & Co., Wissenschaftliche Ergebrisse der Deutschen Atlantischen Expedition auf dem Forschungs- und Vermessungsschiff "*Meteor*" 1925-1927 Ergebnisse; Herausgegeben von A. Defant, **3**, I. Teil, Morphologie des Atlantischen Ozeans, 33-151 + beilagen 2-5.

Sverdrup, H.U., M.W. Johnson and R.H. Fleming, 1942: *The Oceans: Their Physics, Chemistry, and General Biology*. Prentice-Hall, Englewood Cliffs, New Jersey, 1087 pp.

Swart, V.P. and J.L. Largier, 1987: Thermal structure of Agulhas Bank water, *South African Journal of Marine Science*, **5**, 243-253.

UNESCO, 1983: Algorithms for computation of fundamental properties of sea water. Unesco Technical Papers in Marine Science, **44**, 53 pp.

Valentine, H.R., C.M. Duncombe Rae, R.C. van Ballegooyen and J.R.E. Lutjeharms, 1988: The Subtropical Convergence and Agulhas Retroflection Cruise (SCARC) Data Report, *CSIR Report T/SEA 8804*, 258 pp.

Van Foreest, D., F.A. Shillington and R. Legeckis, 1984: Large scale, stationary, frontal features in the Benguela Current system, *Continental Shelf Research*, **3**, 465-474.

Veronis, G., 1973: Model of world ocean circulation, I, Wind-driven, two layer, *Journal of Marine Research*, **31**, 228-288.

Visser, G.A., 1969: Analysis of Atlantic waters off the west coast of southern Africa, *Investigational Report of the Division for Sea Fisheries of South Africa*, **75**, 26 pp.

Waldron, H.N., 1985: Influences on the hydrology of Cape Columbine/ St Helena Bay region, *M.Sc. thesis, University of Cape Town:* 138 pp.

Walker, N.D., 1986: Satellite observations of the Agulhas Current and episodic upwelling south of Africa, *Deep-Sea Research*, **33**, 1083-1106.

Walker, N.D., 1990: Links between South African summer rainfall and temperature variability of the Agulhas and Benguela Current systems, *Journal of Geophysical Research*, in press.

Walker, N.D. and R.D. Mey, 1988: Ocean-atmosphere heat fluxes within the Agulhas Retroflection region, *Journal of Geophysical Research*, **93**, 15473-15483.

Wenner, F., E.H. Smith and F.M. Soule, 1930: Apparatus for determination aboard ship of the salinity of sea water by the electrical conductivity method, *Bureau of Standards Journal of Research*, **5**, 711-732.

Worthington, L.V. 1976: On the North Atlantic circulation. *The John Hopkins Oceanographic Studies*, **6**, 110 pp.

Worthington, L.V., 1981: The water masses of the world ocean: Some results of a fine-scale census, In *Evolution of Physical Oceanography, Scientific Surveys in Honour of Henry Stommel*, B.A. Warren and C. Wunsch (Eds.), pp. 42-69, MIT Press, Cambridge, Massachusetts.

Wright, W.R. and L.V. Worthington, 1970: The water masses of the North Atlantic Ocean; a volumetric census of temperature and salinity, *Serial Atlas of the Marine Environment*, Folio 19, American Geographical Society, New York, 8 pp + 7 plates.

Wüst, G., W. Brogmus and E. Noodt, 1954: Die zonale Verteilung von Salzgehalt, Niederschlag, Verdunstung, Temperatur und Dichte an der Oberfläche der Ozeane, *Kieler Meeresforschungen*, 10, 137-161.

Wyrtki, K., 1971: *Oceanographic Atlas of the International Indian Ocean Expedition*, National Science Foundation, Washington, D.C., 531 pp.

ADDENDA

ADDENDUM I

TABLE 4.1: List of stations used for the volumetric analyses. The (B) after the station number implies a bottom station.

STATION NO	LATITUDE	LONGITUDE	SHIP	CRUISE
55(B)	41°41.8'S	06°38.0'E	R.V. Knorr	Ajax
56(B)	40°35.6	08°19.0	R.V. Knorr	Ajax
57(B)	39°30.6	09°59.7	R.V. Knorr	Ajax
58(B)	38°30.5	11°49.7	R.V. Knorr	Ajax
59(B)	37°13.7	13°45.5	R.V. Knorr	Ajax
1(B)	33°51.9	14°59.5	R.V. Knorr	ARC
2(B)	34°10.2	17°19.7	R.V. Knorr	ARC
3	34°39.2	16°42.8	R.V. Knorr	ARC
4(B)	35°07.7	16°08.8	R.V. Knorr	ARC
7(B)	36°32.7	14°24.2	R.V. Knorr	ARC
9(B)	36°00.1	13°46.8	R.V. Knorr	ARC
14	35°59.2	17°06.9	R.V. Knorr	ARC
15(B)	35°59.9	18°00.1	R.V. Knorr	ARC
17(B)	36°00.6	19°59.1	R.V. Knorr	ARC
18(B)	36°59.2	18°37.2	R.V. Knorr	ARC
22	38°18.5	14°00.4	R.V. Knorr	ARC
23(B)	38°24.1	12°59.7	R.V. Knorr	ARC
24(B)	38°33.2	14°29.9	R.V. Knorr	ARC
27(B)	38°51.0	17°30.8	R.V. Knorr	ARC
32	39°14.6	17°18.3	R.V. Knorr	ARC
36	39°16.0	18°37.2	R.V. Knorr	ARC
37	39°59.9	19°14.9	R.V. Knorr	ARC
39(B)	42°00.0	20°59.7	R.V. Knorr	ARC
42(B)	40°00.6	21°00.7	R.V. Knorr	ARC
45(B)	38°00.3	20°59.2	R.V. Knorr	ARC
46(B)	37°20.5	21°00.0	R.V. Knorr	ARC
47(B)	36°39.9	21°00.2	R.V. Knorr	ARC
48(B)	35°00.1	23°00.0	R.V. Knorr	ARC
49(B)	35°34.8	23°23.6	R.V. Knorr	ARC
50(B)	36°10.1	23°47.6	R.V. Knorr	ARC
51(B)	36°44.3	24°14.3	R.V. Knorr	ARC
52(B)	37°19.2	24°40.2	R.V. Knorr	ARC
53(B)	37°54.3	25°04.7	R.V. Knorr	ARC
54(B)	38°28.7	25°27.6	R.V. Knorr	ARC
55(B)	39°09.6	25°39.5	R.V. Knorr	ARC
56(B)	40°10.1	25°40.6	R.V. Knorr	ARC
58(B)	42°00.6	25°40.5	R.V. Knorr	ARC
59	40°30.9	24°27.0	R.V. Knorr	ARC
71	38°17.0	16°39.9	R.V. Knorr	ARC
74	37°02.6	14°40.6	R.V. Knorr	ARC
77	35°30.6	14°04.3	R.V. Knorr	ARC
78	34°52.8	13°59.7	R.V. Knorr	ARC
79	34°37.2	13°43.4	R.V. Knorr	ARC
81	34°00.0	14°06.8	R.V. Knorr	ARC
83	34°00.2	15°18.1	R.V. Knorr	ARC
209(B)	34°30.9	18°04.9	R.V. Thomas Washington	Marathon
218(B)	36°30.0	15°48.9	R.V. Thomas Washington	Marathon
222(B)	38°19.0	15°10.3	R.V. Thomas Washington	Marathon

STATION NO	LATITUDE	LONGITUDE	SHIP	CRUISE
224(B)	39°00.5	14°12.7	R.V. Thomas Washington	Marathon
226(B)	39°24.9	15°32.4	R.V. Thomas Washington	Marathon
227(B)	39°43.3	16°00.6	R.V. Thomas Washington	Marathon
229(B)	40°43.5	17°02.3	R.V. Thomas Washington	Marathon
232(B)	42°30.3	17°59.3	R.V. Thomas Washington	Marathon
234(B)	43°30.5	17°56.8	R.V. Thomas Washington	Marathon
236(B)	44°27.5	17°52.5	R.V. Thomas Washington	Marathon
239(B)	35°59.7	19°59.8	R.V. Thomas Washington	Marathon
245(B)	37°33.2	18°44.0	R.V. Thomas Washington	Marathon
248(B)	38°29.7	19°29.9	R.V. Thomas Washington	Marathon
251(B)	38°29.9	21°33.1	R.V. Thomas Washington	Marathon
252(B)	38°30.2	22°16.1	R.V. Thomas Washington	Marathon
259(B)	36°31.8	22°27.1	R.V. Thomas Washington	Marathon
268(B)	37°29.8	26°15.0	R.V. Thomas Washington	Marathon
270(B)	36°30.4	26°45.7	R.V. Thomas Washington	Marathon
272(B)	35°40.1	26°41.2	R.V. Thomas Washington	Marathon
274(B)	35°06.3	25°52.0	R.V. Thomas Washington	Marathon
276(B)	34°46.4	25°43.9	R.V. Thomas Washington	Marathon
280(B)	38°36.3	26°24.4	R.V. Thomas Washington	Marathon
283(B)	39°30.5	26°58.2	R.V. Thomas Washington	Marathon
288(B)	39°17.3	24°31.0	R.V. Thomas Washington	Marathon
289(B)	38°59.8	23°58.5	R.V. Thomas Washington	Marathon
290(B)	38°45.7	23°26.6	R.V. Thomas Washington	Marathon
293(B)	37°39.6	19°59.7	R.V. Thomas Washington	Marathon
11464(B)	37°14.2	23°04.1	R.V. Discovery	ARZ
11467(B)	40°07.9	19°47.5	R.V. Discovery	ARZ
11468(B)	38°58.0	18°33.3	R.V. Discovery	ARZ
11469(B)	37°57.2	15°34.0	R.V. Discovery	ARZ
11470(B)	40°11.1	16°34.8	R.V. Discovery	ARZ
11471(B)	41°57.3	17°46.4	R.V. Discovery	ARZ
03	36°01.0	16°48.0	R.V. S.A. Agulhas	SCARC
08	33°57.0	13°40.0	R.V. S.A. Agulhas	SCARC
09	34°30.0	12°51.0	R.V. S.A. Agulhas	SCARC
11	35°11.0	11°43.0	R.V. S.A. Agulhas	SCARC
13	36°31.0	11°29.0	R.V. S.A. Agulhas	SCARC
15	37°38.0	10°27.0	R.V. S.A. Agulhas	SCARC
16	37°41.0	09°29.0	R.V. S.A. Agulhas	SCARC
17	37°53.0	08°29.0	R.V. S.A. Agulhas	SCARC
18	38°00.0	06°44.0	R.V. S.A. Agulhas	SCARC
22	36°30.0	08°30.0	R.V. S.A. Agulhas	SCARC
23	37°40.8	11°09.6	R.V. S.A. Agulhas	SCARC
25	37°31.2	12°43.8	R.V. S.A. Agulhas	SCARC
27	37°24.6	17°57.6	R.V. S.A. Agulhas	SCARC
29	37°45.0	16°00.0	R.V. S.A. Agulhas	SCARC
32	39°00.6	13°00.0	R.V. S.A. Agulhas	SCARC
33	39°08.4	12°42.6	R.V. S.A. Agulhas	SCARC
34	40°03.0	11°52.8	R.V. S.A. Agulhas	SCARC
36	41°31.8	11°31.2	R.V. S.A. Agulhas	SCARC
37	40°57.0	14°22.2	R.V. S.A. Agulhas	SCARC
40	40°56.7	18°45.2	R.V. S.A. Agulhas	SCARC
42	41°56.2	19°44.6	R.V. S.A. Agulhas	SCARC
43	43°54.7	20°10.4	R.V. S.A. Agulhas	SCARC
44	44°18.8	20°48.0	R.V. S.A. Agulhas	SCARC
45	40°59.5	20°30.2	R.V. S.A. Agulhas	SCARC

STATION NO	LATITUDE	LONGITUDE	SHIP	CRUISE
46	41°51.5	21°43.2	R.V. S.A. Agulhas	SCARC
47	43°02.2	21°53.6	R.V. S.A. Agulhas	SCARC
48	42°50.5	22°25.0	R.V. S.A. Agulhas	SCARC
50	42°07.4	23°47.8	R.V. S.A. Agulhas	SCARC
51	41°03.8	23°14.5	R.V. S.A. Agulhas	SCARC
52	40°10.9	22°32.0	R.V. S.A. Agulhas	SCARC
53	39°37.0	22°10.5	R.V. S.A. Agulhas	SCARC
56	37°14.9	20°27.7	R.V. S.A. Agulhas	SCARC

ADDENDUM II

Census of the water masses of the Agulhas Retroflection Area (0-1500 m) ranked by volume per bivariate class (°θ x ‰).

RANK NUMBER	TEMPERATURE RANGE °θ	SALINITY RANGE ‰	VOLUME
1	2,7 - 2,8	34,66 - 34,67	4985,0
2	2,7 - 2,8	34,64 - 34,65	4791,4
3	2,7 - 2,8	34,65 - 34,66	4723,7
4	2,8 - 2,9	34,62 - 34,63	4597,8
5	2,9 - 3,0	34,58 - 34,59	4423,6
6	2,7 - 2,8	34,63 - 34,64	4365,5
7	2,7 - 2,8	34,67 - 34,68	4210,7
8	3,0 - 3,1	34,54 - 34,55	4152,6
9	2,8 - 2,9	34,61 - 34,62	4104,2
10	2,8 - 2,9	34,60 - 34,61	4094,5
11	3,1 - 3,2	34,52 - 34,53	3968,7
12	3,0 - 3,1	34,55 - 34,56	3939,6
13	2,7 - 2,8	34,61 - 34,62	3804,1
14	2,7 - 2,8	34,62 - 34,63	3678,3
15	3,1 - 3,2	34,53 - 34,54	3542,8
16	2,8 - 2,9	34,63 - 34,64	3533,1
17	3,0 - 3,1	34,56 - 34,57	3484,7
18	2,8 - 2,9	34,59 - 34,60	3465,3
19	2,8 - 2,9	34,58 - 34,59	3446,0
20	2,9 - 3,0	34,57 - 34,58	3368,5
21	2,6 - 2,7	34,69 - 34,70	3155,6
22	2,9 - 3,0	34,59 - 34,60	3078,1
23	2,8 - 2,9	34,64 - 34,65	2971,7
23	2,9 - 3,0	34,60 - 34,61	2971,7
24	3,1 - 3,2	34,54 - 34,55	2952,3
25	2,6 - 2,7	34,70 - 34,71	2923,3
26	3,0 - 3,1	34,53 - 34,54	2913,6
27	2,8 - 2,9	34,56 - 34,57	2903,9
28	3,2 - 3,3	34,52 - 34,53	2884,5
29	3,2 - 3,3	34,48 - 34,49	2865,2
30	2,7 - 2,8	34,68 - 34,69	2739,4
31	3,0 - 3,1	34,52 - 34,53	2632,9
32	2,7 - 2,8	34,60 - 34,61	2584,5
33	2,7 - 2,8	34,57 - 34,58	2545,8
33	2,9 - 3,0	34,56 - 34,57	2545,8
34	3,2 - 3,3	34,51 - 34,52	2516,7
35	3,0 - 3,1	34,57 - 34,58	2507,0
35	3,3 - 3,4	34,52 - 34,53	2507,0
36	2,7 - 2,8	34,58 - 34,59	2449,0
37	2,8 - 2,9	34,55 - 34,56	2400,6
38	3,1 - 3,2	34,51 - 34,52	2381,2
39	2,8 - 2,9	34,65 - 34,66	2342,5
39	2,7 - 2,8	34,59 - 34,60	2342,5
40	2,8 - 2,9	34,57 - 34,58	2332,8
41	2,6 - 2,7	34,68 - 34,69	2323,1
42	2,9 - 3,0	34,55 - 34,56	2294.1
43	2,8 - 2,9	34,54 - 34,55	2245,7
44	2,7 - 2,8	34,55 - 34,56	2226,3
45	2,9 - 3,0	34,54 - 34,55	2197,3

RANK NUMBER	TEMPERATURE RANGE °θ	SALINITY RANGE ‰	VOLUME
46	2,6 - 2,7	34,71 - 34,72	2187,6
47	3,4 - 3,5	34,50 - 34,51	2177,9
48	3,1 - 3,2	34,55 - 34,56	2129,5
49	3,4 - 3,5	34,47 - 34,48	2119,9
50	2,9 - 3,0	34,53 - 34,54	2061,8
50	2,8 - 2,9	34,53 - 34,54	2061,8
51	2,7 - 2,8	34,56 - 34,57	2042,4
51	3,7 - 3,8	34,44 - 34,45	2042,4
52	3,1 - 3,2	34,49 - 34,50	2023,1
53	3,2 - 3,3	34,53 - 34,54	2003,7
53	3,3 - 3,4	34,46 - 34,47	2003,7
53	3,4 - 3,5	34,46 - 34,47	2003,7
54	3,5 - 3,6	34,48 - 34,49	1945,6
55	3,0 - 3,1	34,50 - 34,51	1935,9
55	3,2 - 3,3	34,50 - 34,51	1935,9
56	2,8 - 2,9	34,51 - 34,52	1916,6
57	3,6 - 3,7	34,45 - 34,46	1848,8
58	3,6 - 3,7	34,38 - 34,39	1829,5
59	3,4 - 3,5	34,49 - 34,50	1810,1
60	3,2 - 3,3	34,54 - 34,55	1790,7
61	3,0 - 3,1	34,51 - 34,52	1781,1
61	3,5 - 3,6	34,45 - 34,46	1781,1
62	3,4 - 3,5	34,52 - 34,53	1771,4
63	3,6 - 3,7	34,40 - 34,41	1761,7
64	3,5 - 3,6	34,51 - 34,52	1752,0
65	3,3 - 3,4	34,53 - 34,54	1732,7
66	3,0 - 3,1	34,58 - 34,59	1723,0
66	3,4 - 3,5	34,30 - 34,31	1723,0
67	2,9 - 3,0	34,41 - 34,42	1693,9
68	3,1 - 3,2	34,57 - 34,58	1684,3
68	2,8 - 2,9	34,52 - 34,53	1684,3
69	2,9 - 3,0	34,61 - 34,62	1664,9
70	3,0 - 3,1	34,49 - 34,50	1626,2
71	3,1 - 3,2	34,50 - 34,51	1616,5
71	3,7 - 3,8	34,47 - 34,48	1616,5
72	3,8 - 3,9	34,40 - 34,41	1606,8
73	3,2 - 3,3	34,47 - 34,48	1597,1
73	4,0 - 4,1	34,40 - 34,41	1597,1
74	3,4 - 3,5	34,51 - 34,52	1587,5
74	3,6 - 3,7	34,46 - 34,47	1587,5
75	2,9 - 3,0	34,52 - 34,53	1577,8
75	3,5 - 3,6	34,50 - 34,51	1577,8
75	3,2 - 3,3	34,49 - 34,50	1577,8
75	3,7 - 3,8	34,48 - 34,49	1577,8
75	3,4 - 3,5	34,45 - 34,46	1577,8
76	3,6 - 3,7	34,47 - 34,48	1558,4
77	4,1 - 4,2	34,42 - 34,43	1548,7
78	3,5 - 3,6	34,52 - 34,53	1539,1
79	3,3 - 3,4	34,50 - 34,51	1519,7
79	3,9 - 4,0	34,46 - 34,47	1519,7
80	3,1 - 3,2	34,42 - 34,43	1510,0
80	4,1 - 4,2	34,40 - 34,41	1510.0
81	3,9 - 4,0	34,29 - 34,30	1500,4

RANK NUMBER	TEMPERATURE RANGE °θ	SALINITY RANGE ‰	VOLUME
82	3,6 - 3,7	34,50 - 34,51	1490,7
82	3,3 - 3,4	34,47 - 34,48	1490,7
83	2,8 - 2,9	34,66 - 34,67	1481,0
83	3,5 - 3,6	34,47 - 34,48	1481,0
83	8,9 - 9,0	34,72 - 34,73	1481,0
84	2,7 - 2,8	34,54 - 34,55	1471,3
84	3,3 - 3,4	34,48 - 34,49	1471,3
85	3,6 - 3,7	34,34 - 34,35	1461,6
86	3,6 - 3,7	34,44 - 34,45	1442,2
87	3,6 - 3,7	34,48 - 34,49	1432,6
88	3,1 - 3,2	34,56 - 34,57	1422,9
88	3,5 - 3,6	34,40 - 34,41	1422,9
89	2,9 - 3,0	34,63 - 34,64	1413,2
90	2,7 - 2,8	34,69 - 34,70	1403,6
90	3,0 - 3,1	34,59 - 34,60	1403,6
90	3,0 - 3,1	34,45 - 34,46	1403,6
90	3,6 - 3,7	34,37 - 34,38	1403,6
90	16,4 -16,5	35,58 - 35,59	1403,6
91	3,9 - 4,0	34,41 - 34,42	1393,9
92	2,7 - 2,8	34,53 - 34,54	1384,2
93	2,9 - 3,0	34,62 - 34,63	1374,5
93	3,7 - 3,8	34,50 - 34,51	1374,5
93	3,5 - 3,6	34,44 - 34,45	1374,5
94	3,5 - 3,6	34,46 - 34,47	1355,2
94	3,5 - 3,6	34,41 - 34,42	1355,2
95	3,4 - 3,5	34,53 - 34,54	1345,5
95	3,9 - 4,0	34,45 - 34,46	1345,5
95	3,8 - 3,9	34,47 - 34,48	1345,5
96	3,0 - 3,1	34,61 - 34,62	1335,8
96	3,7 - 3,8	34,46 - 34,47	1335,8
97	2,6 - 2,7	34,67 - 34,68	1326,1
97	3,6 - 3,7	34,49 - 34,50	1326,1
97	3,7 - 3,8	34,45 - 34,46	1326,1
97	3,6 - 3,7	34,39 - 34,40	1326,1
98	3,6 - 3,7	34,43 - 34,44	1316,4
98	3,0 - 3,1	34,40 - 34,41	1316,4
99	4,0 - 4,1	34,41 - 34,42	1306,8
99	4,3 - 4,4	34,31 - 34,32	1306,8
100	8,8 - 8,9	34,71 - 34,72	1297,1
101	3,3 - 3,4	34,51 - 34,52	1287,4
101	3,5 - 3,6	34,49 - 34,50	1287,4
101	3,7 - 3,8	34,42 - 34,43	1287,4
101	3,5 - 3,6	34,37 - 34,38	1287,4
101	10,4 -10,5	34,88 - 34,89	1287,4
101	12,1 -12,2	35,09 - 35,10	1287,4
102	3,0 - 3,1	34,44 - 34,45	1277,7
103	2,8 - 2,9	34,50 - 34,51	1268,0
104	2,9 - 3,0	34,48 - 34,49	1258,4
104	4,5 - 4,6	34,37 - 34,38	1258,4
104	4,7 - 4,8	34,33 - 34,34	1258,4
104	3,8 - 3,9	34,29 - 34,30	1258,4
104	9,6 - 9,7	34,79 - 34,80	1258,4
104	11,5 -11,6	35,01 - 35,02	1258,4

RANK NUMBER	TEMPERATURE RANGE °θ	SALINITY RANGE ‰	VOLUME
105	3,7 - 3,8	34,49 - 34,50	1248,7
105	9,0 - 9,1	34,73 - 34,74	1248,7
106	3,7 - 3,8	34,43 - 34,44	1239,0
106	2,9 - 3,0	34,36 - 34,37	1239,0
107	3,9 - 4,0	34,49 - 34,50	1229,3
107	3,3 - 3,4	34,37 - 34,38	1229,3
108	3,2 - 3,3	34,41 - 34,42	1219,6
108	4,2 - 4,3	34,30 - 34,31	1219,6
108	9,2 - 9,3	34,75 - 34,76	1219,6
109	3,8 - 3,9	34,50 - 34,51	1210,0
109	3,0 - 3,1	34,46 - 34,47	1210,0
109	12,2 -12,3	35,10 - 35,11	1210,0
110	2,9 - 3,0	34,64 - 34,65	1200,3
110	3,6 - 3,7	34,51 - 34,52	1200,3
110	4,2 - 4,3	34,40 - 34,41	1200,3
110	10,5 -10,6	34,89 - 34,90	1200,3
110	12,8 -12,9	35,18 - 35,19	1200,3
111	3,9 - 4,0	34,43 - 34,44	1190,6
111	9,5 - 9,6	34,78 - 34,79	1190,6
112	3,1 - 3,2	34,60 - 34,61	1180,9
112	3,1 - 3,2	34,43 - 34,44	1180,9
112	9,3 - 9,4	34,76 - 34,77	1180,9
113	10,3 -10,4	34,87 - 34,88	1171,2
114	3,3 - 3,4	34,40 - 34,41	1162,0
115	3,3 - 3,4	34,55 - 34,56	1161,6
115	2,9 - 3,0	34,50 - 34,51	1161,6
115	3,3 - 3,4	34,49 - 34,50	1161,6
115	4,2 - 4,3	34,39 - 34,40	1161,6
115	8,6 - 8,7	34,69 - 34,70	1161,6
115	9,5 - 9,6	34,77 - 34,78	1161,6
116	4,6 - 4,7	34,36 - 34,37	1151,9
116	4,4 - 4,5	34,30 - 34,31	1151,9
116	3,6 - 3,7	34,29 - 34,30	1151,9
116	9,4 - 9,5	34,77 - 34,78	1151,9
116	11,1 -11,2	34,96 - 34,97	1151,9
117	4,5 - 4,6	34,41 - 34,42	1142,2
117	12,5 -12,6	35,13 - 35,14	1142,2
118	3,4 - 3,5	34,48 - 34,49	1132,5
118	4,2 - 4,3	34,35 - 34,36	1132,5
118	9,1 - 9,2	34,74 - 34,75	1132,5
118	11,0 -11,1	34,95 - 34,96	1132,5
118	11,2 -11,3	34,98 - 34,99	1132,5
119	3,8 - 3,9	34,44 - 34,45	1122,8
119	3,0 - 3,1	34,43 - 34,44	1122,8
119	9,2 - 9,3	34,74 - 34,75	1122,8
119	10,2 -10,3	34,86 - 34,87	1122,8
120	3,2 - 3,3	34,45 - 34,46	1113,2
120	8,5 - 8,6	34,68 - 34,69	1113,2
120	11,3 -11,4	34,99 - 35,00	1113,2
121	3,0 - 3,1	34,47 - 34,48	1103,5
121	4,2 - 4,3	34,41 - 34,42	1103,5
121	8,3 - 8,4	34,67 - 34,68	1103,5
121	9,7 - 9,8	34,80 - 34,81	1103,5

RANK NUMBER	TEMPERATURE RANGE °θ	SALINITY RANGE ‰	VOLUME
122	3,2 - 3,3	34,37 - 34,38	1093,8
122	3,5 - 3,6	34,34 - 34,35	1093,8
122	11,7 - 11,8	35,04 - 35,05	1093,8
123	2,6 - 2,7	34,60 - 34,61	1084,1
123	3,7 - 3,8	34,52 - 34,53	1084,1
123	2,9 - 3,0	34,47 - 34,48	1084,1
124	3,3 - 3,4	34,56 - 34,57	1074,4
124	12,6 -12,7	35,14 - 35,15	1074,4
125	3,9 - 4,0	34,40 - 34,41	1064,8
125	4,3 - 4,4	34,39 - 34,40	1064,8
125	11,8 -11,9	35,05 - 35,06	1064,8
125	12,3 -12,4	35,11 - 35,12	1064,8
126	3,6 - 3,7	34,42 - 34,43	1055,1
126	3,6 - 3,7	34,41 - 34,42	1055,1
126	3,5 - 3,6	34,29 - 34,30	1055,1
126	8,2 - 8,3	34,66 - 34,67	1055,1
126	8,7 - 8,8	34,70 - 34,71	1055,1
126	10,8 -10,9	34,93 - 34,94	1055,1
127	3,0 - 3,1	34,48 - 34,49	1045,4
127	4,3 - 4,4	34,43 - 34,44	1045,4
127	3,5 - 3,6	34,43 - 34,44	1045,4
127	4,6 - 4,7	34,41 - 34,42	1045,4
127	3,9 - 4,0	34,30 - 34,31	1045,4
127	11,4 -11,5	35,00 - 35,01	1045,4
127	16,3 -16,4	35,53 - 35,54	1045,4
127	22,3 - 22,4	35,58 - 35,59	1045,4
128	2,9 - 3,0	34,49 - 34,50	1035,7
128	4,6 - 4,7	34,32 - 34,33	1035,7
128	4,1 - 4,2	34,30 - 34,31	1035,7
128	10,6 -10,7	34,90 - 34,91	1035,7
129	2,8 - 2,9	34,49 - 34,50	1026,0
129	3,1 - 3,2	34,41 - 34,42	1026,0
129	3,4 - 3,5	34,37 - 34,38	1026,0
129	3,8 - 3,9	34,33 - 34,34	1026,0
129	4,0 - 4,1	34,30 - 34,31	1026,0
130	3,3 - 3,4	34,54 - 34,55	1016,4
130	3,0 - 3,1	34,34 - 34,35	1016,4
130	12,4 -12,5	35,12 - 35,13	1016,4
130	12,9 -13,0	35,19 - 35,20	1016,4
131	4,0 - 4,1	34,42 - 34,43	1006,7
131	4,3 - 4,4	34,38 - 34,39	1006,7
131	3,8 - 3,9	34,30 - 34,31	1006,7
131	8,3 - 8,4	34,66 - 34,67	1006,7
131	10,9 -11,0	34,94 - 34,95	1006,7
132	2,9 - 3,0	34,65 - 34,66	997,0
132	2,6 - 2,7	34,65 - 34,66	997,0
132	4,5 - 4,6	34,32 - 34,33	997,0
133	3,3 - 3,4	34,57 - 34,58	987,3
133	3,2 - 3,3	34,38 - 34,39	987,3
133	3,9 - 4,0	34,33 - 34,34	987,3
133	9,6 - 9,7	34,78 - 34,79	987,3
133	10,0 -10,1	34,83 - 34,84	987,3

RANK NUMBER	TEMPERATURE RANGE °θ	SALINITY RANGE ‰	VOLUME
134	2,9 - 3,0	34,44 - 34,45	977,6
134	3,9 - 4,0	34,44 - 34,45	977,6
134	4,1 - 4,2	34,43 - 34,44	977,6
134	3,4 - 3,5	34,43 - 34,44	977,6
134	4,3 - 4,4	34,42 - 34,43	977,6
134	3,1 - 3,2	34,40 - 34,41	977,6
134	3,0 - 3,1	34,32 - 34,33	977,6
134	9,9 -10,0	34,82 - 34,83	977,6
134	11,6 -11,7	35,02 - 35,03	977,6
134	11,9 -12,0	35,07 - 35,08	977,6
134	12,3 -12,4	35,12 - 35,13	977,6
135	2,6 - 2,7	34,59 - 34,60	968,0
135	3,8 - 3,9	34,46 - 34,47	968,0
135	3,7 - 3,8	34,39 - 34,40	968,0
135	3,9 - 4,0	34,38 - 34,39	968,0
135	3,6 - 3,7	34,31 - 34,32	968,0
135	3,0 - 3,1	34,31 - 34,32	968,0
135	8,1 - 8,2	34,65 - 34,66	968,0
135	9,4 - 9,5	34,76 - 34,77	968,0
135	10,1 -10,2	34,85 - 34,86	968,0
135	12,7 -12,8	35,17 - 35,18	968,0
136	3,5 - 3,6	34,42 - 34,43	958,3
136	4,4 - 4,5	34,42 - 34,43	958,3
136	4,5 - 4,6	34,30 - 34,31	958,3
136	8,2 - 8,3	34,64 - 34,65	958,3
137	3,2 - 3,3	34,60 - 34,61	948,6
137	3,5 - 3,6	34,53 - 34,54	948,6
137	8,0 - 8,1	34,63 - 34,64	948,6
137	9,0 - 9,1	34,72 - 34,73	948,6
137	11,9 -12,0	35,06 - 35,07	948,6
138	3,8 - 3,9	34,43 - 34,44	938,9
138	3,8 - 3,9	34,36 - 34,37	938,9
138	4,7 - 4,8	34,36 - 34,37	938,9
138	8,2 - 8,3	34,65 - 34,66	938,9
138	12,9 -13,0	35,20 - 35,21	938,9
139	3,9 - 4,0	34,42 - 34,43	929,2
139	4,7 - 4,8	34,42 - 34,43	929,2
139	8,4 - 8,5	34,67 - 34,68	929,2
140	3,2 - 3,3	34,40 - 34,41	919,6
140	2,9 - 3,0	34,32 - 34,33	919,6
140	3,8 - 3,9	34,25 - 34,26	919,6
140	12,0 -12,1	35,08 - 35,09	919,6
141	3,2 - 3,3	34,55 - 34,56	909,9
141	4,4 - 4,5	34,41 - 34,42	909,9
141	4,5 - 4,6	34,38 - 34,39	909,9
141	6,0 - 6,1	34,47 - 34,48	909,9
141	6,8 - 6,9	34,52 - 34,53	909,9
141	11,6 -11,7	35,03 - 35,04	909,9
141	12,0 -12,1	35,07 - 35,08	909,9
142	3,0 - 3,1	34,62 - 34,63	900,2
142	3,4 - 3,3	34,58 - 34,59	900,2
142	3,6 - 3,7	34,35 - 34,36	900,2
142	3,3 - 3,4	34,34 - 34,35	900,2
142	9,3 - 9,4	34,75 - 34,76	900,2

RANK NUMBER	TEMPERATURE RANGE °θ	SALINITY RANGE ‰	VOLUME
143	3,9 - 4,0	34,25 - 34,26	890,7
144	4,2 - 4,3	34,44 - 34,45	890,5
144	3,6 - 3,7	34,36 - 34,37	890,5
144	5,1 - 5,2	34,34 - 34,35	890,5
144	3,6 - 3,7	34,33 - 34,34	890,5
144	3,0 - 3,1	34,33 - 34,34	890,5
144	6,3 - 6,4	34,44 - 34,45	890,5
144	8,7 - 8,8	34,69 - 34,70	890,5
144	8,8 - 8,9	34,70 - 34,71	890,5
144	9,7 - 9,8	34,79 - 34,80	890,5
144	13,1 -13,2	35,22 - 35,23	890,5
144	16,4 -16,5	35,59 - 35,60	890,5
145	2,6 - 2,7	34,64 - 34,65	880,9
145	3,2 - 3,3	34,59 - 34,60	880,9
145	4,0 - 4,1	34,43 - 34,44	880,9
145	3,4 - 3,5	34,41 - 34,42	880,9
145	3,3 - 3,4	34,36 - 34,37	880,9
145	4,2 - 4,3	34,36 - 34,37	880,9
145	3,8 - 3,9	34,35 - 34,36	880,9
145	4,9 - 5,0	34,33 - 34,34	880,9
145	19,9 -20,0	35,57 - 35,58	880,9
145	19,2 -19,3	35,54 - 35,55	880,9
146	2,9 - 3,0	34,51 - 34,52	871,2
146	4,0 - 4,1	34,44 - 34,45	871,2
146	2,8 - 2,9	34,43 - 34,44	871,2
146	4,6 - 4,7	34,38 - 34,39	871,2
146	4,7 - 4,8	34,37 - 34,38	871,2
146	3,5 - 3,6	34,35 - 34,36	871,2
146	9,1 - 9,2	34,73 - 34,74	871,2
146	10,7 -10,8	34,92 - 34,93	871,2
146	13,2 -13,3	35,23 - 35,24	871,2
147	2,8 - 2,9	34,42 - 34,43	861,5
147	5,0 - 5,1	34,41 - 34,42	861,5
147	5,0 - 5,1	34,38 - 34,39	861,5
147	7,0 - 7,1	34,54 - 34,55	861,5
147	8,1 - 8,2	34,64 - 34,65	861,5
148	2,8 - 2,9	34,47 - 34,48	851,8
148	4,1 - 4,2	34,45 - 34,46	851,8
148	3,3 - 3,4	34,44 - 34,45	851,8
148	3,2 - 3,3	34,42 - 34,43	851,8
148	4,2 - 4,3	34,38 - 34,39	851,8
148	4,7 - 4,8	34,38 - 34,39	851,8
148	4,4 - 4,5	34,31 - 34,32	851,8
148	7,0 - 7,1	34,55 - 34,56	851,8
148	7,6 - 7,7	34,56 - 34,57	851,8
148	10,6 -10,7	34,91 - 34,92	851,8
149	3,1 - 3,2	34,39 - 34,40	842,1
149	2,9 - 3,0	34,34 - 34,35	842,1
149	3,6 - 3,7	34,28 - 34,29	842,1
149	4,2 - 4,3	34,28 - 34,29	842,1
149	6,9 - 7,0	34,53 - 34,54	842,1
149	10,1 -10,2	34,84 - 34,85	842,1
149	11,2 -11,3	34,97 - 34,98	842,1
149	12,2 -12,3	35,09 - 35,10	842,1

RANK NUMBER	TEMPERATURE RANGE °θ	SALINITY RANGE ‰	VOLUME
150	3,7 - 3,8	34,51 - 34,52	832,5
150	3,0 - 3,1	34,41 - 34,42	832,5
150	3,7 - 3,8	34,40 - 34,41	832,5
150	4,5 - 4,6	34,31 - 34,32	832,5
150	8,0 - 8,1	34,64 - 34,65	832,5
150	8,4 - 8,5	34,65 - 34,66	832,5
150	9,8 - 9,9	34,81 - 34,82	832,5
150	10,0 -10,1	34,84 - 34,85	832,5

ADDENDUM III

Census of the water masses of the Agulhas Retroflection Area (bottom stations) ranked by volume per bivariate class (°θ x ‰).

RANK	TEMPERATURE RANGE °θ	SALINITY RANGE ‰	VOLUME
1	2,1 - 2,2	34,84 - 34,85	46704,5
2	2,2 - 2,3	34,83 - 34,84	38718,7
3	2,0 - 2,1	34,83 - 34,84	35911,6
4	2,0 - 2,1	34,84 - 34,85	34701,7
5	1,9 - 2,0	34,83 - 34,84	34421,0
6	2,1 - 2,2	34,83 - 34,84	33636,9
7	0,7 - 0,8	34,73 - 34,74	31943,0
8	2,3 - 2,4	34,82 - 34,83	29910,2
9	2,2 - 2,3	34,84 - 34,85	29135,8
10	1,8 - 1,9	34,83 - 34,84	26328,6
11	0,6 - 0,7	34,73 - 34,74	25931,9
12	0,9 - 1,0	34,75 - 34,76	25902,5
13	1,7 - 1,8	34,82 - 34,83	24576,7
14	0,5 - 0,6	34,72 - 34,73	24189,5
15	2,3 - 2,4	34,83 - 34,84	23957,2
16	0,8 - 0,9	34,74 - 34,75	22940,8
17	1,0 - 1,1	34,76 - 34,77	21905,1
18	2,4 - 2,5	34,80 - 34,81	21382,4
19	2,2 - 2,3	34,82 - 34,83	21246,9
20	0,7 - 0,8	34,74 - 34,75	20617,7
21	0,6 - 0,7	34,72 - 34,73	19069,0
22	1,9 - 2,0	34,84 - 34,85	17955,8
23	0,8 - 0,9	34,75 - 34,76	17810,6
24	1,6 - 1,7	34,81 - 34,82	17771,9
25	1,8 - 1,9	34,82 - 34,83	17762,2
26	2,4 - 2,5	34,79 - 34,80	17558,9
27	2,3 - 2,4	34,81 - 34,82	16842,6
28	2,5 - 2,6	34,76 - 34,77	16339,3
29	2,4 - 2,5	34,81 - 34,82	16203,8
30	1,2 - 1,3	34,77 - 34,78	16068,3
31	2,4 - 2,5	34,82 - 34,83	15903,7
32	1,5 - 1,6	34,80 - 34,81	15632,7
33	1,4 - 1,5	34,79 - 34,80	15226,1
34	0,4 - 0,5	34,71 - 34,72	14984,1
35	1,1 - 1,2	34,77 - 34,78	14877,9
36	2,5 - 2,6	34,75 - 34,76	14877,7
37	2,5 - 2,6	34,77 - 34,78	14325,9
38	2,1 - 2,2	34,82 - 34,83	14171,1
39	1,2 - 1,3	34,78 - 34,79	13454,8
40	2,6 - 2,7	34,70 - 34,71	13377,3
41	1,1 - 1,2	34,76 - 34,77	13367,6
42	1,7 - 1,8	34,81 - 34,82	13309,6
43	2,5 - 2,6	34,78 - 34,79	13077,3
44	1,3 - 1,4	34,78 - 34,79	12912,7
45	2,6 - 2,7	34,71 - 34,72	12825,6
46	2,6 - 2,7	34,72 - 34,73	12012,5
47	2,5 - 2,6	34,74 - 34,75	11741,5
48	2,4 - 2,5	34,78 - 34,79	11683,4
49	1,9 - 2,0	34,82 - 34,83	11422,0
50	2,6 - 2,7	34,69 - 34,70	11044,5

RANK	TEMPERATURE RANGE °θ	SALINITY RANGE ‰	VOLUME
51	1,3 - 1,4	34,79 - 34,80	10996,1
52	1,6 - 1,7	34,80 - 34,81	10812,2
53	2,0 - 2,1	34,82 - 34,83	10560,5
54	2,3 - 2,4	34,84 - 34,85	10454,1
55	0,4 - 0,5	34,72 - 34,73	10328,2
56	0,9 - 1,0	34,76 - 34,77	9921,7
57	2,6 - 2,7	34,73 - 34,74	9853,9
58	1,0 - 1,1	34,75 - 34,76	9428,0
59	2,5 - 2,6	34,79 - 34,80	9031,1
60	2,6 - 2,7	34,68 - 34,69	8798,9
61	2,4 - 2,5	34,83 - 34,84	8421,3
62	2,7 - 2,8	34,65 - 34,66	7792,1
63	1,5 - 1,6	34,81 - 34,82	7598,6
63	1,6 - 1,7	34,82 - 34,83	7598,6
64	1,4 - 1,5	34,80 - 34,81	7501,8
65	1,5 - 1,6	34,79 - 34,80	7375,9
66	2,7 - 2,8	34,64 - 34,65	7317,8
67	2,6 - 2,7	34,74 - 34,75	7153,3
68	1,8 - 1,9	34,81 - 34,82	7114,6
69	2,5 - 2,6	34,80 - 34,81	6988,7
70	2,7 - 2,8	34,66 - 34,67	6882,3
71	2,5 - 2,6	34,73 - 34,74	6872,6
72	2,3 - 2,4	34,80 - 34,81	6746,7
73	2,4 - 2,5	34,77 - 34,78	6591,9
74	2,7 - 2,8	34,67 - 34,68	6543,5
75	2,7 - 2,8	34,63 - 34,64	6456,3
76	0,9 - 1,0	34,74 - 34,75	6437,0
77	1,4 - 1,5	34,78 - 34,79	6388,6
78	2,6 - 2,7	34,67 - 34,68	6369,2
79	2,5 - 2,6	34,81 - 34,82	6349,9
80	0,8 - 0,9	34,73 - 34,74	5856,2
80	1,0 - 1,1	34,77 - 34,78	5856,2
80	1,2 - 1,3	34,76 - 34,77	5856,2
81	2,0 - 2,1	34,85 - 34,86	5420,6
82	0,6 - 0,7	34,74 - 34,75	5391,6
83	0,5 - 0,6	34,71 - 34,72	5227,0
83	1,8 - 1,9	34,84 - 34,85	5227,0
84	1,7 - 1,8	34,83 - 34,84	5130,2
85	2,7 - 2,8	34,68 - 34,69	5091,5
86	2,8 - 2,9	34,62 - 34,63	5004,4
87	0,3 - 0,4	34,71 - 34,72	4956,0
88	0,3 - 0,4	34,70 - 34,71	4907,6
89	1,3 - 1,4	34,77 - 34,78	4839,8
90	2,6 - 2,7	34,75 - 34,76	4791,4
91	2,7 - 2,8	34,62 - 34,63	4646,2
92	2,8 - 2,9	34,63 - 34,64	4588,2
93	2,5 - 2,6	34,72 - 34,73	4472,0
94	0,7 - 0,8	34,75 - 34,76	4355,9
95	1,7 - 1,8	34,80 - 34,81	4346,2
96	0,5 - 0,6	34,73 - 34,74	4239,7
97	1,9 - 2,0	34,85 - 34,86	4162,3
98	2,1 - 2,2	34,86 - 34,87	4065,5
98	2,2 - 2,3	34,81 - 34,82	4065,5
99	2,6 - 2,7	34,76 - 34,77	4007,4

RANK	TEMPERATURE RANGE °θ	SALINITY RANGE ‰	VOLUME
100	2,6 - 2,7	34,66 - 34,67	3900,9
101	1,1 - 1,2	34,78 - 34,79	3871,9
102	2,4 - 2,5	34,85 - 34,86	3775,1
103	2,9 - 3,0	34,58 - 34,59	3658,9
104	2,9 - 3,0	34,60 - 34,61	3639,6
105	2,6 - 2,7	34,65 - 34,66	3629,9
106	2,9 - 3,0	34,59 - 34,60	3484,7
107	2,8 - 2,9	34,61 - 34,62	3475,0
108	2,5 - 2,6	34,71 - 34,72	3426,6
109	2,1 - 2,2	34,85 - 34,86	3387,9
109	2,4 - 2,5	34,76 - 34,77	3387,9
110	2,8 - 2,9	34,64 - 34,65	3358,9
111	2,1 - 2,2	34,81 - 34,82	3291,1
112	3,0 - 3,1	34,56 - 34,57	3155,6
113	2,7 - 2,8	34,69 - 34,70	3136,2
114	2,7 - 2,8	34,61 - 34,62	3039,4
115	0,4 - 0,5	34,70 - 34,71	3000,7
116	2,5 - 2,6	34,83 - 34,84	2913,6
117	3,0 - 3,1	34,55 - 34,56	2855,5
118	2,6 - 2,7	34,77 - 34,78	2749,0
119	2,4 - 2,5	34,84 - 34,85	2661,9
119	2,8 - 2,9	34,60 - 34,61	2661,9
120	2,5 - 2,6	34,70 - 34,71	2536,1
121	2,7 - 2,8	34,60 - 34,61	2303,8
122	2,4 - 2,5	34,75 - 34,76	2226,3
123	0,2 - 0,3	34,69 - 34,70	2197,3
124	0,7 - 0,8	34,72 - 34,73	2177,9
125	3,1 - 3,2	34,52 - 34,53	2168,2
126	2,6 - 2,7	34,78 - 34,79	2158,6
127	0,2 - 0,3	34,70 - 34,71	2119,9
128	2,9 - 3,0	34,57 - 34,58	2100,5
128	3,0 - 3,1	34,54 - 34,55	2100,5
129	2,3 - 2,4	34,85 - 34,86	2081,1
130	3,0 - 3,1	34,57 - 34,58	2042,4
131	2,0 - 2,1	34,86 - 34,87	2032,7
132	2,5 - 2,6	34,82 - 34,83	1994,0
133	2,8 - 2,9	34,65 - 34,66	1965,0
134	2,8 - 2,9	34,59 - 34,60	1955,3
134	2,9 - 3,0	34,61 - 34,62	1955,3
135	2,5 - 2,6	34,69 - 34,70	1945,6
136	3,1 - 3,2	34,53 - 34,54	1935,9
136	1,1 - 1,2	34,75 - 34,76	1935,9
137	3,3 - 3,4	34,52 - 34,53	1926,3
138	2,3 - 2,4	34,79 - 34,80	1916,6
139	2,7 - 2,8	34,57 - 34,58	1848,8
140	2,3 - 2,4	34,86 - 34,87	1839,1
141	2,7 - 2,8	34,70 - 34,71	1810,1
142	3,1 - 3,2	34,55 - 34,56	1781,1
143	2,7 - 2,8	34,59 - 34,60	1771,4
143	2,8 - 2,9	34,56 - 34,57	1771,4
143	2,8 - 2,9	34,58 - 34,59	1771,4
144	1,6 - 1,7	34,79 - 34,80	1742,3
144	2,6 - 2,7	34,79 - 34,80	1742,3
145	2,7 - 2,8	34,58 - 34,59	1732,7
145	3,2 - 3,3	34,51 - 34,52	1732,7

RANK	TEMPERATURE RANGE °θ	SALINITY RANGE ‰	VOLUME
146	2,6 - 2,7	34,64 - 34,65	1674,6
147	2,2 - 2,3	34,86 - 34,87	1645,5
148	3,2 - 3,3	34,52 - 34,53	1616,5
149	2,6 - 2,7	34,83 - 34,84	1606,8
150	3,0 - 3,1	34,58 - 34,59	1568,1
151	1,9 - 2,0	34,81 - 34,82	1548,7
151	2,0 - 2,1	34,81 - 34,82	1548,7
151	2,7 - 2,8	34,55 - 34,56	1548,7
152	2,5 - 2,6	34,68 - 34,69	1500,4
153	2,9 - 3,0	34,53 - 34,54	1481,0
154	2,2 - 2,3	34,85 - 34,86	1452,0
154	0,8 - 0,9	34,76 - 34,77	1452,0
155	2,8 - 2,9	34,57 - 34,58	1442,3
156	3,7 - 3,8	34,44 - 34,45	1432,6
157	2,9 - 3,0	34,56 - 34,57	1422,9
158	3,0 - 3,1	34,52 - 34,53	1413,2
159	2,2 - 2,3	34,80 - 34,81	1403,6
159	2,5 - 2,6	34,84 - 34,85	1403,6
160	3,0 - 3,1	34,59 - 34,60	1393,9
161	2,6 - 2,7	34,60 - 34,61	1384,2
162	3,4 - 3,5	34,50 - 34,51	1364,8
162	3,5 - 3,6	34,48 - 34,49	1364,8
163	0,3 - 0,4	34,69 - 34,70	1355,2
163	2,3 - 2,4	34,78 - 34,79	1344,2
163	2,6 - 2,7	34,61 - 34,62	1344,2
163	2,6 - 2,7	34,63 - 34,64	1355,2
164	2,9 - 3,0	34,54 - 34,55	1335,8
165	2,8 - 2,9	34,55 - 34,56	1326,1
165	3,1 - 3,2	34,54 - 34,55	1326,1
166	2,5 - 2,6	34,66 - 34,67	1306,8
167	3,3 - 3,4	34,50 - 34,51	1297,1
168	3,5 - 3,6	34,52 - 34,53	1268,0
169	1,9 - 2,0	34,86 - 34,87	1258,4
169	2,6 - 2,7	34,81 - 34,82	1258,4
170	2,6 - 2,7	34,62 - 34,63	1248,7
171	3,2 - 3,3	34,48 - 34,49	1229,3
171	3,2 - 3,3	34,54 - 34,55	1229,3
172	2,5 - 2,6	34,67 - 34,68	1219,6
173	2,6 - 2,7	34,80 - 34,81	1210,0
173	2,9 - 3,0	34,62 - 34,63	1210,0
174	2,7 - 2,8	34,54 - 34,55	1190,6
175	2,9 - 3,0	34,52 - 34,53	1180,9
176	1,2 - 1,3	34,79 - 34,80	1161,6
176	1,6 - 1,7	34,83 - 34,84	1161,6
176	2,4 - 2,5	34,74 - 34,75	1161,6
176	2,5 - 2,6	34,85 - 34,86	1161,6
176	2,7 - 2,8	34,53 - 34,54	1161,6
176	3,0 - 3,1	34,50 - 34,51	1161,6
177	3,2 - 3,3	34,50 - 34,51	1151,9
177	3,2 - 3,3	34,53 - 34,54	1151,9
178	3,6 - 3,7	34,38 - 34,39	1142,2
178	2,9 - 3,0	34,65 - 34,66	1142,2
179	2,6 - 2,7	34,59 - 34,60	1132,5
179	2,6 - 2,7	34,82 - 34,83	1132,5
179	3,0 - 3,1	34,53 - 34,54	1132,5

RANK	TEMPERATURE RANGE °θ	SALINITY RANGE ‰	VOLUME
180	3,2 - 3,3	34,55 - 34,56	1122,8
180	3,3 - 3,4	34,51 - 34,52	1122,8
180	3,5 - 3,6	34,40 - 34,41	1122,8
181	3,4 - 3,5	34,49 - 34,50	1113,2
182	2,7 - 2,8	34,56 - 34,57	1103,5
182	2,9 - 3,0	34,41 - 34,42	1103,5
183	3,1 - 3,2	34,42 - 34,43	1084,1
183	3,8 - 3,9	34,40 - 34,41	1084,1
184	2,9 - 3,0	34,63 - 34,64	1074,4
184	2,9 - 3,0	34,64 - 34,65	1074,4
185	2,8 - 2,9	34,66 - 34,67	1064,8
186	3,5 - 3,6	34,47 - 34,48	1045,4
186	22,3 -22,4	35,58 - 35,59	1045,4
187	12,1 -12,2	35,09 - 35,10	1035,7
188	3,4 - 3,5	34,46 - 34,47	1026,0
188	9,0 - 9,1	34,73 - 34,74	1026,0
189	16,3 -16,4	35,53 - 35,54	1016,4
190	2,5 - 2,6	34,65 - 34,66	1006,7
190	3,5 - 3,6	34,45 - 34,46	1006,7
190	3,6 - 3,7	34,45 - 34,46	1006,7
191	2,7 - 2,8	34,71 - 34,72	997,0
192	2,9 - 3,0	34,68 - 34,69	987,3
192	3,1 - 3,2	34,57 - 34,58	987,3
193	3,0 - 3,1	34,40 - 34,41	977,6
193	11,1 -11,2	34,96 - 34,97	977,6
194	1,5 - 1,6	34,82 - 34,83	968,0
194	2,6 - 2,7	34,85 - 34,86	968,0
194	2,7 - 2,8	34,81 - 34,82	968,0
194	3,1 - 3,2	34,51 - 34,52	968,0
195	2,9 - 3,0	34,55 - 34,56	958,3
195	3,2 - 3,3	34,63 - 34,64	958,3
195	10,4 -10,5	34,88 - 34,89	958,3
195	11,0 -11,1	34,95 - 34,96	958,3
196	3,0 - 3,1	34,49 - 34,50	948,6
196	3,1 - 3,2	34,60 - 34,61	948,6
196	3,3 - 3,4	34,48 - 34,49	948,6
196	3,7 - 3,8	34,50 - 34,51	948,6
197	2,8 - 2,9	34,68 - 34,69	938,9
197	3,1 - 3,2	34,49 - 34,50	938,9
197	4,2 - 4,3	34,35 - 34,36	938,9
197	4,0 - 4,1	34,40 - 34,41	938,9
197	9,6 - 9,7	34,79 - 34,80	938,9
198	2,8 - 2,9	34,54 - 34,55	929,2
198	3,0 - 3,1	34,62 - 34,63	929,2
198	3,7 - 3,8	34,47 - 34,48	929,2
198	8,6 - 8,7	34,69 - 34,70	929,2
198	11,5 -11,6	35,01 - 35,02	929,2
199	8,9 - 9,0	34,72 - 34,73	919,6
199	12,2 -12,3	35,10 - 35,11	919,6
200	3,3 - 3,4	34,60 - 34,61	909,9
200	3,1 - 3,2	34,56 - 34,57	909,9
200	8,8 - 8,9	34,71 - 34,72	909,9
200	9,1 - 9,2	34,74 - 34,75	909,9
200	12,5 -12,6	35,14 - 35,15	909,9
201	11,2 - 11,3	34,98 - 34,99	900,2